INFLUENCE OF BASE ALLOY COMPOSITION ON PROCESSING TIME DURING TRANSIENT LIQUID PHASE BONDING OF NICKEL-BASE SUPERALLOYS

By

JUHAINA FAROUK HUNEDY

A thesis submitted to the Faculty of Graduate Studies of

The University of Manitoba

in partial fulfillment of the requirements for the degree of

Master of Science

Department of Mechanical and Manufacturing Engineering

University of Manitoba

Winnipeg

Abstract

An experimental investigation to study the influence of base metal composition on the time required to achieve complete isothermal solidification (t_f) during TLP bonding of three Ni-base superalloys was performed. Alloys IN 738, DS Rene80 and DS IC 6 show similar behaviour when bonded at 1100 ^{o}C, with comparable t_f. However, at higher temperatures, IN 738 requires extended period of time (as compared to DS Rene80 and DS IC 6) to achieve complete isothermal solidification. The prolonged t_f in IN 738 appears to be caused by a more pronounced reduction in concentration gradient of the diffusing solute within the material during bonding. In contrast, the shorter complete isothermal solidification time experienced by alloy DS IC6 is attributable to its capability to better accommodate the diffusing solute, through the formation of densely packed second-phase precipitates in the diffusion affected zone (DAZ).

Acknowledgement

I wish to express my sincere thanks to my supervisor Dr. Olanrewaju Ojo. His close supervision and continuous advice are greatly appreciated.

I would also like to express my gratitude to the Libyan government for their financial support throughout my studies. The efforts of the Canadian Bureau for International Education (CBIE) are also appreciated. Special thanks are due to Diane Cyr, my academic manager, for her continuous support and close attendance to all problems.

I thank laboratory technicians Don Mardis, John van Dorp, and Mike Boswick for their continual assistance and friendly manner.

Special thanks and heartfelt appreciation are due to my friends Omudhohwo Oshobe and Rekha Chaudhari. Their kindness and encouragement was invaluable.

Last but not least, I am grateful and indebted to my family, who's love and support were vital for me to accomplish this work. I thank my parents, Farouk and Lesley, who instilled within me the love of knowledge. A big thank you goes to my siblings, especially to my sister Nissreen for her technical assistance in this thesis. Finally, I wish to express my gratitude to my dear husband Mustafa for his continual motivation and emotional support.

Dedication

I wish to dedicate this work to my dear father, Farouk Mohammed Hunedy, who unfortunately is not here with us to see its completion. His never ending encouragement of my self and my six siblings to aim for our highest potential in our studies and to be satisfied with no less than a search for complete truth and integrity in all our undertakings, has been a constant source of inspiration. I count my self truly blessed to be his daughter.

Table of Contents

List of Tables

List of Figures

1 Introduction

Nickel (Ni) base superalloys are utilised in manufacturing complex-shaped hot-section components that are designed to withstand the stringent operating conditions of modern aircraft and industrial power generation gas turbine engines. The high work temperatures of these engines lead to component degradation through creep, fatigue and oxidation reaction. In most cases, it is economically more feasible to refurbish these components as opposed to complete replacement. Since some of the Ni base superalloys that contain significant amounts of titanium (Ti) and aluminum (Al) are difficult to weld due to their high susceptibility to hot cracking during welding and post-weld heat treatment [1] , a process known as transient liquid phase (TLP) bonding was developed by Duval et al [2]. TLP bonding has evolved into an attractive alternative joining technique for these difficult to weld alloys owing to its ability to combine the beneficial features of liquid phase joining and diffusion bonding, without the need for high localised heat input or high bonding pressures involved in these techniques.

The TLP bonding process involves the use of an interlayer alloy that contains a melting point depressant (MPD) element, such as boron (B), silicon (Si) or phosphorus (P), which melts between the faying surfaces of the base metal that will be joined. Following this, base metal dissolution (melt-back) occurs to dilute the liquated interlayer to an equilibrium composition at the bonding temperature. While holding at the bonding temperature, the inter-diffusion of the alloying elements occurs between the base metal and the liquid. This results in an increase in the melting point of the liquid interlayer,

and thus isothermal solidification of the liquid. The amount of liquid present in the joint gradually decreases, such that the liquid-solid interface recedes towards the center of the joint. For the joint to be of sound quality, sufficient holding time must be provided, to allow for complete isothermal solidification of the liquid to occur, as well as homogenisation of the joint with the base metal. In such cases where the isothermal solidification process was not completed, owing to insufficient holding time, the remaining liquid transforms into eutectic microconstituents at the center of the joint. These microconstituents are brittle and can render a joint with poor mechanical properties.

An important aspect of producing joints with excellent mechanical properties by using TLP bonding is the processing time (t_f) required to achieve complete isothermal solidification. Therefore, for this bonding technique to be economically effective and efficient, complete isothermal solidification must be achieved within a reasonable holding time (t_f). Minimizing processing time can reduce component repair duration and labour time, which can translate into significant cost reduction in commercial applications. This has been the drive for many studies to investigate the effect of different parameters, such as temperature and filler alloy type, on the rate of isothermal solidification, which determines the t_f. An important factor that can greatly influence the isothermal solidification rate is base alloy composition. This factor, however, is overlooked and seldom reported in the literature, especially as it is thought that diffusivity of the MPD solute within alloys that have the same base element is comparable.

In view of the aforementioned, the main objective of this work is to investigate how the base alloy composition can influence the time required to achieve complete isothermal solidification (t_f) during the TLP bonding of Ni-base superalloys.

To fulfil this objective, three Ni-base superalloys are chosen, namely, polycrystalline IN738, directionally solidified (DS) Rene80, and directionally solidified (DS) IC6. These alloys are bonded at varying temperatures and holding time by using NB150 (Ni-Cr-B) as the filler alloy. When bonded at 1100^{o}C, all three alloys behave similarly, with comparable t_f, and the experimental data are concurrent with conventional TLP bonding analytical models, which assume a parabolic relationship between solid/liquid interface migration and holding time. As these three alloys are all Ni-base superalloys, it would be expected that the rate at which the MPD solute diffuses into the base alloy would be comparable, thus, the t_f for all three alloys would also be comparable. However, an increase in the bonding temperature would show incomparable behaviour of the three alloys. At a higher bonding temperature, alloy IN738 shows deviation from the expected parabolic behaviour, while alloy DS IC6 maintains a parabolic relationship to the end, and alloy DS Rene80 suffers a slight deviation towards the end of the isothermal solidification stage. This incomparable behaviour of the alloys at higher temperatures would result in an excessively prolonged holding time for alloy IN738, compared to DS IC6 and DS Rene80. The ability of alloy DS IC6 to complete isothermal solidification within a reasonable time frame is attributed to its capability to accommodate the diffusing MPD solute, through the formation of a densely packed diffusion affected zone (DAZ) of the second-phase precipitates.

In furthering this study, an experimental investigation is carried out to explore the effectiveness of using a composite powder mixture (which comprises filler and base alloy powders) as an alternative to filler alloy alone in reducing the t_f in alloys, such as IN738, which show deviation from parabolic behaviour. It is found that by using a composite powder with a 7:3 mixing ratio of NB150 filler alloy powder to IN738 base alloy powder, this can reduce the t_f by 50%, as compared to using NB150 filler alloy alone.

In the course of this investigation, it is found that a composite powder mixture, in which the gap-filler particles remain unmelted at the bonding temperature, would produce a joint with large porosity. In contrast, complete melting of the gap-filler in the composite powder mixture would produce a joint free of porosity. As such, a complementary experimental investigation is carried out to study the effect of various factors on the dissolution of gap-filler powder particles. The factors studied include: bonding temperature, mixing ratio of filler alloy to gap-filler alloy ($R_{F:G}$), type of MPD solute, type of gap filler, and size of gap filler powder particles.

2 Literature review

2.1 Ni-base superalloys

The development of superalloys in general was brought about through the need to produce materials that can endure severe high temperature environments with a lengthy operating time as that found for gas turbine engines. Superalloys are special materials because they exhibit a unique combination of excellent mechanical properties and superior resistance to hot corrosion at elevated temperatures. Ni-base superalloys are amongst the most complex and sophisticated alloy systems. They possess outstanding tensile strength, creep rupture strength, as well as excellent corrosion and oxidation resistance [1].

A wide variety of alloying elements are added to Ni-base superalloys. Most of these alloys contain 10-20% chromium (Cr), up to 8% Al and Ti, 5-10% cobalt (Co), and small amounts of B, zirconium (Zr), and carbon (C). Other common additions include molybdenum (Mo), tungsten (W), niobium (Nb), tantalum (Ta) and hafnium (Hf) [3].

Gamma (γ) Matrix

The γ matrix is a solid-solution Ni-based austenitic phase that typically contains considerable amounts of elements, such as Co, Cr, Mo, W, iron (Fe), Al and Ti [3, 4]. These solid solution elements differ from Ni in atomic radii by up to 10%; therefore, a considerable distortion of the lattice is generated [5] which can impart strength to the matrix by increasing the resistance to dislocation motion.

Gamma prime (γ'), Gamma Double prime (γ'') and Delta (δ) phases

The γ' phase (Figure 2.1) is the principal high temperature strengthening phase in most of the Ni-base superalloys. Elements that promote the formation of γ' include Al, Ti and Ta. The ordered FCC $L1_2$-type Ni_3(Al, Ta, Ti) γ' phase particles have a lattice parameter that is very close to that of the γ matrix, thus enabling the coherent and homogeneous precipitation of the γ' phase in the γ matrix and imparting stability at high temperatures [6]. Furthermore, the inherent ductility of γ' prevents it from being a source of fracture. The morphology of the γ' precipitates largely depends on their mismatch with the γ matrix. Hagel [7] reported that the γ' exhibits a spherical shape at a lattice mismatch of 0 – 0.2%, then becomes cubic at a mismatch of around 0.5 – 1%, and above 1.25%, they have a plate-like morphology.

For Ni-base superalloys that contain significant amounts of Fe and Nb, the major strengthening phase is a body-centered-tetragonal ordered precipitate called γ''. This kind of precipitate exhibits a disc-shaped morphology with a thickness as little as 10 nm, and a diameter around 50 nm, and generally coherent with the matrix. Upon aging, Ni-Fe alloys that contain γ'' precipitates become susceptible to the formation of an orthorhombic δ phase (Figure 2.2), which is incoherent with the γ matrix; thus, it does not confer strength even if present in significant amounts [6].

Carbides

Common Ni-base alloy carbides are MC, $M_{23}C_6$, and M_6C. Alloying elements that react with carbon to produce these carbides include Cr, W, Mo, Ta, Nb and Ti.

MC carbides usually form during freezing, and adopt a coarse cubic or script morphology, as shown in Figure 2.1. They are often found in interdendritic regions with no particular preference for intergranular or transgranular positions [3].

MC carbides are the primary type of carbides in Ni-base superalloys, but tend to degenerate during heat treatment and service, thus yielding other carbides such as $M_{23}C_6$ and/or M_6C [8]. $M_{23}C_6$ carbides tend to form during lower temperature heat treatment and service (760-980^{o}C); they usually have the tendency to form along grain boundaries as irregular discontinuous blocky particles. M_6C carbides however, tend to form at slightly higher temperatures, 815-980^{o}C, as opposed to $M_{23}C_6$ [3].

There has been some dispute over whether carbides are beneficial or detrimental to the properties of Ni-base superalloys. In general, when carbides are properly situated at grain boundaries, they can strengthen and retard grain boundary sliding. If formed as discrete particles along the grain boundaries, $M_{23}C_6$ carbides can significantly improve the creep life of an alloy. It was reported that a carbon addition of up to 0.09 wt% contributes to improving the creep rupture life from 10 to 100 hours, as a result of fine $M_{23}C_6$ carbides that form intergranulary [9]. However, if they form as a continuous cellular structure, they can actually enhance crack propagation through grain boundary/matrix decohesion. Carbides can also act as dispersion strengtheners for the γ-matrix when precipitated in a fine form.

Topologically Close-Packed Phases

In certain cases where the composition of the alloy has not been carefully controlled,

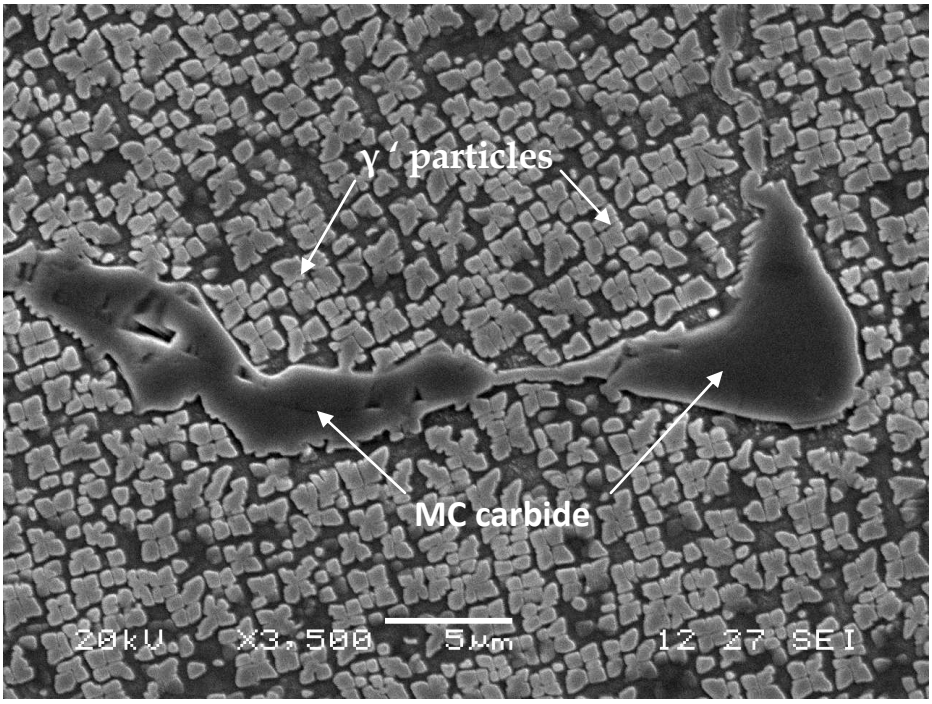

Figure 2.1: SEM micrograph showing γ' precipitates and MC carbides in as cast IN738

Figure 2.2: SEM micrograph showing the microstructure of IN718 heat treated at 900/1hr/AC [10]

some detrimental phases can form either during heat treatment or service. These detrimental phases are referred to as topologically close-packed (TCP) phases, and their precipitation is promoted by excessive quantities of elements, such as Cr, W, molybdenum (Mo), and rhenium (Re) [11]. TCP phases normally have a high and uniform packing density of atoms with a complex crystal structure and a degree of non-metallic, directional bonding [12]. They often nucleate on grain boundary carbides and appear as thin linear plates that are brittle in nature and can act as crack initiators [3]. In general, TCP phases, such as μ, σ, P and R, have the chemical formulae A_xB_y, where A and B are transition metals. The μ phase is based on the ideal stoichiometry A_6B_7 and has a rhombohedral cell which contains 13 atoms. The σ phase is based on the stoichiometry A_2B and has a tetragonal cell that contains 30 atoms. The P phase is primitive orthorhombic, which contains 56 atoms per cell. Finally, the R phase has a rhombohedral cell that contains 53 atoms [6]. The phases commonly found in Ni alloys are σ and μ. The σ phase acts as an excellent source for crack initiation, therefore, leading to low-temperature brittle failure. However, its effect on elevated temperature rupture strength is more of a concern. Since σ contains high amounts of refractory metals extracted from the γ matrix, this can cause a loss of solution strengthening [3].

2.2 Joining and repair techniques for Ni-base superalloy components

2.2.1 Fusion welding

Fusion welding involves the joining of faying surfaces by controlled melting through a localised application of heat and subsequent solidification of the liquid metal pool. Heat sources that are often utilised include electron beams, plasma arcs, electrical resistance, and lasers. During welding operations, the base material remains at a much lower temperature than the weld pool, which results in a sharp temperature gradient between the base material and weld area [13]. In cases where the joint gap is wide or has varying width, it is common practice to use filler metals that have a slightly lower melting point than the component so as to ensure complete melting and flow of filler metal into the joint [14]. Figure 2.3 shows the general macrostructural components of a typical fusion welded joint.

Welding processes

The three main types of fusion welding are as follows.

1. Gas Welding

    Oxyacetylene welding

2. Arc Welding

    Shielded metal arc welding

    Plasma arc welding

    Gas-tungsten arc welding

    Gas-metal arc welding

Flux cored arc welding

Submerged arc welding

Electro-slag welding

3. High-energy beam welding

Electron beam welding

Laser beam welding

The heat sources for these three types, as their names suggest, are gas flames, electric arcs, and high energy beams, respectively. The gas welding process is well suited for maintenance and repair applications, especially as the equipment is simple, portable, and inexpensive. However, it produces the highest heat input in a work piece and lowest power density compared to both the arc welding and high energy beam welding processes. The low power density of gas welding makes it necessary to carry out the welding operation at low speed, which in turn, produces a high heat input, thus resulting in a large heat affected zone (HAZ) and severe distortion of the joined components. In contrast, high energy beam welding, which generates the lowest heat input, can produce welds with deeper penetration and enhanced general quality. Joints that require multiple-pass arc welding can be welded into a single pass by electron beam welding at high speeds, which results in a very narrow HAZ and little distortion [13]. However, the equipment required for electron beam welding is very expensive and the requirement for high vacuum and x-ray shielding is inconvenient and time consuming.

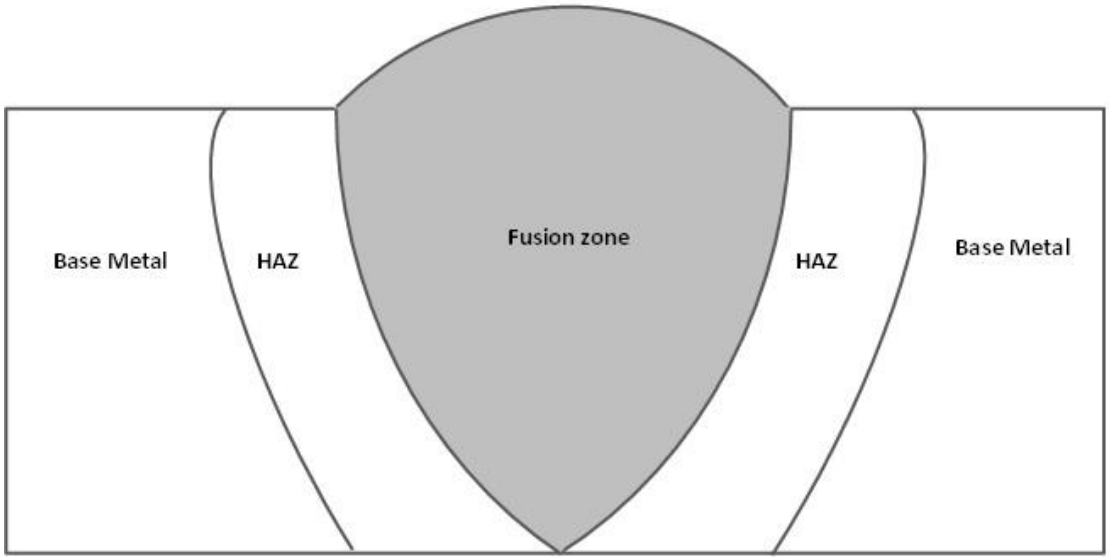

Figure 2.3: Macrostructure of a typical fusion weld

Fusion welding has been successfully employed for joining many materials over a long period of time; nevertheless, it still has limitations inherent to the process which restrict its use as a joining technique. These limitations include:

- the detrimental effect of localised heat input on the microstructure of the components around the joint region, termed the HAZ. For instance, Ni-base superalloys that contain substantial amounts of Al and Ti are difficult to weld due to their high susceptibility to HAZ cracking during welding and subsequent heat treatments [1]. This is because Ni-base superalloys develop large shrinkage stresses due to the rapid precipitation of the γ' particles during cooling down from the welding temperature [15]. Additionally, there is localised melting at the grain boundaries, thus causing thermally induced welding strains and very low ductility in the alloy, which can also induce cracking in the HAZ [16],
- the fatigue resistance of welded components is generally inferior to that of the base alloy. This is attributed to the stress concentration generated by the high thermal gradients produced during welding. These thermal gradients can also result in the distortion of welded components in the HAZ region [1],
- that fusion welding cannot be used to join metals to non-metals [13], and
- the difficulty in welding complex geometries since some surfaces may not be easily accessible to heat sources.

2.2.2 Diffusion Bonding

Diffusion bonding is a solid-state joining process by which two nominally flat surfaces can be joined at an elevated temperature by utilising an applied pressure and holding for a time that ranges from a few minutes to a few hours. The International Institute of Welding (IIW) has adopted a definition of diffusion bonding as proposed by Kazakov [17] : "Diffusion bonding of materials in the solid state is a process for making a monolithic joint through the formation of bonds at atomic level, as a result of closure of the mating surfaces (Figure 2.4) due to the local plastic deformation at elevated temperature which aids interdiffusion at the surface layers of the materials being joined".

Advantages of diffusion bonding

The diffusion bonding technique has been used in many applications due to the following reasons:

- the ability to produce parts with high quality joints, and since no metallurgical discontinuities occur across the joint interface, repaired components can be used in high temperature services,
- the ability to join dissimilar metals with reduced generation of thermal expansion mismatch stresses. This is because the process is performed at relatively low temperatures, and
- elimination of the need for wetting and spreading of fillers, which is contrary to the TLP bonding process where a controlled atmosphere is necessary [14].

Figure 2.4: Sequence of metallurgical stages in diffusion bonding process [18]

Limitations of diffusion bonding

The use of diffusion bonding as a joining technique tends to have limited applications due to the following reasons:

- the demand for high bonding pressures (e.g. 500-5000 psi), thoroughly prepared surfaces with exact fit-up, as well as the possibility of deformation that occurs in the parts during bonding, thus making this technique prohibitively expensive [2],
- the initial investment cost is fairly high and production of large components is limited by the size of the bonding equipment used. Also, limitations to joint design are set as the process is intolerant to joints of variable widths,
- since diffusion bonding is controlled by the solid-state diffusion of atoms across the joint's interface, the technique thus involves a relatively long processing time, and
- alloys based on Al, Ni, Fe, and Co, which exhibit very low solubility for interstitial elements, tend to be difficult to bond when using this technique.

2.2.3 Brazing

Brazing is a joining process wherein metals are bonded together by using a filler metal with a liquidus temperature greater than 450°C, but lower than the solidus temperature of the base metal [19]. At the brazing temperature, the filler metal melts and wets the faying surfaces of the joint by capillary action. The molten filler is retained within the joint by surface tension. Metallurgical reactions take place between the molten filler

and the base material, causing erosion (melt-back) in the original surfaces of the joint. The joined component is then cooled in order to solidify the molten filler metal. Conventional brazing processes normally involve short holding times, therefore, only a limited amount of solid state diffusion of the solute elements is feasible [13].

2.2.3.1 Brazing techniques

During brazing, effective capillary action, necessary for joining, largely depends on the efficient transfer of heat from the heat source into the joint. The size of individual assemblies, numbers required, and rate of production influence the selection of heating method used. Other factors that must be taken into consideration when choosing a heating method include: rate of heating, thermal gradient and cooling rate, all of which can enormously vary with different heating methods.

Some of the most common methods of heating include [19]:

- torch brazing,
- furnace brazing,
- induction brazing,
- resistance brazing,
- dip brazing, and
- wide-gap brazing.

Torch brazing, both manual and automatic, utilises a gas (oxyfuel) flame to heat an assembly. A flux is normally required with the process to promote wetting of the filler metal. It is widely used as a joining process because it is portable and inexpensive [19].

Furnace brazing is a high volume production process for self-fixtured assemblies with a filler metal preplaced near or in the joint. The furnace is typically purged with a gaseous atmosphere or evacuated of air and heated to a temperature above the liquidus of the filler metal, but less than the solidus of the base metal. Heating is often by resistance, but furnaces that utilise both radiation and natural gas convection heating can reduce the heating time by 50%. Preplaced filler metal can be in the form of wire, foil, powder, paste, slugs or preformed shapes. Fluxing is usually required except when a reducing atmosphere is introduced into the furnace [19].

Induction brazing makes use of a material's resistance to the flow of electricity induced by coils positioned around a work piece to provide the heat required for brazing. High-frequency alternating currents flow through the induction coils and create an electromagnetic field around the work piece. This induces an opposing current in the work piece which in turn generates the heat required for brazing. Preplaced filler metals are utilised and may be in the form of wire, strip, or powder. Induction brazing is suitable for high-volume production applications that can be remotely controlled. Due to the precise and selective heating capabilities of the process, high-strength components can be brazed with little loss of strength [19].

Resistance brazing is most suited for simple joints in metals with high electrical conductivity. The work piece with the preplaced filler is made to be part of an electric circuit. Brazing heat comes from either placing carbon electrodes in contact with the brazement to conduct heat into the work or by relying on the resistance of the

brazement to generate heat. Resistance brazing is considered a fast, non-contaminating, and easily controlled process. However, it cannot be used for joining large work pieces or those with non uniform cross sections [19].

Dip brazing involves the immersion of an assembly into a heated bath of either molten metal or a flux bath of molten salt. In both of these processes, the parts to be joined are held together and immersed into a bath of molten bonding metal that flows into the joints. This joining technique is usually used for the manufacturing of electronics and similar small parts [19].

Wide-gap brazing is often used in the repair of large defects and wide gap cracks, and to rebuild large worn surface areas of airfoils. This technique involves the use of a filler which is a mixture of a filler metal and a high-temperature-melting powder (usually referred to as gap-filler). During brazing, the filler metal will completely melt while the gap-filler powder particles remain mostly unmelted, as shown in Figure 2.5, and provide the necessary capillary forces to the molten filler metal within the joint. The mixture, thus, behaves like slurry with sufficient bridging power to fill large cracks or surface defects [19].

2.2.3.2 Brazing atmosphere

Many applications demand that the brazing of an assembly be carried out under a protective atmosphere, including assemblies intended for vacuum environment services, to avoid volatile contaminants and the formation of oxides within the joints. Protective atmosphere categories include gaseous atmosphere and vacuum.

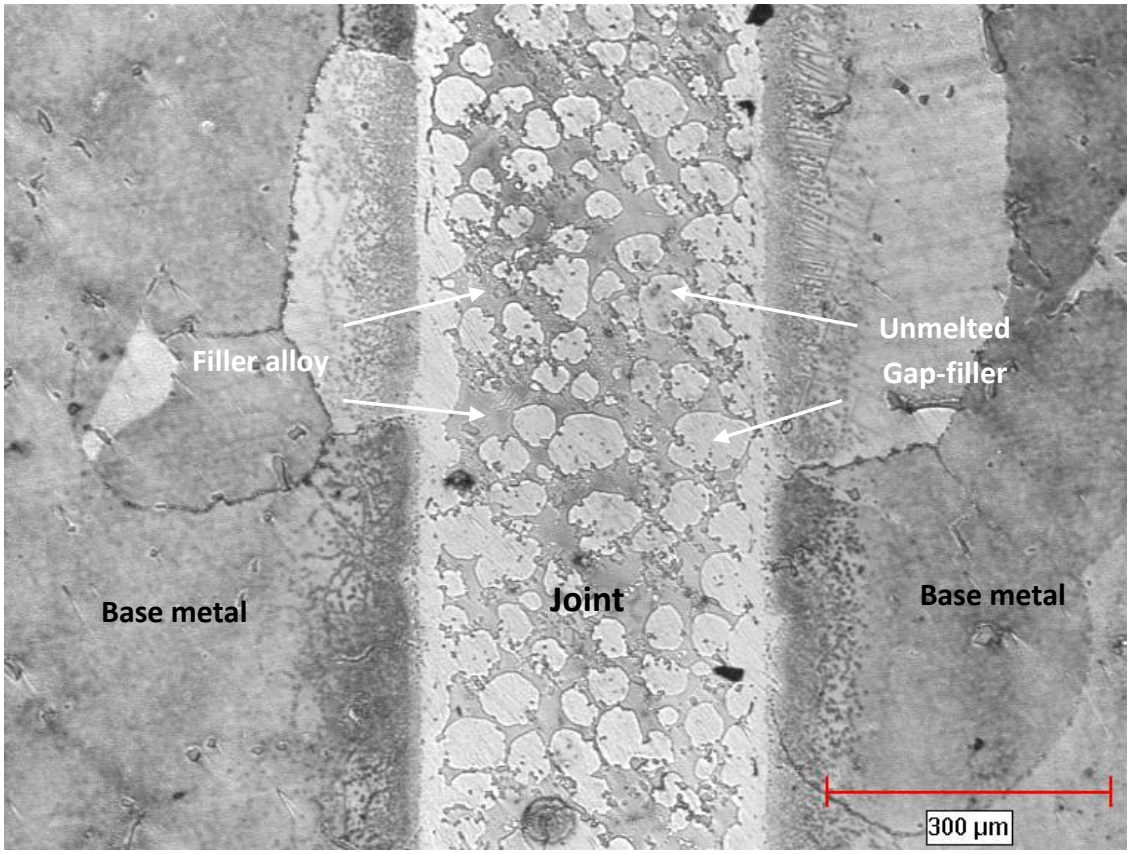

Figure 2.5: Optical micrograph showing a wide gap joint brazed with a mixture of filler alloy and gap-filler powders

Gaseous atmospheres include chemically inert and chemically active gas atmospheres. Chemically inert gases, such as argon, helium, or nitrogen, function by excluding oxygen and other gaseous elements that might react with the components to form surface films and restrain the flowing and wetting of liquated filler alloys [20]. Chemically active gases, such as hydrogen, carbon monoxide or ammonia, are designed to react with the surface films present on the component and filler metal during brazing, and remove them in the process. For instance, a hydrogen atmosphere has been frequently used in the past as it has the ability to decompose certain oxide and sulphide layers. However, its effectiveness is reduced if utilised with Ti and Al bearing alloys, such as Ni-base superalloys [20].

Brazing carried out under a high vacuum atmosphere utilises the same principle of chemically inert gases in which oxygen is excluded to prevent the formation of oxides on the faying surfaces of a joint and the liquated filler alloy. Some of the advantages of using a vacuum atmosphere over a gaseous atmosphere include reduction in the formation of certain oxides, prevention of furnace hot corrosion, and elimination of volatile gases and impurities. A vacuum atmosphere may be used in combination with an inert atmosphere by obtaining a roughing vacuum, purging with an inert gas, and then roughing out again [20].

Controlled gas atmospheres necessitate the use of a confining vessel such as a furnace. This offers many advantages such as economising on the cost of flux and reduction in post-processing operations (e. g. cleaning and removal of flux residues). However,

certain metals may not be compatible with standard atmospheres. For instance, hydrogen atmospheres can cause hydrogen embrittlement of some metals including Ti, Ta and Zr. Similarly, nitrogen atmospheres cannot be used when the parent materials or filler metals contain elements that are susceptible to nitriding, such as Bo, Mo, Ti and Zr. Other potential disadvantages of employing controlled gaseous atmospheres include the capital costs of the equipment, as well as recurring costs due to the consumption of the gas atmosphere used for the processing and maintenance of vacuum pumps [19].

2.2.3.3 Surface cleaning and preparation

The preparation of surfaces to be brazed is of utmost importance, as this will help ensure the production of sound quality joints. All contaminants, such as grease, oils, wax and oxides, should be carefully removed to allow for the wetting, flow and diffusivity of the liquated filler alloy across the faying surfaces of the joint. Cleaning methods used to prepare the surfaces of the joint for brazing include mechanical, chemical, and fluoride cleaning.

Mechanical cleaning methods, including grit blasting, grinding, filing, machining and wire brushing, are usually used to remove heavy oxide scales on the surfaces to be joined. These cleaning methods also cause the roughening of the joint surfaces which can optimise the spreading of the molten filler alloy. Mechanical cleaning methods are less widely used than chemical cleaning methods; however, they may be necessary for removing stubborn lubricants, such as pigmented drawing compounds [19].

Chemical cleaning is the most successful way to remove oil and grease residues. Degreasing solutions are normally used to clean the parts by soaking, spraying or suspension in a hot vapour of the cleaning solution. Immersion in phosphate acid is also used for parts that contain hard-to-remove surface oxides. Following any chemical cleaning operation, the parts must be ultrasonically cleaned in alcohol or clean hot water to remove any traces of the cleaning solutions.

The fluoride cleaning method is usually employed for the cleaning of narrow cracks to be repaired by brazing. Such cracks may be produced by thermal fatigue and are not easily accessible, but need to be effectively cleaned to remove any oxides on the surface layer. The parts to be cleaned are exposed to fluoride ions in a reducing atmosphere but proper control of the process is necessary to effectively clean the surfaces without excessively depleting them of the alloying elements.

2.2.3.4 Fluxes

The main purpose for employing brazing fluxes is to promote the wetting of the base metal by the molten filler metal. For this reason, a flux must be capable of dissolving any oxides that remain on the base metal surface after cleaning operations, and also any oxide films on the molten filler metal. In some cases, fluxes are utilised to suppress the vitalisation of high-vapour-pressure constituents in filler metals; however, fluxes are not designed to remove oils or grease [19]. A flux must be applied as an even coating on the base metal surface and should protect the surfaces until the brazing temperature is reached, and remain active throughout the brazing cycle. It is recommended that fluxes

are used in their proper temperature ranges and on the materials for which they are designed to be used, because molten filler metal should displace flux from the joint at the brazing temperature. Therefore, the recommended temperature will ensure that the viscosity and interfacial energy between the flux and mating surfaces will encourage good wetting [19].

Many chemical elements and compounds are used in the preparation of fluxes. The most common ingredients of chemical fluxes are [19]:

- borates (sodium, potassium, lithium, etc.),
- fused borax,
- elemental boron,
- fluoborates (potassium, sodium, etc.),
- fluorides (sodium, potassium, etc.),
- chlorides,
- alkalis (potassium hydroxide, sodium hydroxide, etc.),
- wetting agents, and
- water.

Some filler metals contain alloy additions of deoxidisers, such as phosphorous, lithium and other elements that have strong affinities for oxygen. These additions can make the filler metal self-fluxing without the application of prepared fluxes or controlled atmospheres. It must be realised however, that these fillers are self-fluxing only in the

molten state and will oxidise during the heating cycle [19]. It is therefore recommended that a protective atmosphere or fluxes in combination with these fillers be used.

When the brazing cycle is complete, it is necessary to remove the residual flux to avoid problems such as corrosion or oxidation of the brazed parts when in service. This is usually done by washing the brazed parts in warm or cold water, or by using an abrasive such as a wire brush to dislodge stubborn flux residue [19].

2.2.3.5 Filler alloys

There are several characteristics that a brazing filler alloy must possess so that it is compatible with a particular base alloy. A filler alloy must have a liquidus temperature that is less than the solidus temperature of the base metal. In practice, heat-resistant alloys are normally brazed with Ni or Co-base filler alloys that contain an MPD element(s) such as B, Si, and P. Other elements such as Al, Ti and C are deliberately excluded or kept to a minimum in the filler alloy as they are found to form stable interfacial phases in the bond [2]; these phases are brittle and can weaken the joint. A filler alloy must also be able to produce a joint with the required mechanical properties as well as attractive chemical properties (e.g. oxidation/corrosion resistance). For this reason, Cr is added to many filler alloys at an amount as high as 20% [21]. Another important feature that a filler alloy must possess is proper fluidity at the brazing temperature to ensure wetting and flow by capillary action. The best spreading characteristics are usually associated with filler alloys with eutectic compositions rather than those with hypo- or hyper-eutectic compositions [22]. The filler alloy must also be

capable of producing a bond at a temperature that will not damage the properties of the base metal.

Filler alloys are available in several forms to suit the shape of the surface to be joined or repaired. Available filler alloy forms include powder, paste, tape, foil, and sheet. Brazing powders are usually produced by inert gas atomization and available in specified particle sizes. The powders may be mixed with organic binders to facilitate positioning onto the base metal surface. Brazing tapes are made of powders that are uniformly applied to a flexible organic backing strip, with or without an adhesive backing [23]. Brazing foils are amorphous and made by rapid solidification during melt spinning operations. Brazing tapes and foils are usually utilised for applications that require a large bond area, good fit-up, or where flow and wettability are a challenge [24].

2.2.3.6 Base alloy characteristics

In order to produce satisfactory braze joints, it is important to consider certain characteristics of the base metal. The base metal must be able to adequately accommodate the diffusing MPD element. It is also desirable to utilise base metals which do not form second phases at the brazing temperature. The base alloy should possess sufficient strength and thermodynamic stability at the brazing temperature. It is also important that the solidus temperature of the base alloy be considerably higher than the liquidus temperature of the filler alloy. Another factor that must be considered is that base alloys with an initial concentration of the MPD element may behave differently compared to base alloys which contain no MPD element [20].

Advantages of brazing

- Strong, uniform and leak proof joints can be rapidly and simultaneously made.
- Components with complex geometries and varying thickness can usually be brazed together.
- Ability to preserve protective metal coating or cladding on the materials that are being joined.
- Multicomponent assemblies can be joined with low distortion and good resistance to thermal shock. This is made possible by heating the entire part to the brazing temperature.
- Cast and wrought alloys can be joined together to produce an integral component.
- It is possible to cosmetically produce neater joints without the need for costly secondary operations.

Limitations of brazing

Having mentioned the attractive features of brazing, the fact still remains that a brazed joint is not a homogeneous body, but rather, is heterogeneous, composed of different phases with differing physical and chemical properties.

2.2.4 Transient liquid phase (TLP) bonding

TLP bonding is a high temperature fluxless process that came about as an advancement to vacuum brazing [25]. This fairly newly developed process incorporates the beneficial

features of liquid phase joining and solid-state diffusion bonding. This offers the potential to produce joints with microstructures and mechanical properties close to those of the base material [14]. It differs from diffusion bonding in that the formation of a liquid interlayer eliminates the necessity for a high bonding force [26].

As shown in Figure 2.6, the TLP bonding process involves the use of an interlayer that contains an MPD element, such as B, Si and/or P. As the temperature of the joint assembly is raised to the bonding temperature, which is well below the solidus temperature of the base material, the interlayer melts and interdiffusion of alloying elements takes place between the base material and the fused interlayer. As a result, changes in the composition of the solid and liquid phases will occur until a state of equilibrium is attained at the interface of the joint. The continuous diffusion of the MPD element into the base material raises the melting point of the liquid filler, which results in isothermal solidification. Therefore, for a joint to achieve complete isothermal solidification, it must be held at the bonding temperature for a sufficient amount of time before cooling to an ambient temperature. This is to allow for the diffusion of the entire MPD element into the base material. Following complete isothermal solidification, holding the joint at the bonding temperature for a longer time is usually necessary to homogenise both the microstructure and the composition of the bonded material.

Advantages of TLP bonding process

- Compared to diffusion bonding, diffusion brazing has the advantage of not requiring the rather high pressure typically involved in a solid-state diffusion

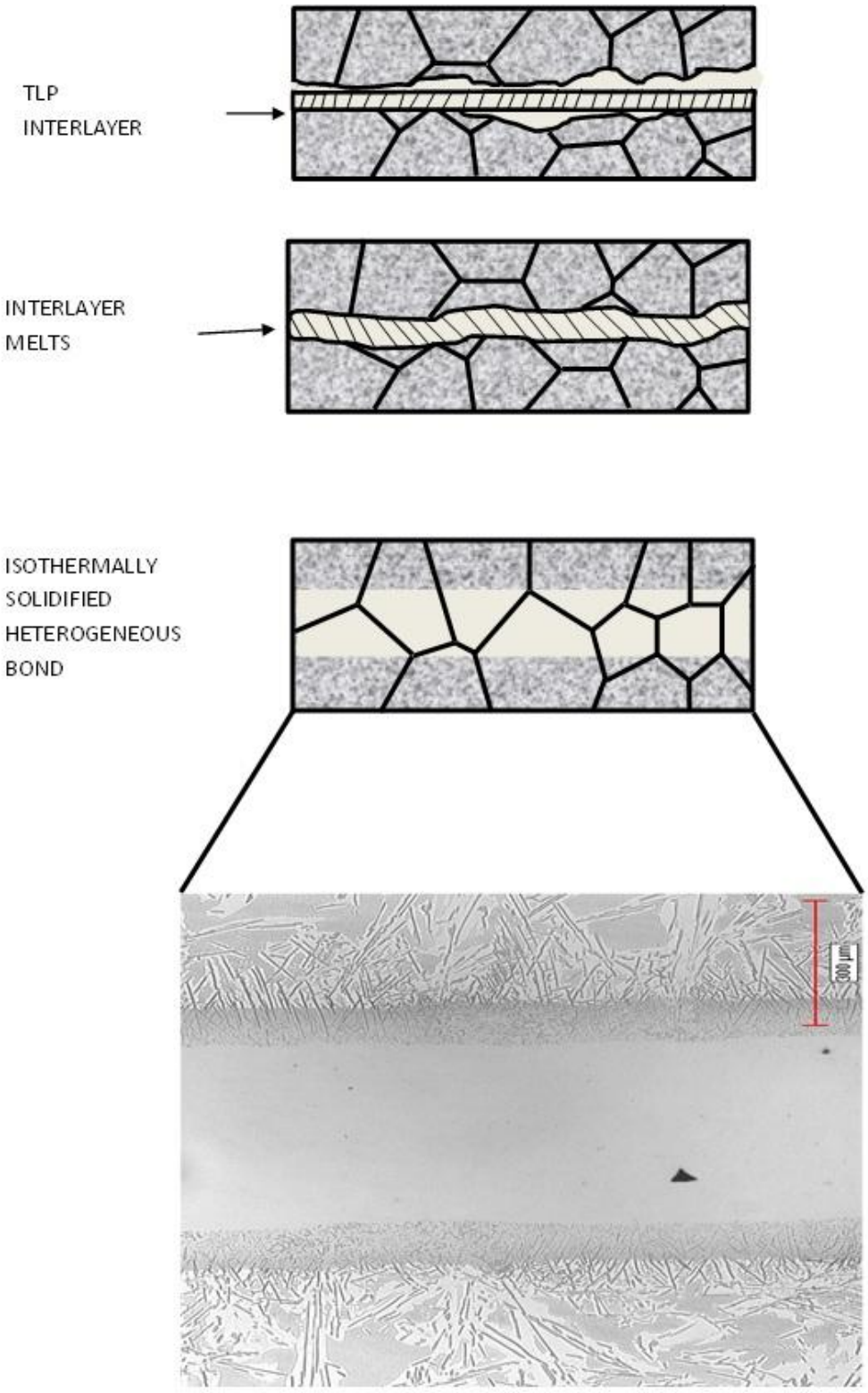

Figure 2.6: Illustration of TLP bonding process

bonding process [27]. Moreover, it can be suitably employed for joining intermetallic base materials, which have stable oxide films and are difficult to joint by diffusion bonding techniques [28].

- It is capable of successfully joining heat resistant alloys that are inherently susceptible to HAZ cracking during welding or post-weld heat treatment [2, 29, 30]. It is also capable of producing sound joints between dissimilar alloy combinations and metal-matrix composites.
- Complex-shaped parts can be joined by using simple tooling and joint surface preparation.
- It allows for the mass production of parts and hence processing costs can be significantly reduced.
- Joints with microstructural and mechanical properties similar to those of the parent metal can be produced. It is also possible to enhance the quality of the joints by employing a suitable post-joining heat treatment.

Limitations of TLP bonding process

- Long processing times that can typically be several hours. This is due to the dependence of the isothermal solidification stage on the solid-state diffusion of the solute element from the liquid interlayer into the base metal.
- Insufficient holding time at the bonding temperature can result in the formation of brittle phases. These brittle phases generally tend to degrade the mechanical and chemical properties of the joint.

- Diffusion of the MPD solute from the liquid interlayer into the base metal causes the precipitation of second phase particles at the brazed joint interface. These particles can have adverse effects on the mechanical properties and corrosion resistance of the joint.

2.2.4.1 Mechanisms of TLP Bonding

Duvall et al. [2] developed TLP bonding as an alternate method to join heat resistant alloys. In their study, where a eutectic composition interlayer was used, they described four basic stages for TLP bonding, namely: melting of the interlayer, base metal dissolution, isothermal solidification, and solid bond homogenisation. Tuah-Poku et al. [27] carried out a comprehensive study on TLP bonding. By utilising a pure interlayer, a four-stage process was defined as: dissolution of the pure interlayer, homogenisation of the liquid interlayer, isothermal solidification, and homogenisation of the bonded region. To account for the possible loss of the MPD solute during heating to the bonding temperature, MacDonald and Eager [26] added an initial stage (stage 0) prior to the base metal dissolution stage. This effect was reported by Niemann and Garret [31] and Nakagawa et al [32] for slow heating rates which allow for the premature diffusion of the MPD solute into the base material, resulting in a lack of liquid formation at the joint interface.

To simplify the theoretical description of the TLP bonding stages (as shown in Figure 2.7), it is most appropriate to use an interlayer with a eutectic composition of C_E. This is

Figure 2.7: Schematic of the mechanisms controlling TLP bonding process [33]

inserted between two pure A base metals of composition C_A. Therefore, the assembly can be described as an A/A-B/A system, where B is the MPD solute.

a) Heating and melting of the Interlayer

During this stage (Figure 2.7a), the assembly to be bonded is heated to the bonding temperature, T_B, which is normally above the melting point (eutectic temperature), $T_{M,}$ of the filler alloy. Thus, the filler alloy melts and fills the joint. During the heating stage, before the interlayer reaches the melting point, some solid state diffusion may take place between the filler alloy and the base metal. The amount of diffusion will depend on several factors amongst which are the heating rate and the diffusivity of the MPD element. As mentioned earlier, very slow heating rates may cause the MPD solute to diffuse out of the filler before reaching the melting temperature; therefore, very little or no liquid will form upon reaching the bonding temperature. This problem is more pronounced when using very thin filler alloys and fillers with low MPD solute concentrations [31].

b) Base Metal Dissolution

Base metal dissolution occurs after the liquation of the filler alloy at its melting point and continues until the bonding temperature is achieved. The local melt-back of the base metal occurs as a result of the continuous diffusion of the MPD solute (atoms of B) from the liquid filler into the base metal, consequently increasing the concentration of B at the base metal mating surfaces to amounts greater than $C_{\alpha L}$. Therefore, in order to attain equilibrium at the solid-liquid interface (i.e. interfacial

melts back into the liquid filler, and results in an increase in the volume of the interlayer liquid phase as shown in Figure 2.7b). The interfacial reactions causing base metal dissolution are rapid and controlled by liquid diffusion.

The dissolution stage becomes of great importance in applications such as those by the aerospace industry. Excessive base metal dissolution of structures such as honeycomb and rocket fins cannot be tolerated, as this can lower the load bearing capability of thin sections. The extent of base metal melt-back depends on several factors, including the initial concentration of the MPD solute in the filler C_E, initial filler thickness and solubility of the MPD solute into the base metal.

c) Isothermal Solidification

It is normally assumed that isothermal solidification is initiated after the dissolution stage at a constant bonding temperature, T_B, during which the MPD solute diffuses out of the liquid interlayer and into the base metal. A state of local equilibrium is maintained at the solid-liquid interface at all times during the isothermal solidification stage and the composition of the liquid and adjoining solid remains fixed at $C_{L\alpha}$ and $C_{\alpha L}$ respectively. However, as the MPD solute continues to diffuse into the base metal, the volume of liquid which can be maintained at equilibrium progressively decreases in order to satisfy the solute mass balance across the interface. Therefore, solidification occurs inward from both mating surfaces by the migration of the solid-liquid interface towards the centerline of the joint [2]. Once the maximum concentration of the MPD solute within the joint region has been

reduced to $C_{\alpha L}$, then the liquid is entirely removed and isothermal solidification is completed (Figure 2.7d).

The isothermal solidification stage is very slow compared to the dissolution stage as it is controlled by the solid-state diffusion of the MPD solute into the base metal. The time necessary to achieve complete isothermal solidification depends on the diffusion flux of the solute in the base metal and on the amount of solute that needs to be diffused. These depend on several factors, including initial filler thickness, diffusion of the MPD solute into the base metal, solubility of the MPD solute and its concentration gradient in the base metal.

d) Joint Homogenisation

Following the isothermal solidification stage, a homogenisation process is carried out at a temperature which may be different from the bonding temperature. During homogenisation, the remainder of the MPD solute diffuses out of the joint and its concentration is decreased whilst other alloying elements diffuse from the base alloy into the joint [34]. Ideally, at the end of the homogenisation process, the joint will be identical both in chemistry and microstructure to the base alloy. After homogenisation is completed, there can be a tolerable amount of the MPD solute that remains in the joint, which generally depends on the material and the intended application of the repaired part as well as the practicality of the homogenisation treatment.

2.2.4.2 Modeling of Isothermal Solidification Kinetics

An extensive body of work on modeling the TLP bonding process has been built over many years in an effort to accurately predict the conditions needed to complete bonding. One of the common goals that drive the modeling work is to predict the completion times required for each stage of the process (i.e., base metal dissolution, isothermal solidification, and homogenisation). However, the bulk of the work has been geared towards modeling of the isothermal solidification stage, as its kinetics are controlled by the slow solid state diffusion of the solute element into the base metal, and thus, requires a much longer completion time than that required for the other stages. For this reason, it was suggested that a reasonable estimation of the completion time for the isothermal solidification stage can be used as an approximation for the whole process [26, 35]. Other common goals of the modeling work include the ability to select an optimum filler alloy (i.e. composition and thickness) and bonding parameters (e. g. temperature and time), which will optimise the completion time of the TLP bonding process [36].

The following is a review of some of the research work that has been done on the modeling of the isothermal solidification stage. In these models, some fundamental assumptions are made, amongst which, local equilibrium is assumed to exist at the solid-liquid interface at the bonding temperature. They also assume that the effect of convection in the liquid is negligible due to the small thickness of the liquid interlayer [27]. The interdiffusion coefficients in the solid and liquid (D_S and D_L) are considered to

be independent of the composition [27] and the base metal is assumed to be a semi-infinite medium.

Premised on the previous assumptions, the analytical modeling of the isothermal completion time can be classified into two major categories, single-phase solution and two-phase solution. In the single-phase solution, the system is treated as a single semi-infinite phase, with the base metal having a constant solute concentration ($C_{\alpha L}$) at its surface. The two-phase solution, however, treats the system as two semi-infinite phases with a diffusion-controlled solid-liquid moving interface [37]. The latter solution is much more accurate in approximating real situations, especially as it allows for the advancement of the interface towards the centerline as the liquid is consumed.

Based on the single-phase model approach, Tuah-Poku et al [27] utilised an error function to represent the solute distribution in a semi-infinite base metal, as described below:

$$C(x,t) = C_{\alpha L} + (C_M - C_{\alpha L})erf\left[\frac{x}{\sqrt{4D_s t}}\right] \qquad (1)$$

where $C_{\alpha L}$ is the solute concentration at the surface of the base metal

C_M is the initial solute concentration in the base metal

D_s is the solute diffusivity in the base metal_

t is the solidification time

x is the distance along the specimen length from the surface.

By using the above error function, the total amount of solute (M_t) diffused into the base metal at time (t) is given by:

$$M_t = \int_0^t \frac{dc}{dx} dt = 2(C_{\alpha L} - C_M)\sqrt{\frac{D_s t}{\pi}} \qquad (2)$$

If the amount of solute diffused into the base metal during the heating and dissolution stages is assumed to be negligible, then the total amount of solute diffused into the base metal at the end of the isothermal solidification stage can be considered equal to the original solute concentration of the filler metal [35], such that:

$$C_E W_o = 4(C_{\alpha L} - C_M)\sqrt{\frac{D_s t}{\pi}} \qquad (3)$$

where C_E and W_o are the original solute concentration and the initial width of the filler metal, respectively.

Upon rearrangement of Equation (3), the isothermal solidification completion time may be expressed as follows:

$$t = \frac{\pi}{16 D_s}\left[\frac{C_E W_o}{C_{\alpha L} - C_M}\right]^2 \qquad (4)$$

The above approach was also followed by Onzawa et al [38], Ikawa et al [39], and Nakao et al [40] to model the isothermal solidification stage.

By adopting a two-phase analytical approach, Lesoult [41] aimed for a more accurate treatment of the problem. A general error function was employed to represent the solute distribution in the solid phase as shown below:

$$C(x,t) = A_1 + A_2 erf\left\{\frac{x}{\sqrt{4D_s t}}\right\} \qquad (5)$$

where A_1 and A_2 are constants determined by the specific boundary conditions:

$$When\ x \to \infty,\ C(\infty,t) = A_1 + A_2 = C_M \qquad (6)$$

and at the moving solid/liquid interface, i.e. x = X(t)

$$C(X(t),t) = A_1 + A_2 erf\left\{\frac{X(t)}{\sqrt{4D_s t}}\right\} = C_{\alpha L} \qquad (7)$$

where $C_{\alpha L}$ is the solute concentration of the solid phase at the interface.

Since Equation (7) must be satisfied for all values of t, X(t) must be proportional to $t^{1/2}$ i.e.,

$$X(t) = k\sqrt{4D_s t} \qquad (8)$$

where k is the rate constant. An increasing k results in a faster solid/liquid interface motion and a shorter isothermal solidification completion time.

Mass balance at the interface produces the following expression:

$$(C_{L\alpha} - C_{\alpha L}) \bullet \frac{dX(t)}{dt} = D\left[\frac{\partial C(x,t)}{\partial x}\right]_{x=X(t)} \qquad (9)$$

where $C_{L\alpha}$ is the solute concentration in the liquid phase at the moving solid/liquid interface.

The solving of Equations (5) and (9) produces:

$$\frac{k(1+erf(k))\pi^{\frac{1}{2}}}{\exp(-k^2)} = \frac{C_{\alpha L} - C_M}{C_{L\alpha} - C_{\alpha L}} \qquad (10)$$

Numerical methods were employed by Lesoult [41] to calculate the rate constant k in Equation (10), which is eventually used to compute the time necessary for complete isothermal solidification as shown in the expression below:

$$t = \frac{W_{\max}^2}{16k^2 D} \qquad (11)$$

where W_{max} is the maximum liquid width calculated by using the mass balance method [27]. Comparable solutions to the above were also derived by Sakamoto et al [42] and Ramirez and Liu [43] by using a similar approach.

The single-phase solution (Equation (4)) derived by Tuah-Poku et al [27] was found to greatly overestimate the isothermal solidification completion time. They explained this overestimation with the possibility that the solidification process has been accelerated due to ledge-type interface migration, as well as the effect of grain boundary grooving. Work carried out later by Zhou [37] suggested that the overestimated time predicted by

Equation (4) may actually be due to an inaccurate assumption made during the derivation. A major assumption made in the single-phase solution is a stationary interface, and accordingly, Equation (1) is used to represent the distribution of the solute in the solid base metal. This assumption is unsuitable in most cases, since in reality, it is known that the liquid/solid interface migrates during the isothermal solidification stage. There is, however, an exception where Equation (4) can closely estimate the isothermal completion time. In cases where k is very small (this occurs when values of C_M and $C_{\alpha L}$ are very small compared to that of $C_{L\alpha}$ (Tuah-Poku et al [27]), the rate of isothermal solidification becomes very slow and the solid/liquid interface can be considered stationary [35].

The previously discussed models assume that the base metal dissolution and the isothermal solidification stages occur in a sequential fashion. Gale and Wallach [44, 45] , however, took a different approach in which they considered these two stages to be occurring simultaneously rather than sequentially. Nakagawa et al [32] and Lee et al [46] also proposed this same assumption. In this approach, the liquid phase and the solid substrate are treated as a continuum, which is represented by using the following equation:

$$C(x,t) = C_M + \frac{1}{2}(C_E - C_M)\left\{erf\left[\frac{h+x}{\sqrt{4D_s t}}\right] + erf\left[\frac{h-x}{\sqrt{4D_s t}}\right]\right\} \qquad (12)$$

where C_M is the initial solute concentration in the base metal

C_E is the initial solute concentration in the interlayer

C(x,t) is the initial solute concentration as a function of distance from the center of the interlayer (x) and time (t).

This equation presents the solute distribution in a semi-infinite substrate for an unsteady state diffusion of specie from a source with an initial thickness 2h, which is of the order of the diffusion distance $(Dt)^{½}$. At the end of the isothermal solidification stage, the solute concentration at the center of the interlayer is reduced to the solidus value $C_{\alpha L}$ such that $C(x,t) = C_{\alpha L}$ at x = 0. Taking this into account, Equation (12) can be reduced to estimate the isothermal completion time, t_f, as follows:

$$C_{\alpha L} - C_M = (C_E - C_M)\left\{erf\left[\frac{h}{\sqrt{4D_s t_f}}\right]\right\} \qquad (13)$$

This approach has been reported to show reasonable agreement between the estimated and experimental values of t_f [44, 45, 47].

One of the fundamental assumptions made in analytical modeling is considering the base metal to be a semi-infinite medium. This assumption is only valid for applications where the thickness of the parts to be joined is much larger than the diffusion distance. For applications that involve thin sections, such as those found in the microelectronics industry and in honey-comb structures, the assumption of a semi-infinite medium can be greatly incorrect [48].

2.2.4.3 Development and applications of TLP bonding for superalloys

The earliest mention of the modern industrial application of TLP bonding is attributed to Lynch et al [49], in which they prepared an interface free TLP joint in Ti by using an Ni-copper interlayer, and called the process 'eutectic brazing'. Owczarski et al [50] joined dissimilar metals Zircaloy 2 to 304 stainless steel without incorporating an interlayer, but rather, a eutectic was formed that progressively dissolved each metal, and this was termed 'eutectic bonding'. The 'solid-liquid interdiffusion bonding' (SLID) process was introduced by Bernstein and Bartholomew [51, 52] , by which they produced bonds on electrical components through the use of a ternary system Ag-In-Sn. In this variation, isothermal solidification was not completed; however, successive bonds were produced at decreasing temperatures and high temperature exposure helped to homogenise the joint.

By the 1970s, the TLP bonding process was being developed as a bonding technique in the aerospace industry. While working for General Electric at the Air Craft Engine Group, Hoppin and Berry [53] developed 'activated diffusion bonding' (ADB) for joining several superalloys through the use of an Ni-base eutectic interlayer. By using a process patented by Owczarski et al [54], Duvall et al [55] joined superalloy Udimet 700 by using an Ni-Co interlayer at Pratt and Whitney. Later, in 1974, Duvall et al called the joining process 'transient liquid phase bonding' (TLP) and copyrighted the term; they used the TLP process to join several similar alloys by using an Ni foil that contained B as the MPD solute and achieved joints with near base metal properties [2].

Several researchers have reported the use of the TLP technique for a spectrum of superalloys. Besides the application of this technique for joining alike base-metal components, it has also been used for joining dissimilar superalloys as well as single crystal and oxide dispersion strengthened superalloys [56, 25, 57]. Specific applications include the repair of Ni-base superalloy turbine blade components and joining of heat-resistant alloys that are inherently susceptible to hot cracking or post-weld heat treatment cracking [25, 58, 59, 60, 61].

In addition to those previously mentioned, there are other variants of the TLP bonding process. 'Liquid interface diffusion' (LID) was developed to bond honeycomb sandwich structures [62]. Another variant is wide-gap TLP bonding for 100-500 μm gaps by using multiple layers of melting and non-melting constituents within the joint. It was initially developed by Nakao et al [63, 64], and later modified to include the use of powder within the joint [65]. This technique can also be used in conventional TLP bonding to accelerate isothermal solidification [66, 67]. New technologies are also evolving, such as 'temperature gradient TLP' (TG-TLP) bonding [68, 69], where a temperature gradient is imposed across the substrate-joint interface to decrease the time required for complete isothermal solidification.

2.3 Scope of the present work

As discussed in the previous sections, TLP bonding is proving to be a promising technique for the effective joining of difficult-to-weld Ni-base superalloys with a high

volume fraction of the γ' phase. An important process parameter in the consideration of TLP bonding for commercial applications is the holding time (t_f) required to achieve complete isothermal solidification, which is necessary for preventing the formation of eutectic constituents that degrade the properties of the joined material. Several studies have been undertaken to investigate the effect of different parameters and factors, such as bonding temperature, filler alloy thickness and composition, on the rate of the isothermal solidification of the liquated interlayer that determines the t_f during TLP bonding. However, an important factor that can highly influence the TLP bonding process and ultimately affect the processing time (t_f), is the chemical composition of the base-alloy, and this is seldom reported in the literature.

In view of the above, the primary objective of this work is to study the influence of base-alloy composition on t_f during the TLP bonding of different Ni-base superalloys. To achieve this objective, three Ni-base superalloys, namely, polycrystalline IN738, DS Rene80, and DS IC6, are selected to be bonded at various temperature and time combinations. These commercial nickel-base superalloys with different chemical compositions were selected for this study as representatives of the general qualities possessed by different Ni-base superalloy groups. Conventionally cast IN 738, although considered an old generation superalloy, is still heavily utilised in the manufacture of hot section components of air craft engines and power generation turbines, as it is renowned for its high creep rupture strength and remarkable hot corrosion resistance at service temperatures of up to 980^{o}C. Alloy Rene80, a newer generation Ni-base superalloy, is also used at service temperatures close to those of IN 738 and found in

parts such as the blades and vanes of aero-engines and power generating gas turbines. However, directional solidification processing allows Rene80 to be utilised at higher service temperatures with a reported 4 times increase in creep rupture life compared to the conventionally cast material. A newly developed class of Ni-base superalloys are the Ni aluminides. These intermetallic-base alloys have developed as prime alternates for existing Ni-base superalloys which have almost reached their peak temperature limit of application. Alloy DS IC 6 is one of the Ni_3Al-based alloys that has been developed at the Beijing Institute of Aeronautical Materials as a high-temperature structural material for manufacturing advanced jet-engine components. It exhibits advanced creep-rupture properties, and can withstand service temperatures of up to 1100^oC, which is higher than that of the majority of currently used Ni-base superalloys.

This work, as well as other studies, has shown that alloy IN738 suffers from an anomalous behaviour where prolonged holding time is required to achieve complete isothermal solidification, when the bonding temperature is increased. In an effort to reduce the t_f in such alloys, an experimental study is carried out to explore the effectiveness of using a composite powder mixture, which comprises filler and base alloy powders, as an alternative to filler alloy alone.

A complementary experimental investigation is also carried out to study the effect of various factors on the dissolution of gap-filler powder particles present in the composite powder mixtures. The factors studied include: bonding temperature, mixing ratio of

filler alloy to gap-filler alloy ($R_{F:G}$), type of MPD solute, type of gap filler, and size of gap filler powder particles.

3 Experimental techniques

3.1 Base and filler alloys

The Ni-base superalloys used in the experimental investigation of this work are polycrystalline IN738, DS Rene80, and DS IC6. Alloys IN738 and DS IC6 were used in the as-cast condition, while DS Rene80 was used in the solution-treated condition (2 hrs at 1204^{o}C). The chemical compositions of the alloys to be investigated are listed in Table 3.1. The brazing alloys used are Metglass MBF-80 brazing foil and Nicrobraz 150 powder and additive gap-filler alloys Amdry7380 and Amdry7381 powders. The chemical compositions and size of the brazing alloys are listed in Table 3.2.

3.2 Sample Preparation and TLP Bonding

The as-received base material plates were sectioned into various sample configurations by using numerically controlled electro-discharge machining (EDM). Following this, all mating surfaces were grounded by using 600 grade SiC paper, to ensure the removal of any oxide layer formed during the machining operation. After grinding, the specimens were ultrasonically cleaned in an acetone solution for about 15 minutes. A ceramic coating was applied to the non-mating surfaces of the specimens to prevent spillage and escape of the molten filler from the joint during bonding.

When using the foil filler alloy, the bond assembly consisted of two 2.5 x 8 x 10 mm base alloy coupons placed onto one another, with the filler foil placed between them as

Table 3.1: Nominal chemical composition of base materials

Base Material	Nominal Chemical Composition wt%
Inconel 738LC	15.84Cr, 8.5Co, 1.88Mo, 2.48W, 0.92Nb, 3.6Al, 3.47Ti, 0.07Fe, 1.69Ta, 0.11C, 0.012B, 0.04Zr, 0.001S, Bal. Ni
DS Rene80	14.1Cr,9.82Co, 3.98Mo,4.0W, 0.02Nb, 2.9Al, 4.98Ti, 0.18Fe, 0.2C, 0.012B, 0.028Zr, 0.001S, 0.02Hf, Bal. Ni
DS IC 6	14.0Mo, 8.0Al, 0.06B, Bal. Ni

Table 3.2:Nominal composition of filler alloys and gap-filler powder size

Filler Alloy	Nominal Chemical Composition wt%
Nicrobraz 150	15.0Cr, 0.03C, 3.5B, Bal. Ni
MBF80	15.0Cr, 0.06C, 4.0B, Bal. Ni
Additive Gap-Filler	**Nominal Chemical Composition wt% / Powder Size**
Amdry7381 (coarse powder)	Same as IN738 (Table 3.1)/ -120 +325mesh (-125 +45 μm)
Amdry7380 (fine powder)	Same as IN738 (Table 3.1)/ -325 mesh (-45 μm)

schematically shown in Figure 3.1 a. However, when the powder filler alloy was used (with or without the additive gap-filler), a butt-joint configuration was also used, as shown in Figure 3.1 b, in which a gap of 200 or 350 μ was created half way in the 2 x 8 x 5 mm base alloy coupons to facilitate the accommodation of the powder material. The TLP bonding operations were carried in a vacuum furnace, operated at a vacuum of approximately 5 x 10^{-5} torr, and programmed to follow a temperature-time cycle as schematically shown in Figure 3.2.

3.3 Microscopic Examination

Bonded samples were sectioned by using EDM and prepared via a standard metallographic procedure for microstructural examination. The sectioned samples were polished, and then etched by using a Marbles reagent that contained 4 g $CuSO_4$ + 20 ml HCl + 20 ml H_2O. Electrolytic etching was applied to some samples by using a solution of 12 ml H_3PO_4 + 40 ml HNO_3 + 48 ml H_2SO_4 at 6V for 5 seconds. The microstructure of the bonded samples was examined via an inverted optical microscope and a JEOL 5900 scanning electron microscope (SEM) equipped with an ultra thin window Oxford energy dispersive x-ray spectrometer (EDS). For samples that contained a centerline eutectic, an average of 20 measurements was taken across the eutectic to determine its width. Semi-quantitative chemical compositional analysis of the phases formed in the joint was carried out by EDS equipped with INCA analytical software.

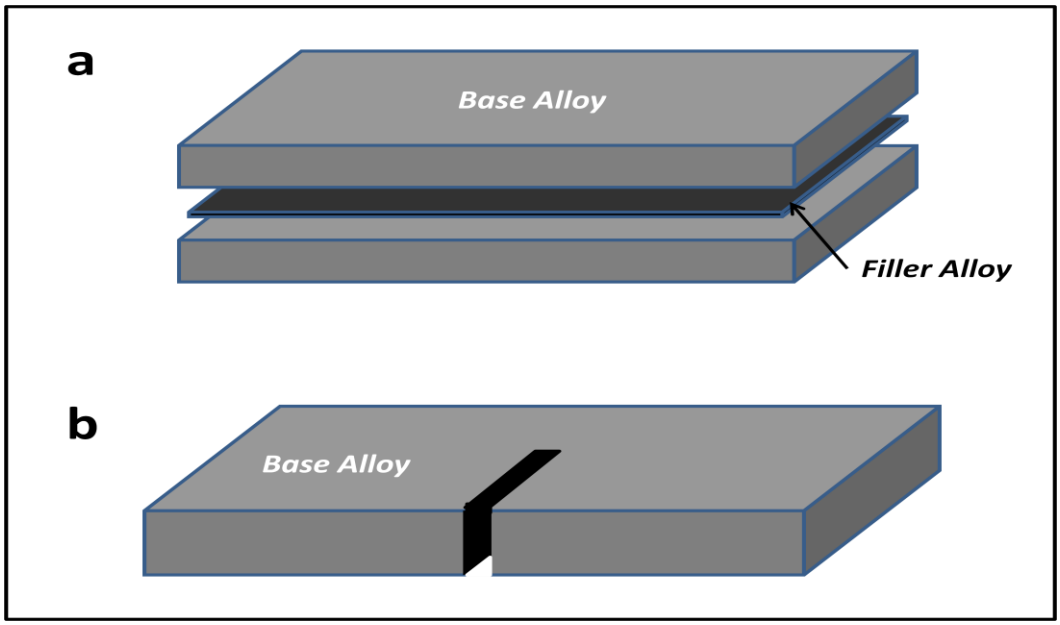

Figure 3.1: Configuration of samples: (a) lap joint, (b) butt-joint

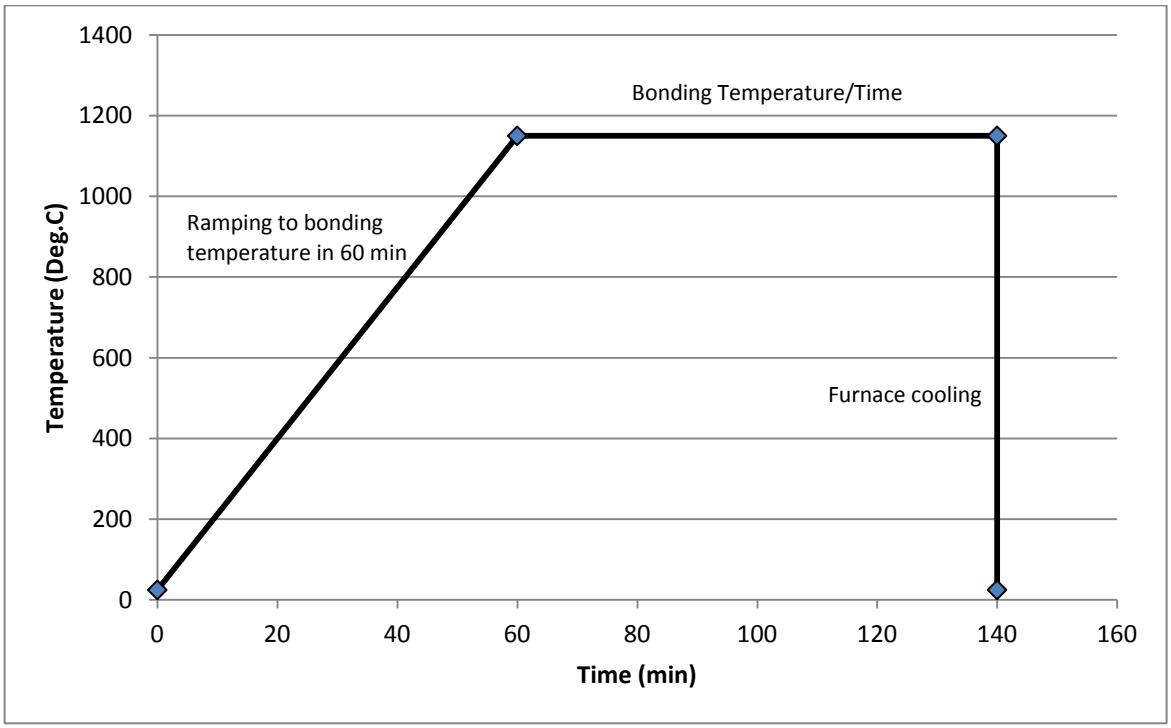

Figure 3.2: Heating cycle used during TLP bonding

4 Results and Discussion

4.1 Microstructural examination of pre-bonded alloys

4.1.1 Microstructure of as received IN738

IN738 has a coarse grain size that ranges from 500 – 800 μm. The grains show well serrated boundaries, as shown in Figure 4.1, which is known to hinder grain boundary sliding and instead promote intragranular deformation [70]. The cast alloy essentially consists of the γ matrix with extensive precipitates of the γ′ intermetallic phase. MC carbides, mainly consisting of Ti (47-50 at.%), Nb (20-27 at.%) and Ta (17-23 at.%), and γ-γ′ eutectics are also present, as shown in Figure 4.2.

4.1.2 Microstructure of as received DS IC 6

The typical microstructure of the as received DS IC6 specimen is shown in Figure 4.3. The back scatter electron image in Figure 4.4 shows three major phases confirmed by the EDS analysis to be γ′, γ, and borides. Area A is the interdendritic area that consists of fine cubic shaped γ′-Ni (Al, Mo), with a chemical composition of 73-74 at.% Ni, 20-21 at.% Al, and 4.9 -5.4 at.% Mo, surrounded by a skeleton of γ and the white particles of boride. Area B is a dendrite arm that consists of large blocky shaped γ′ phase particles surrounded by a two phased (γ′+γ) network similar to that present in Area A.

4.1.3 Microstructure of as received DS Rene 80

The microstructure of the as received DS Rene 80 is shown in Figure 4.5, which depicts the solidification direction of the alloy. The as received alloy mainly consists of

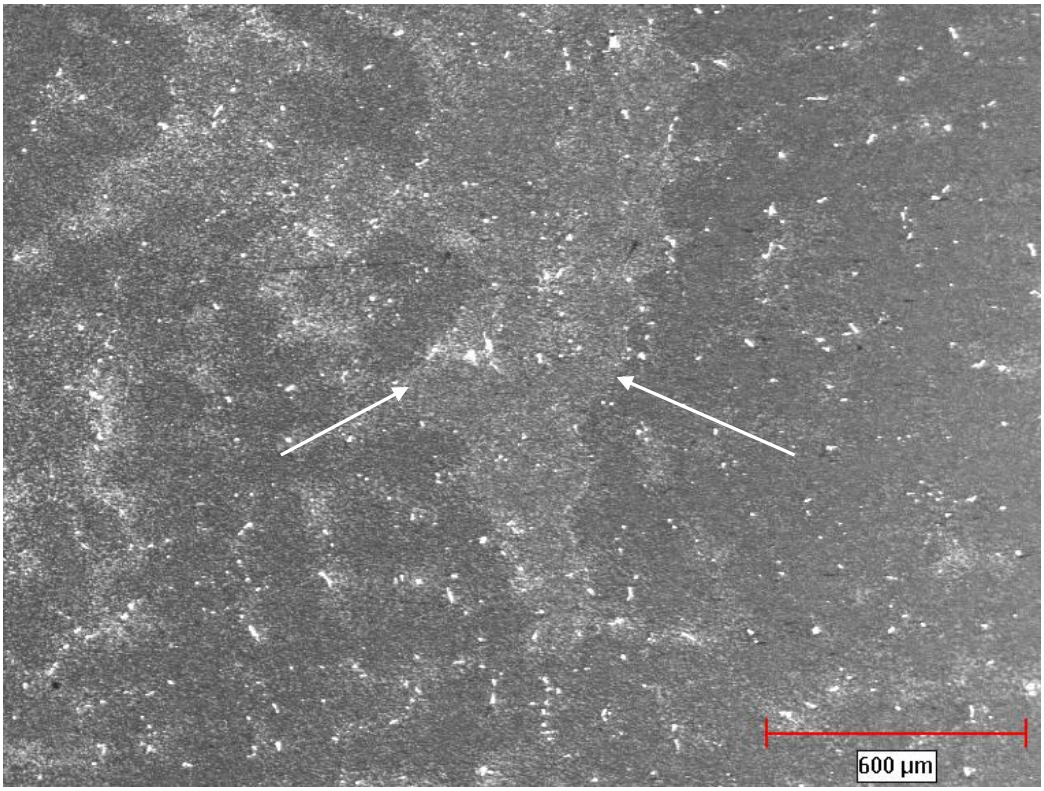

Figure 4.1: Optical micrograph showing serrated grain boundary in as cast IN738

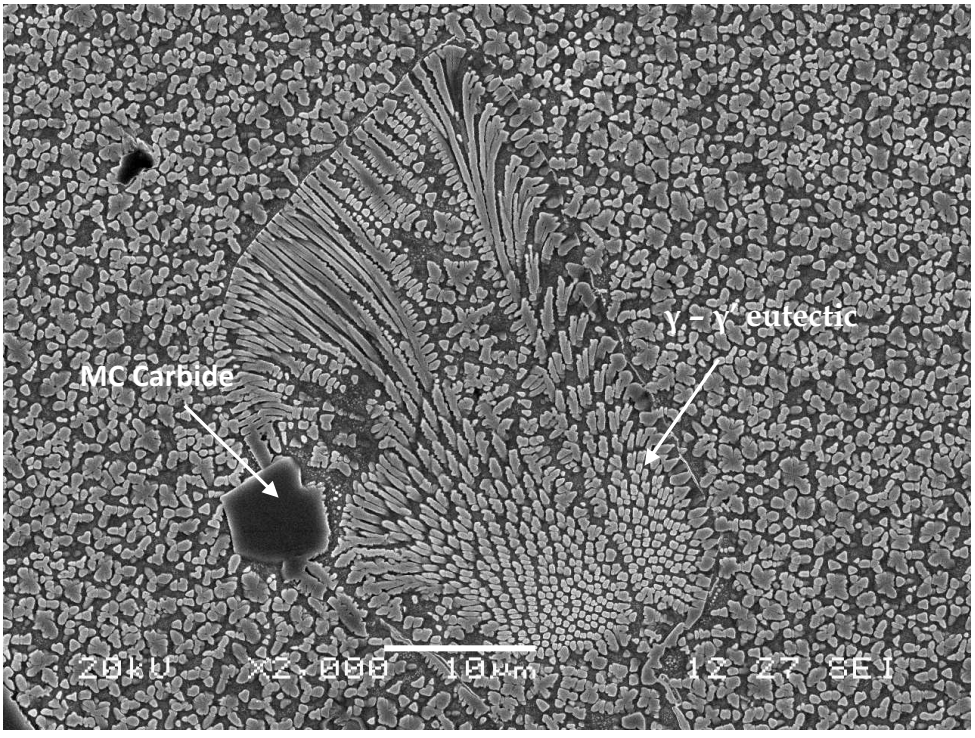

Figure 4.2: SEM micrograph of γ-γ' eutectic island and MC carbide in as cast IN738

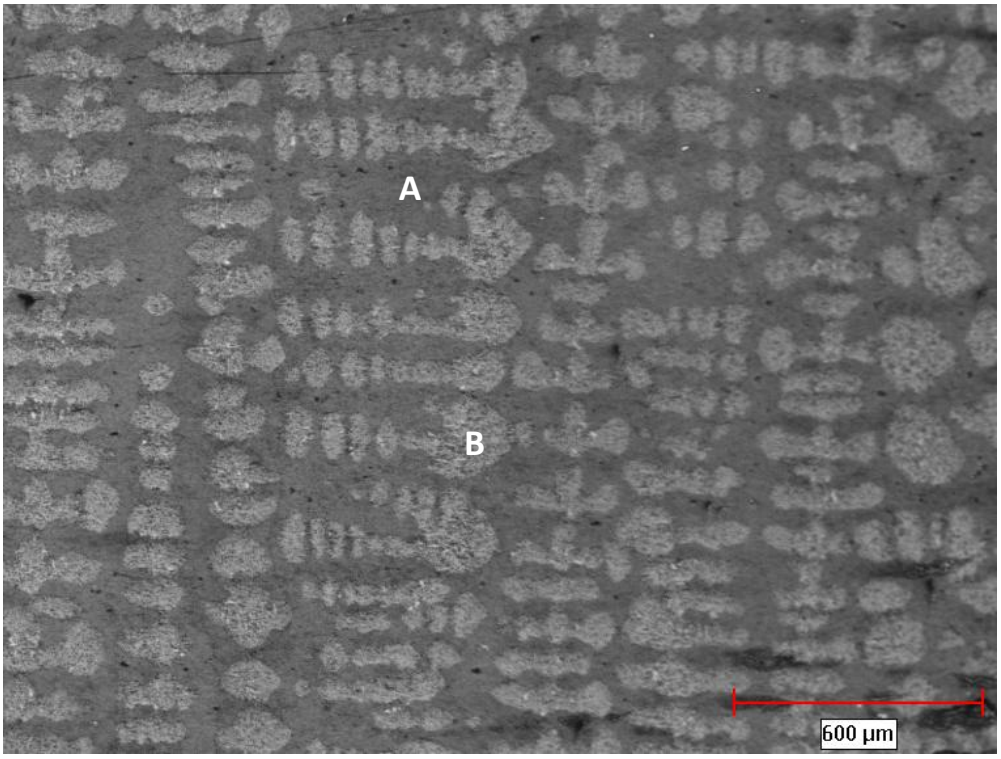

Figure 4.3: Optical micrograph showing interdendritic (A) and dendritic (B) microstructure in as received DS IC6 alloy

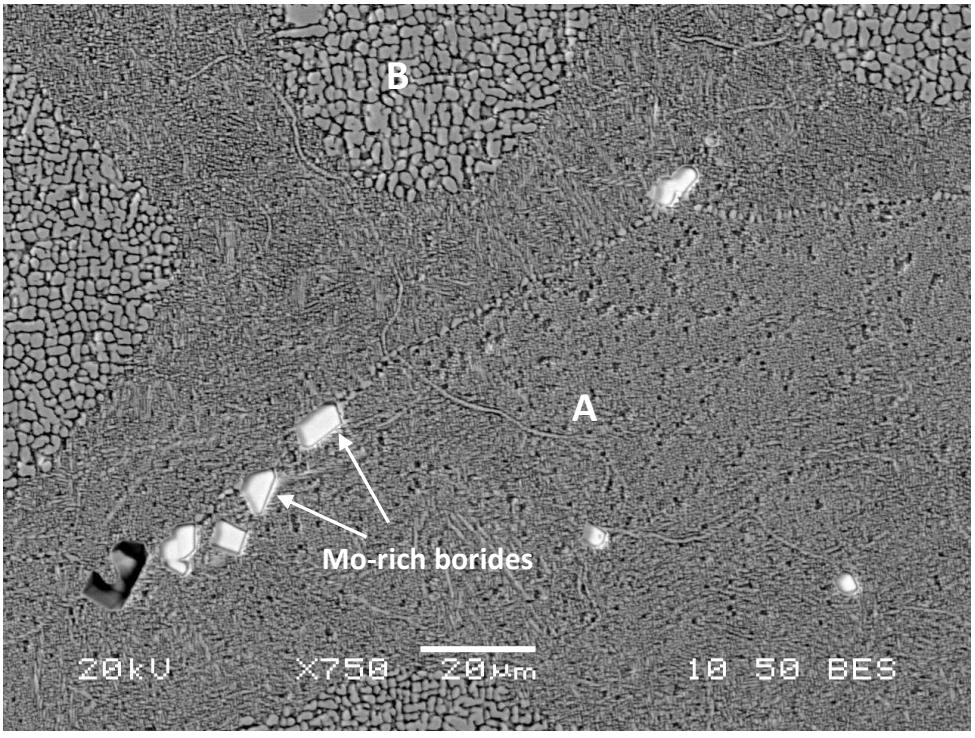

Figure 4.4: SEM micrograph showing Mo-rich borides in the interdendritic area (A) in the as received DS IC6 alloy

secondary γ' particles and MC-type carbides surrounded by the γ phase (Figure 4.6). The SEM EDS analysis of the MC-type carbides shows that the main metallic constituent in most of the carbides is Ti (70-75 at.%) , as well as smaller amounts of Mo (12-15 at.%) and W (6-7.5 at.%). Additionally, many incipiently melted regions were observed in the microstructure (Figure 4.7). Chemical analysis of different phases in these incipiently melted regions by SEM EDS indicates the presence of Cr-Mo-rich borides (Cr 36.4 at.%, Mo 37.7 at.%), and rod-shaped sulfocarbides rich in Ti, Zr and S.

4.2 Microstructural observation of post-bonded alloys

4.2.1 Microstructure of TLP bonded alloys at 1100°C

IN 738 alloy coupons were TLP bonded in vacuum for various holding times that ranged from 30 to 240 min by using an 80 μm thick foil of MBF-80 filler sandwiched between two coupons, at a temperature of 1100°C. The microstructure of a section of the bonded sample after 60 min of holding time is shown in Figure 4.8. It can be seen that the microstructure consists of a centerline eutectic as well as an isothermally solidified pro-eutectic region on either side, bordered with second phase precipitates at the joint-base metal interface. As suggested by the EDS semi-quantitative compositional analysis (Table 4.1), the centerline eutectic is found to consist of Ni-rich and Cr-rich boride phases (presence of B was detected in these phases, but it is not possible to quantify B as a result of the limitation of the EDS analytical software in quantifying light elements

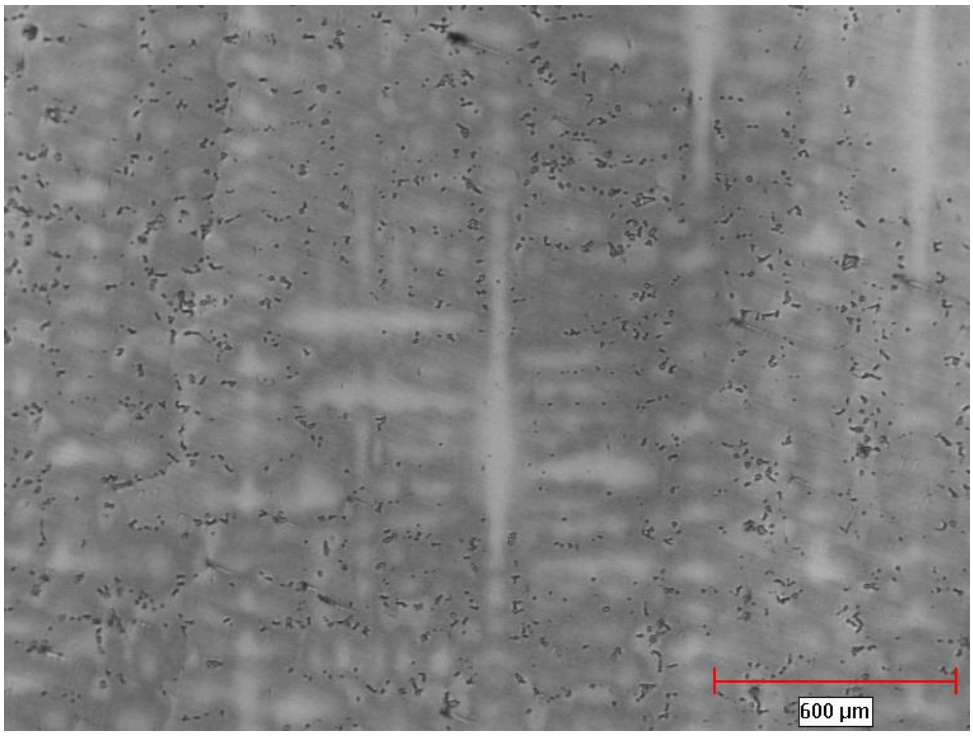

Figure 4.5: Optical micrograph showing direction of solidification in as received DS Rene80

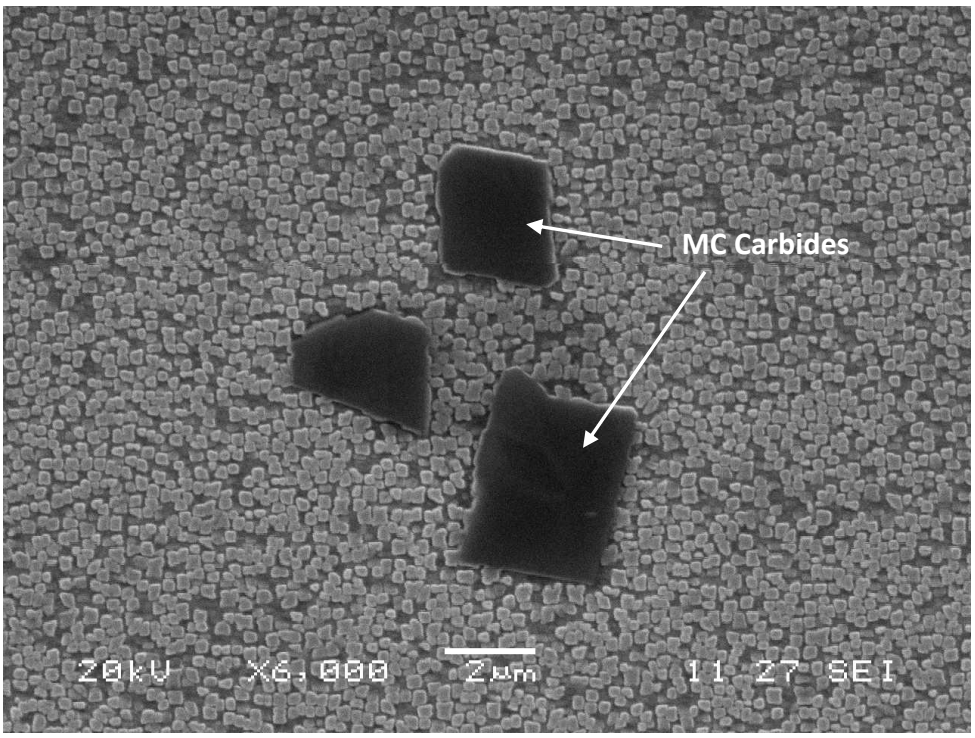

Figure 4.6: SEM micrograph showing secondary γ' and MC carbides in the microstructure of as received DS Rene80

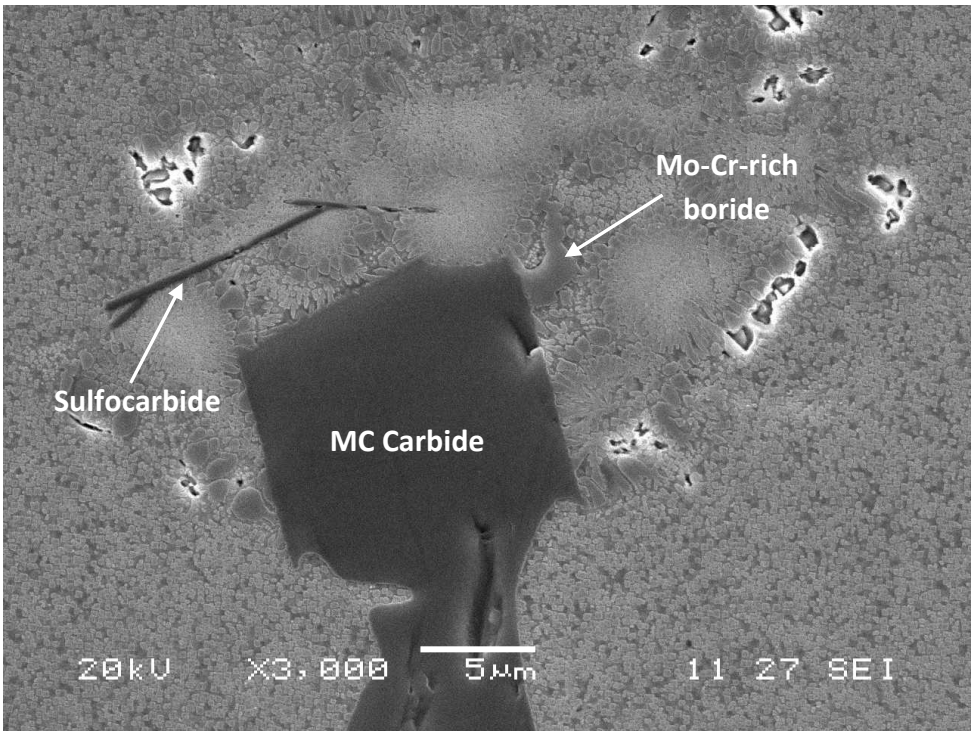

Figure 4.7: SEM micrograph showing an incipiently melted region in the microstructure of as received DS Rene80

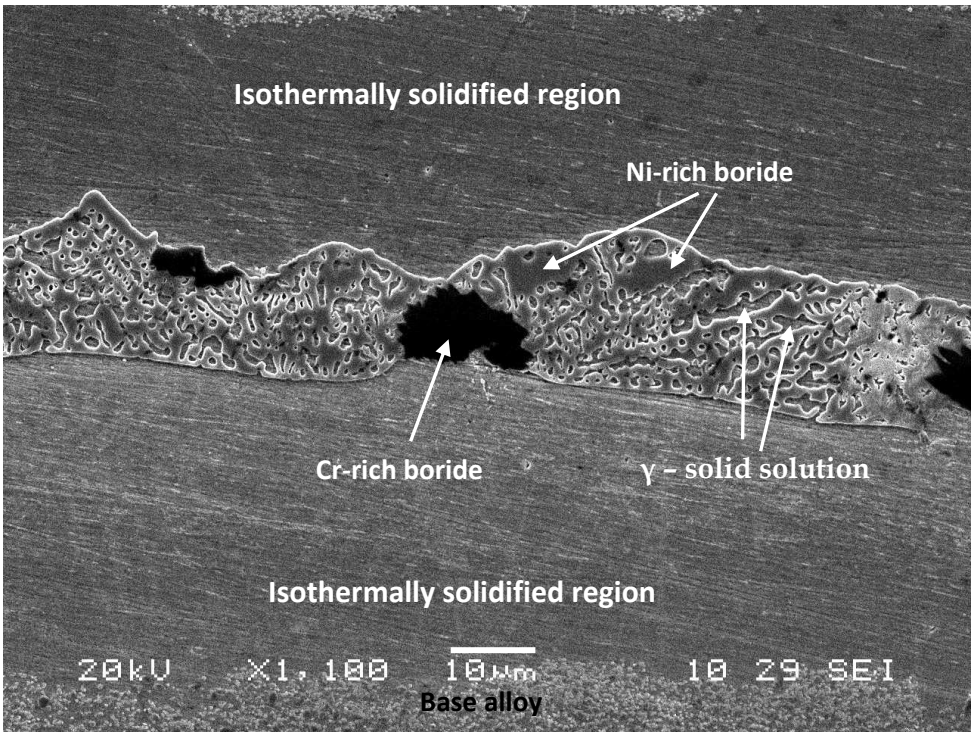

Figure 4.8: SEM microstructure of centerline eutectic for a joint in alloy IN738 bonded at 1100 °C for 1hr using NB150 filler alloy

Table 4.1: Composition of metallic constituents of centerline eutectic for a joint in alloy IN738 bonded at 1100 ^{o}C for 1hr using NB150 filler alloy

Element	Nickel rich boride phase (at.%)	Chromium rich boride phase (at.%)	γ –solid solution phase (at.%)
Al	0.8	-	1.8
Ti	5.4	0.8	0.9
Cr	8.7	90.1	18.4
Co	3.0	0.2	2.3
Ni	80.0	2.7	75.2
Nb	1.1	-	-
Ta	1.0	-	0.5
W	0.3	1.2	0.9
Mo	-	4.9	-

with an atomic number less than 10 [47]), as well as a third phase identified to be an Ni-base γ-solid solution phase. Previous research on diffusion brazing [2, 71], has shown that these phases are formed during the athermal solidification of the residual liquid interlayer as a result of incomplete isothermal solidification at the bonding temperature. Figure 4.8 also shows an isothermally solidified pro-eutectic region on either side of the centerline eutectic. The EDS compositional analysis reveals that this region has a composition similar to that of the Ni-base γ-solid solution phase present in the eutectic centerline. This pro-eutectic region is formed by interdiffusion induced compositional changes, which result in the isothermal solidification of the liquid insert.

Similar to alloy IN738, the coupons of alloys DS IC6 and DS Rene80 were also TLP bonded at 1100^{o}C for holding times that varied between 30 and 240 min by using an 80 μm thick foil of MBF-80 filler alloy. The microstructures of a section of the bonded sample, for both DS IC6 and DS Rene80, after 60 min of holding time, are shown in Figures 4.9 and 4.10 respectively. The SEM EDS compositional analysis of the centerline eutectic of both alloys (Tables 4.2 and 4.3) suggests that it consists of Cr-rich and Ni-rich borides, as well as a γ-solid solution similar to the isothermally solidified region.

Since the centerline eutectic represents the liquid that remains prior to athermal solidification at the end of each holding time, the width of the centerline eutectic (liquid remaining) was found to constantly decrease with increases in holding time (Figure 4.11), such that, complete isothermal solidification of the joints was achieved within 240 min at a temperature of 1100^{o}C. All three alloys showed comparable behaviour in terms

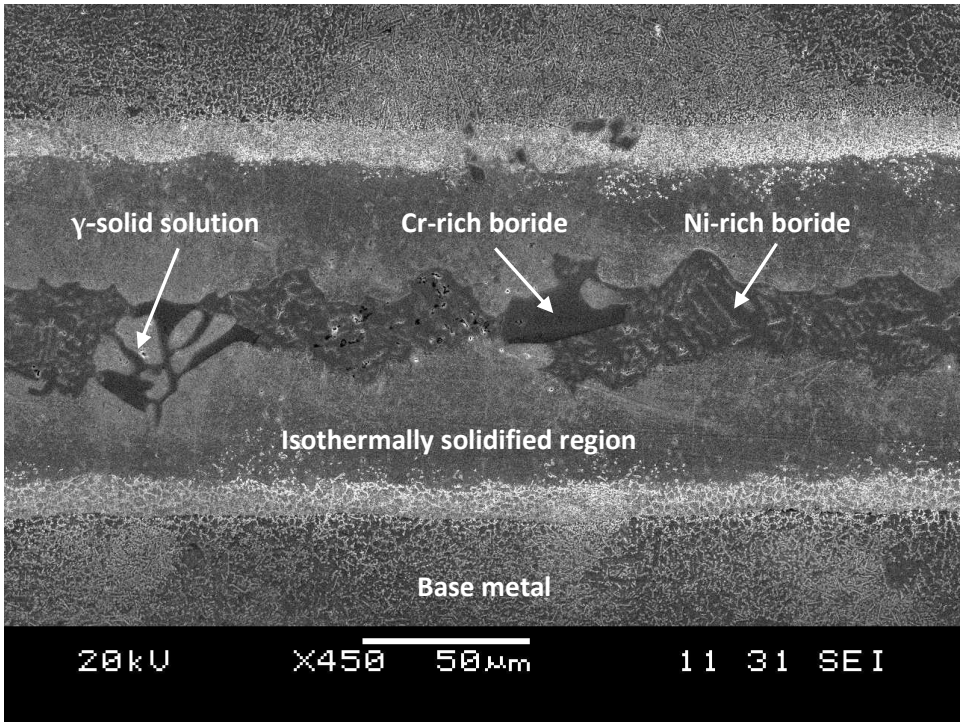

Figure 4.9: SEM microstructure of centerline eutectic for a joint in alloy DS IC6 bonded at 1100 °C for 1hr using NB150 filler alloy

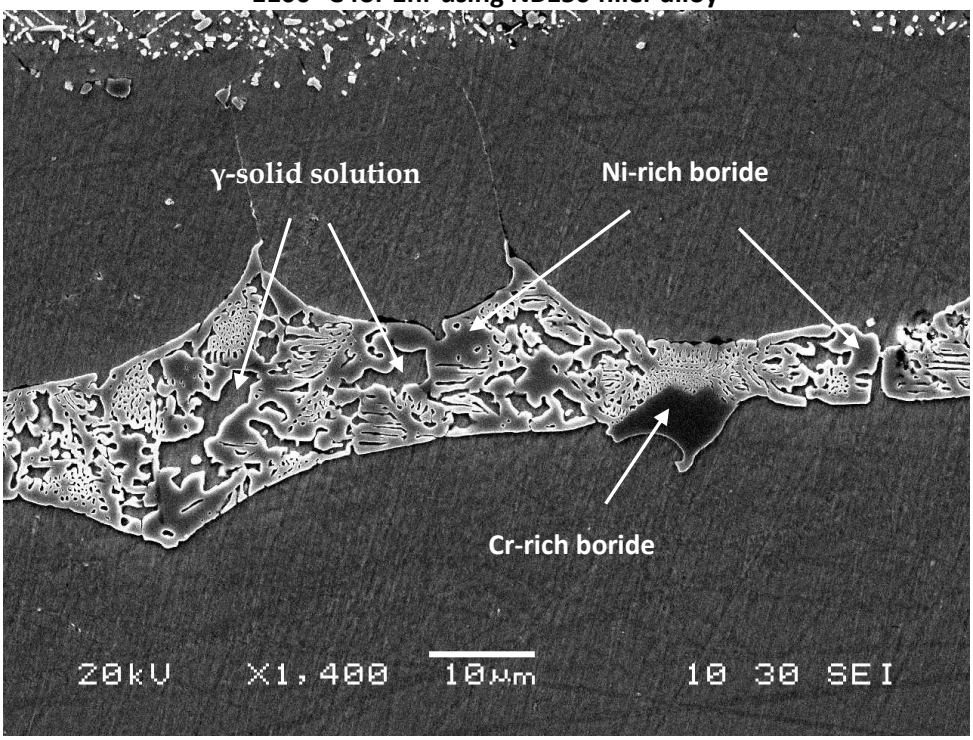

Figure 4.10: SEM microstructure of centerline eutectic for a joint in alloy DS Rene80 bonded at 1100 °C for 1hr using NB150 filler alloy

Table 4.2: Composition of metallic constituents of centerline eutectic for a joint in alloy DS IC6 bonded at 1100 °C for 1hr using NB150 filler alloy

Element	Nickel rich boride phase (at.%)	Chromium rich boride phase (at.%)	γ –solid solution phase (at.%)
Al	2.8	-	5.9
Cr	10.0	61.8	12.3
Mo	1.1	18.0	1.3
Ni	86.1	20.2	80.5

Table 4.3: Composition of metallic constituents of centerline eutectic for a joint in alloy DS Rene80 bonded at 1100 °C for 1hr using NB150 filler alloy

Element	Nickel rich boride phase (at.%)	Chromium rich boride phase (at.%)	γ –solid solution phase (at.%)
Al	1.8	-	1.2
Ti	5.8	1.0	2.3
Cr	7.3	65.7	16.9
Co	3.1	2.3	3.2
Ni	81.5	15.7	74.8
Nb	-	-	0.1
W	0.1	2.4	0.4
Mo	0.4	12.8	1.2

of the rate of isothermal solidification at this temperature and followed the parabolic pattern for the advance of the liquid/solid interface predicted by analytical models [45]. This behaviour is somewhat expected since all three alloys are Ni-base alloys and expected to have comparable solid-state diffusion rates (diffusivity) of B into the base metal substrate.

4.2.2 Microstructure of TLP bonded alloys at 1150°C

A butt-joint configuration (200 μm wide) of IN 738, DS IC6, and DS Rene80 alloys were TLP bonded in vacuum for various holding times that ranged from 1 to 52 hrs by using a filler alloy powder of Nicrobraz150 at a temperature of 1150°C. The microstructure of a section of the bonded sample of IN738 after 1 hr of holding time is shown in Figure 4.12. It can be seen that the microstructure consists of a centerline eutectic as well as an isothermally solidified pro-eutectic region on either side, bordered with second phase precipitates at the joint-base metal interface. This is similar to what was observed in the microstructure of joints bonded at 1100°C. The microstructure of the centerline eutectic found in the joints of DS IC6 and DS Rene80 after 1 hr is analogous to that found in alloy IN738, as shown in Figures 4.13 and 4.14. The SEM EDS compositional analyses of the components of the centerline eutectic for joints made with IN738, DS IC6 and DS Rene80, after 1 hr at 1150°C are listed in Tables 4.4, 4.5 and 4.6 respectively.

Similar to the observation made at 1100°C, the eutectic thickness in all three alloys continued to be comparable up to 7.5 hrs of holding time. Again, this is the expected outcome when taking into consideration that the three alloys studied are all Ni-base

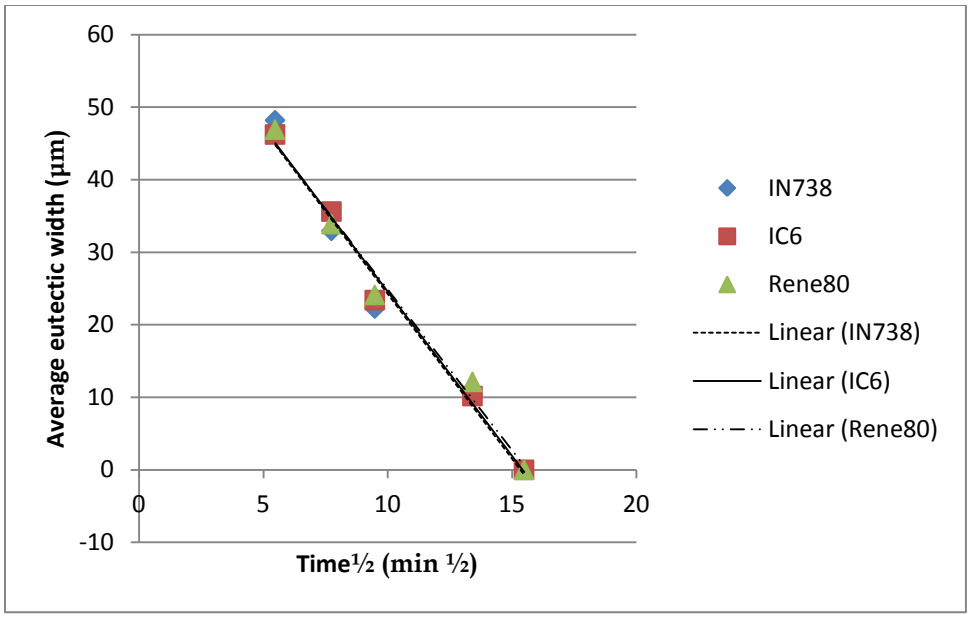

Figure 4.11: Plot of average eutectic width vs. square root of time for alloys IN738, DS IC6, and DS Rene80 bonded at 1100 °C

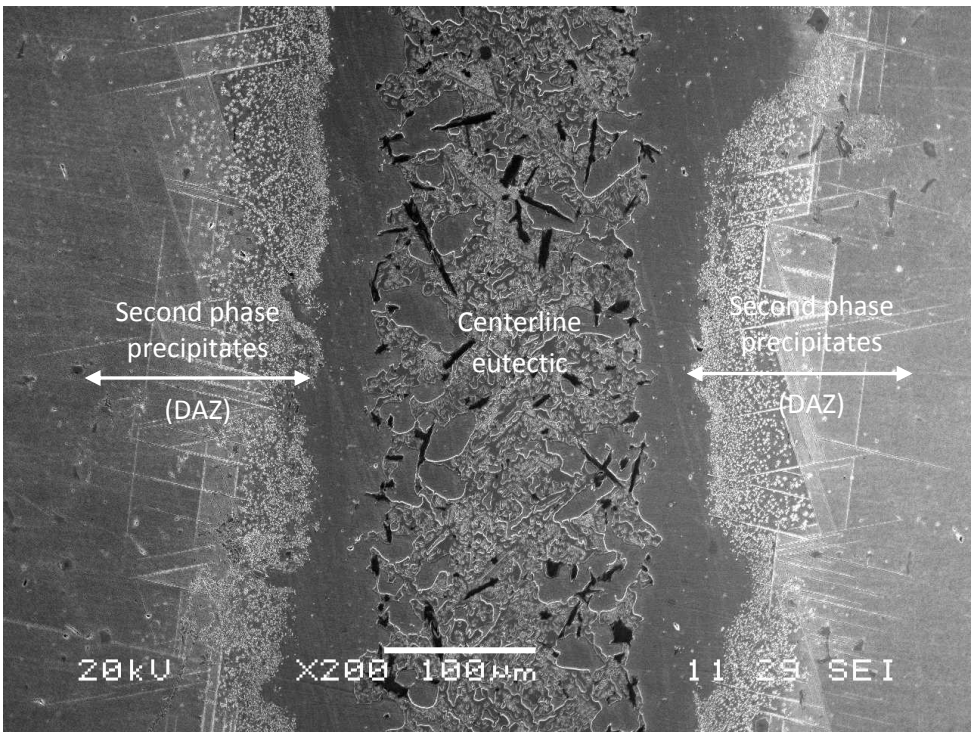

Figure 4.12: SEM microstructure of centerline eutectic for a joint in alloy IN738 bonded at 1150 °C for 1hr using NB150 filler alloy

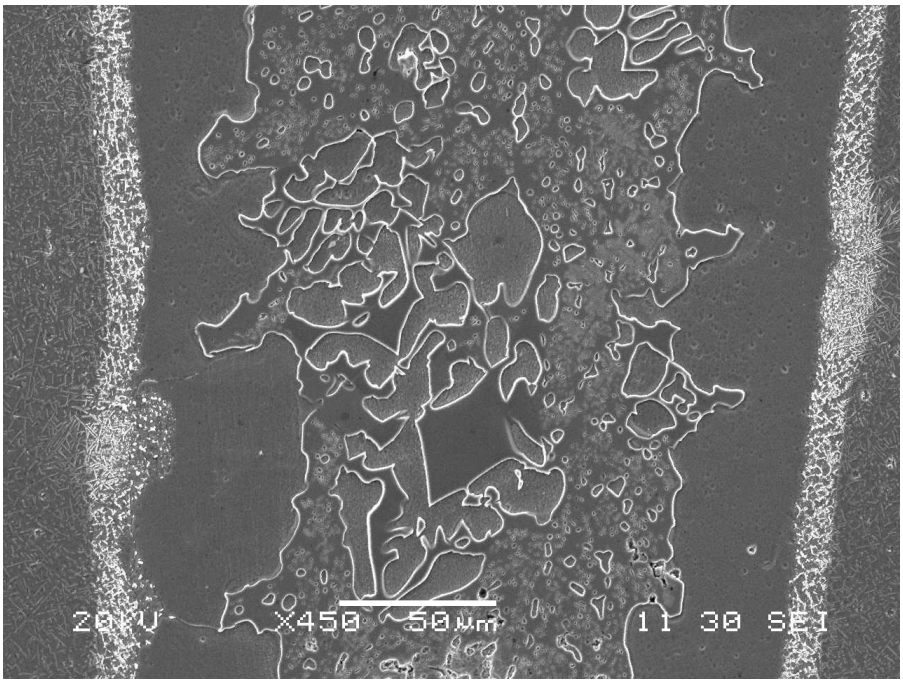

Figure 4.13: SEM microstructure of centerline eutectic for a joint in alloy DS IC6 bonded at 1500 °C for 1hr using NB150 filler alloy

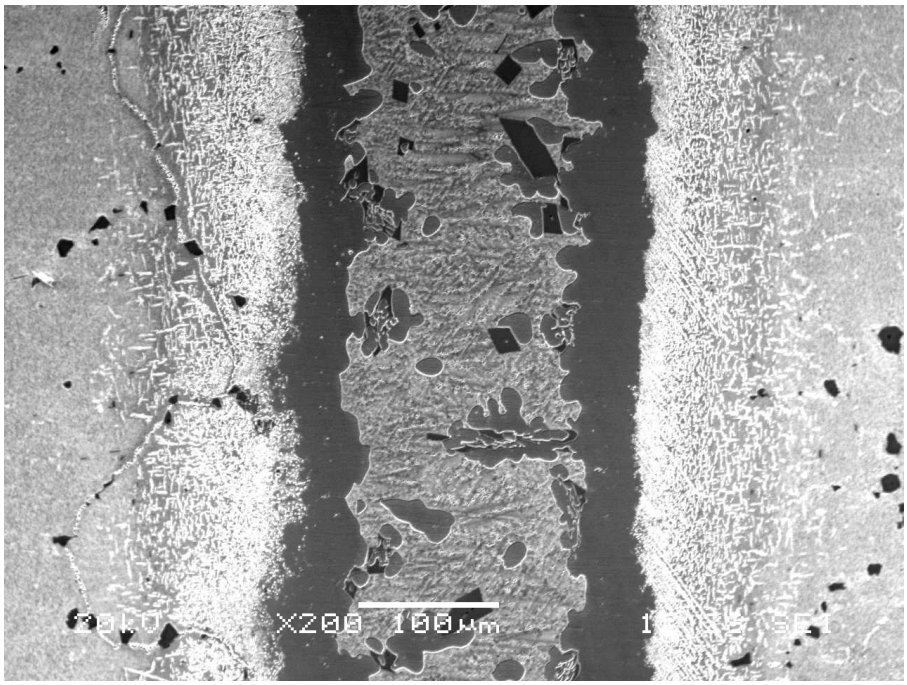

Figure 4.14: SEM microstructure of centerline eutectic for a joint in alloy DS Rene80 bonded at 1500 °C for 1hr using NB150 filler alloy

Table 4.4: Composition of metallic constituents of centerline eutectic for a joint in alloy IN738 bonded at 1150 ^{o}C for 1hr using NB150 filler alloy

Element	Nickel rich boride phase (at.%)	Chromium rich boride phase (at.%)	γ –solid solution phase (at.%)
Al	1.6	-	3.8
Ti	3.7	0.8	1.3
Cr	10.6	84.9	16.9
Co	3.4	0.4	3.3
Ni	79.1	6.2	73.9
Nb	0.5	-	-
Ta	0.7	-	0.4
W	0.3	3.0	0.4
Mo	-	4.7	-

Table 4.5: Composition of metallic constituents of centerline eutectic for a joint in alloy DS IC6 bonded at 1150 ^{o}C for 1hr using NB150 filler alloy

Element	Nickel rich boride phase (at.%)	Chromium rich boride phase (at.%)	γ –solid solution phase (at.%)
Al	3.4	-	6.6
Cr	10.4	55.0	12.4
Mo	1.2	30.1	1.4
Ni	84.7	14.8	79.5

Table 4.6: Composition of metallic constituents of centerline eutectic for a joint in alloy DS Rene80 bonded at 1150 °C for 1hr using NB150 filler alloy

Element	Nickel rich boride phase (at.%)	Chromium rich boride phase (at.%)	γ –solid solution phase (at.%)
Al	1.6	-	3.1
Ti	4.5	2.1	1.9
Cr	11.8	56.5	17.0
Co	3.8	2.4	3.9
Ni	77.7	28.7	72.9
Nb	-	-	0.1
W	0.2	2.7	0.6
Mo	0.5	7.6	0.7

alloys, and it is reasonable to say that the rate at which the MPD solute (B in this case) will diffuse into the base alloy is comparable. However, beyond the 7.5 hr holding period, the comparability in eutectic thickness between the three alloys appears to cease. Figure 4.15 shows the residual liquid (centerline eutectic) in the joints of all three alloys after 12 hrs. It is clear that the average eutectic width for the IN738 alloy is larger than that for the DS Rene80 and DS IC6 alloys. With further increase in the holding time to 16 hrs, alloy DS IC6 shows evidence of a joint with complete isothermal solidification, while alloy IN738 joint continues to show a centerline eutectic as evidence of incomplete isothermal solidification (Figure 4.16). For a joint fabricated by TLP bonding to be of sound quality, complete isothermal solidification of the joint must take place by diffusing the MPD solute out of the joint and gradually reducing the liquid interlayer until it completely disappears. Evidence of residual liquid in the joint in the form of a centerline eutectic indicates the need for an extended holding time to allow for further diffusion of the MPD solute. Thus, the departure from comparability in eutectic thickness experienced by IN738, points to the need for a longer holding time t_f to achieve complete isothermal solidification. As such, a longer processing time is needed to achieve a reliable joint in alloy IN738 as compared to alloy IC6. An experiment showed that even after 52 hrs of holding time, the IN738 joint was still showing evidence of discrete eutectic constituents. Alloy Rene80 also experienced some departure from comparability in eutectic thickness, as it needed 26 hrs of holding time to produce a joint with complete isothermal solidification compared to alloy IC6 which

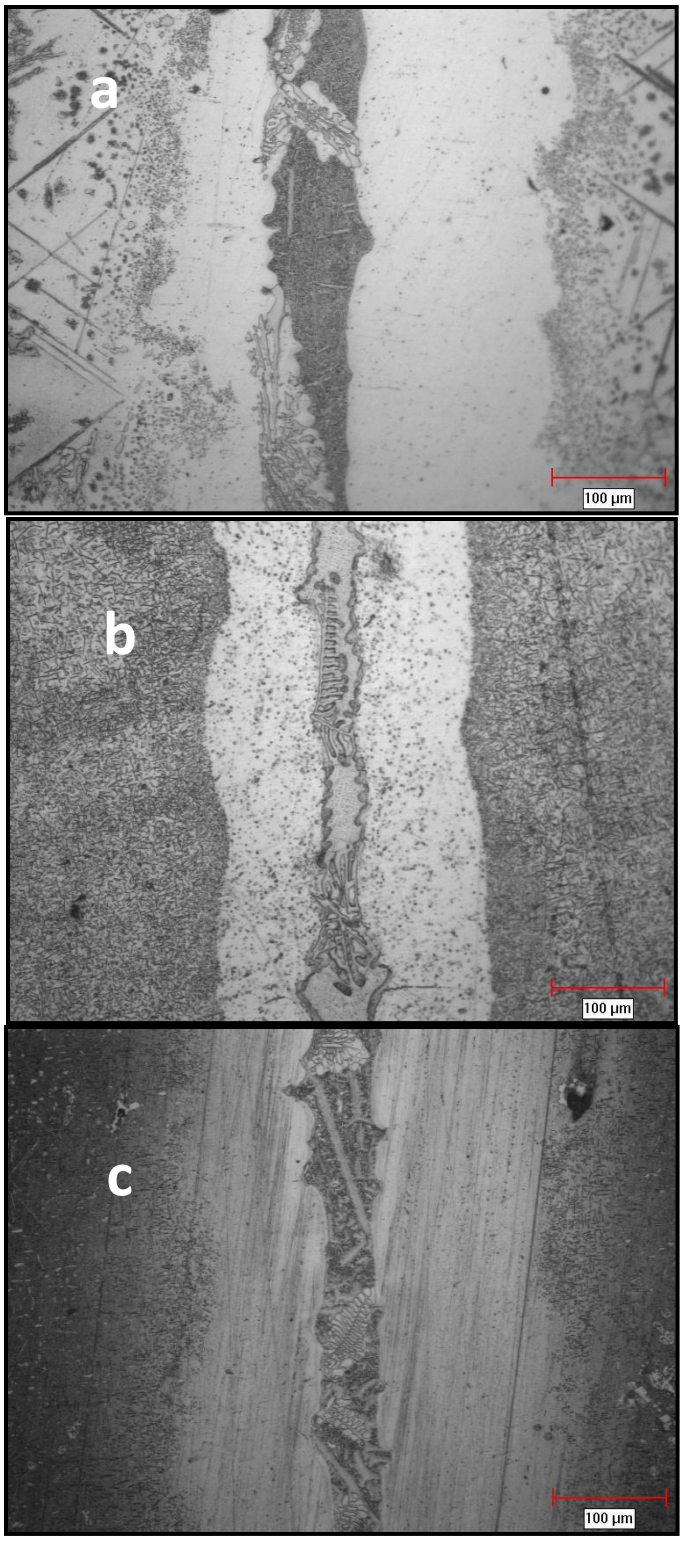

Figure 4.15: SEM micrograph of centerline eutectic for a joint in alloy (a) IN738, (b) DS IC6, and (c) DS Rene80, bonded at 1150 ^{o}C for 12hrs using NB150 filler alloy

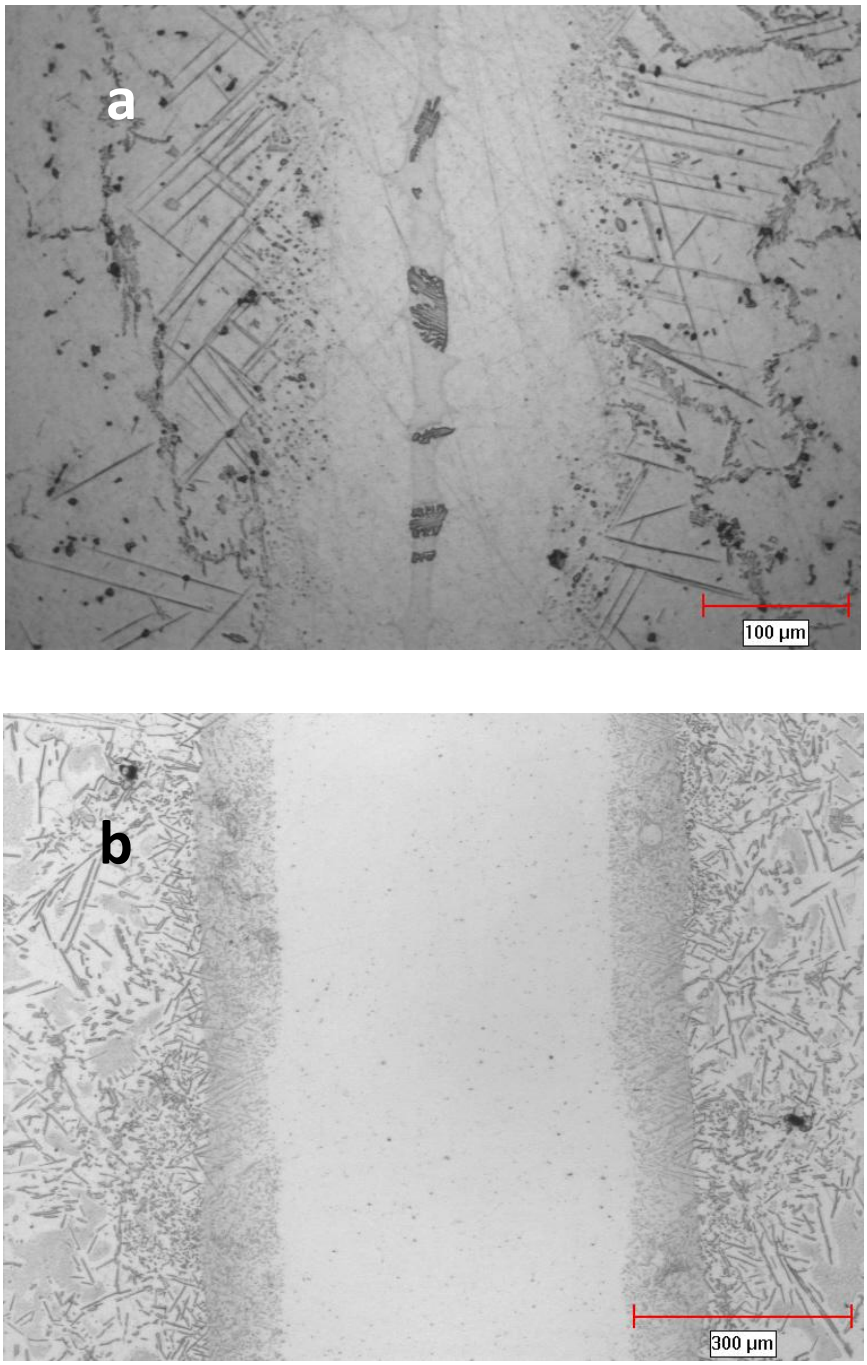

Figure 4.16: SEM micrograph of a joint in alloy (a) IN738 and (b) DS IC6, bonded at 1150 ^{o}C for 16hrs using NB150 filler alloy

needed 16 hrs. However, the extension in t_f required by alloy Rene80 is far less than that required by alloy IN738.

A plot of the average eutectic width against square root of holding time for the three studied alloys at 1150^{o}C is presented in Figure 4.17. It shows a linear relationship up to a holding time of 7.5 hrs, beyond which significant deviation from linearity occurs for alloy IN738, while DS IC6 retains a linear relationship to the end of the isothermal solidification, and DS Rene80 suffers from some deviation towards the end. The relationship between the average eutectic width and the square root of time is predicted by standard analytical models to be of a parabolic nature (linear relationship). Moreover, although deviation from parabolic behaviour has been reported to occur in Ni-base superalloys, it is rather unexpected to see alloys with the same base constituent (Ni in this case) to behave in a different fashion when bonded under the same conditions (temperature, time, and brazing filler alloy), such that an alloy like DS IC6 maintains a constant behaviour until a eutectic-free joint is achieved, while another alloy, such as IN738, significantly deviates from the parabolic behaviour and consequentially suffers an extension in t_f. The difference in the behaviour of the three studied alloys when bonded at 1150^{o}C is especially unexpected in view of the fact that these same alloys had shown comparable behaviour when bonded at a temperature of 1100^{o}C (Figure 4.11). It is well recognised that the diffusivity of the MPD solute into the base-metal substrate is the main factor that controls the rate of isothermal solidification, and thus, the t_f required to achieve a eutectic-free joint. Hence, the comparable behaviour shown by the three studied alloys when bonded at 1100^{o}C,

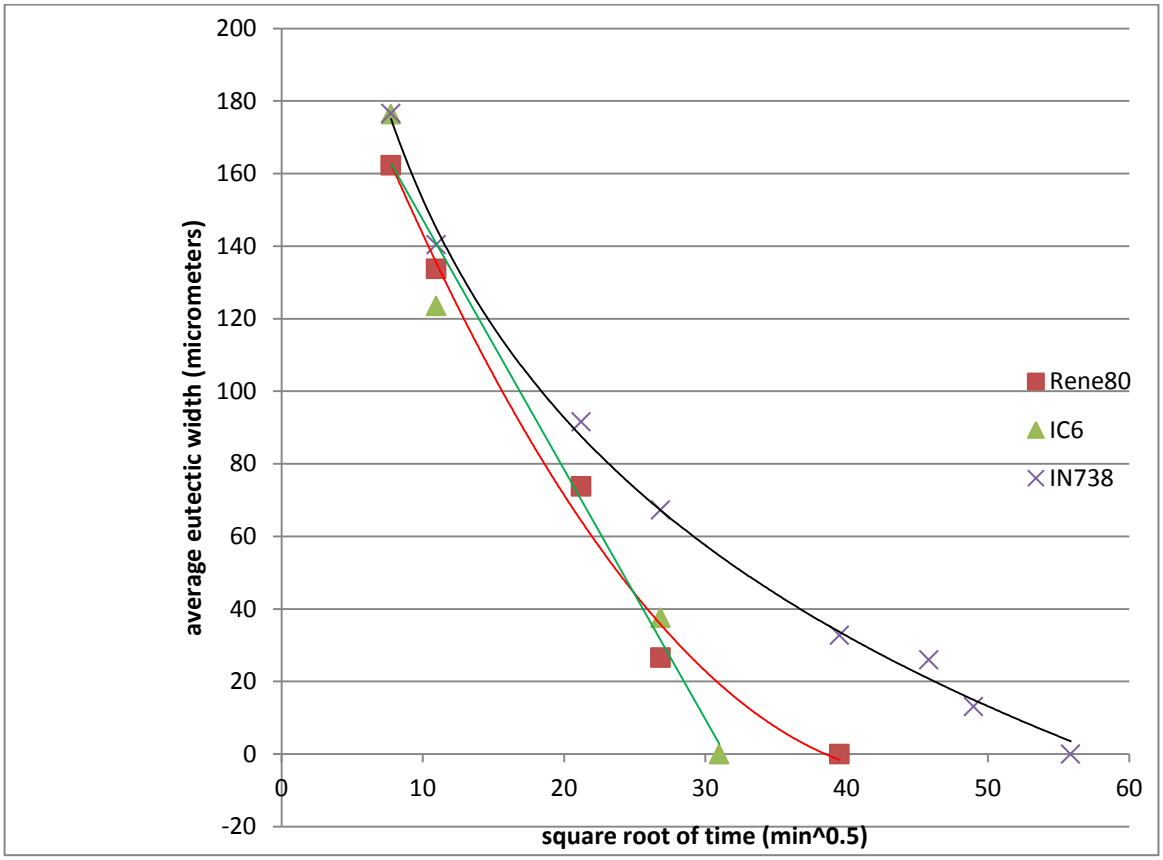

Figure 4.17: : Plot of average eutectic width vs. square root of time for alloys IN738, DS IC6, and DS Rene80 bonded at 1150 ^{o}C

leading to a similar t_f in all three alloys, would suggest that they all have similar diffusivity of MPD solute into the base-alloy substrate. As such, the anomalous difference in the behaviour of the alloys when bonded at a temperature of 1150^{o}C would suggest that another factor other than diffusivity is coming into play at higher bonding temperatures. This factor appears to be overriding the effect of diffusivity at higher bonding temperatures and causing an extension in t_f for some alloys such as IN 738, while aiding in achieving a reasonable t_f for alloys such as DS IC6.

4.2.3 Cause of extension in t_f for alloy IN738 with increase in temperature

Standard analytical TLP bonding models are based on solving Fick's second law of diffusion equation:

$$\frac{\partial C}{\partial t} = D\frac{\partial^2 C}{\partial x^2} \qquad (1)$$

where ∂C/∂t is the change in the solute concentration with time at a given position in the base metal, D is the diffusion coefficient, and $\partial^2 C/\partial x^2$ is the rate of change of the solute concentration gradient (∂C/∂x) with respect to distance (x) [26, 27, 35, 72]. Generally, these standard analytical models make the assumption that during the isothermal solidification stage, diffusion-induced displacement of the solid/liquid interface, h, follows a parabolic law,

$$h = 2\varphi(t^{\frac{1}{2}}) \qquad (2)$$

where t is the holding time and the parameter ϕ indicates the rate of the interface migration. This implies a linear relationship between the residual interlayer liquid thickness and square root of holding time. An inherent assumption in these models is that the base metal is of infinite or semi-infinite thickness; this in turn, permits the use of error function solutions of the Fick's diffusion equation to represent solute distribution in the solid substrate. As such, the advance of the solid-liquid interface is allowed to maintain a parabolic relationship with time during the continual diffusion of the MPD solute into the base metal, even though its concentration gradient in the solid is constantly reducing. Based on this approach, it was previously found that predicted holding times required to achieve complete isothermal solidification agreed reasonably well with experimentally determined values for different alloy systems, including Ni-base alloys. However, recent studies [27, 42, 61, 73, 74, 75] have shown that deviation from this parabolic rule can occur with increases in bonding temperature, with the consequence of an increase in the isothermal solidification time t_f. This behaviour is considered rather anomalous since it is generally perceived that an increase in bonding temperature would reduce the time required to achieve complete isothermal solidification. This is premised on the increased isothermal solidification rate due to higher diffusivity with increased temperature. Several suggestions have been made in the literature for the cause of this anomalous behaviour, namely:

- formation of second phase particles within the base metal at the joint-substrate interface are claimed to slow down the diffusion of the solute elements, and

thus, the solidification process. This can lead to an elongation in the time required to produce a eutectic-free joint [42],

- increase in liquated volume of the filler insert caused by increased base metal dissolution with increases in bonding temperature would seemingly require a longer holding time for complete isothermal solidification [74],

- existence of more than one MPD solute in the filler alloy with one having a slower diffusivity, and thus, slowing down the solidification process and prolonging the holding time [73], and

- decrease in the solubility of the MPD solute into the base metal with increases in the bonding temperature, thus causing a reduction in the rate of isothermal solidification [27].

Experimental observations made by Ramirez and Liu [43] show that the precipitation of second phase particles is considerably reduced with increased bonding temperature. Moreover, the occurrence of the anomalous behaviour in systems that do not form interfacial precipitates cannot be attributed to the formation of second phase particles.

Likewise, attributing this anomalous behaviour to the presence of a second MPD solute in the filler alloy is not reasonable, since its occurrence has been reported in systems that exclusively contain one MPD solute [43].

At first glance, an increase in the liquated volume of the filler insert as a result of base metal 'melt-back' with increase in bonding temperature may appear to be a rational

explanation for deviation from the parabolic rule. As explained by Abdelfatah and Ojo [76], if the effect of reduced solubility with increase in temperature is to be excluded, an increase in liquid size at higher temperatures cannot account for deviation from the parabolic rule, thus causing an increase in holding time. This is because an increase in the bonding temperature is accompanied with an increase in the rate of solute diffusion that would overcome the effect of the increased liquid size and eventually lead to a reduced holding time as compared to a lower temperature.

To investigate the role of a decrease in the MPD solute solubility with increase in temperature towards deviation from the parabolic rule, analytical modeling of TLP bonding was performed while keeping the maximum width of the liquid interlayer constant [77]. While the results of the simulation show that indeed, with an increase in temperature, there exists a critical temperature, T_c, beyond which, a decrease in solute solubility will cause deviation from the parabolic rule and lead to the extension of t_f. However, the analytically predicted T_c was found to be excessively higher than what had been experimentally observed [61].

Recent studies [77, 78] that applied newly developed numerical simulation models to TLP process have shown that the inherent assumption made by analytical models, and by which, a parabolic relationship between holding time and solid/liquid interface migration is maintained with continual diffusion, can only hold while the concentration gradient, $\partial C/\partial x$, decreases to a critical level $(\partial C/\partial x)_c$. Beyond this critical level, any

diffusion-induced decrease in ∂C/∂x would result in considerable deviation from the parabolic rule.

One important consequence of the deviation from parabolic behaviour with increase in temperature is the considerable increase in holding time, t_f, required to produce a eutectic free TLP joint. In the present investigation, while the three alloys studied (IN738, DS IC6, and DS Rene80) show comparable behaviour and follow the parabolic rule predicted by standard analytical models when bonded at 1100^{o}C; however, this is not the case when the bonding temperature is increased to 1150^{o}C. At the start of the bonding process, all three alloys follow the parabolic rule in a comparable fashion (Figure 4.17); however, after 7.5 hrs of holding time, alloy IN738 shows significant deviation. As stated above, a considerable increase in the time required to achieve complete isothermal solidification is the major consequence of deviation from parabolic behaviour at higher temperatures. Notably, while alloy DS IC6 maintained parabolic behaviour throughout the bonding process and a eutectic-free joint was produced after 16 hrs, alloy IN738 which showed significant deviation, required 52 hrs of holding time to produce an almost eutectic-free joint. With less severity than alloy IN738, alloy DS Rene80 also showed deviation from parabolic behaviour towards the end of the solidification, and complete isothermal solidification was achieved after holding for 26 hrs.

As stated above, alloy DS Rene80 showed less deviation than alloy IN738, and hence, required less time to achieve complete isothermal solidification. The onset of deviation

from parabolic behaviour took place at a later stage in alloy DS Rene80 than in alloy IN738 and as such, a narrower deviation zone, and hence, a shorter t_f was observed for alloy DS Rene80.

In applying their newly developed simulation numerical model, Goneim and Ojo [76, 78, 79] explain that at the commencement of deviation, the constant parameter ϕ in Equation (2) becomes unsuitable for representing the isothermal solidification rate because of the continuous reduction in rate within the deviation zone and hence, the size of the zone, which in turn determines that the t_f, is dependent on the magnitude of $\partial c/\partial x$. They further stated that the concentration gradient $\partial C/\partial x$ is influenced by the solubility of the MPD solute into the base metal, such that a decrease in the MPD solute (B) would result in a wider deviation zone and concomitant increase in the t_f due to a reduced $\partial C/\partial x$.

The above discussion demonstrates why alloy IN738 has an extension in t_f upon increase in bonding temperature. The next valid query would be to determine why alloy DS IC6 did not suffer the same anomalous behaviour as alloy IN738. This is especially interesting in light of the fact that all three alloys behave in a similar parabolic fashion, with complete isothermal solidification achieved in a comparable time frame when bonded at a lower temperature of 1100^{o}C.

4.2.4 Diffusion affected zone

Based on the above discussion, it is inferred that any increase in the solubility of the diffusing solute into the base metal would increase $\partial^2 C/\partial x^2$ and hence, result in a higher

rate of diffusion-controlled isothermal solidification. Similarly, any method or mechanism that can enhance the base metal accommodation capability of the diffusing MPD solute, such that ∂C/∂x will not exceed a critical level, can aid in increasing the rate of isothermal solidification, and thus, prevent or minimise an increase in the t_f with an increase in temperature. The formation of solute-rich second-phase precipitates within the base metal region adjacent to the joint has been reported to be a favourable mechanism for the depletion of a substrate matrix of solute atoms and by which, an increase in the rate of isothermal solidification was observed [80]. In the current work, such second-phase particles are noticed to be considerably more pronounced in alloys DS IC6 and DS Rene80 compared to IN738 (Figure 4.18).

Figure 4.19 shows the DAZ in the base metal adjacent to the joint region in alloys IN 738 and DS IC6 bonded for 12 hrs at a temperature of 1150^{o}C, where IN 738 shows considerable deviation from parabolic behaviour compared to alloy DS IC6.

The Zeiss Axiovert 25 inverted reflected-light optical microscope equipped with a CLEMEX vision 3.0 image analyzer was used to determine the volume fraction of the second-phase precipitates formed in the DAZ of the bonded specimens, and the volume fraction of these precipitates for alloys IN 738 and DS IC6 was found to be 8% and 20% respectively.

As alloys DS IC 6 and IN 738 represent both ends of the spectrum where no deviation and significant deviation from parabolic behaviour occurs respectively at a bonding temperature of 1150^{o}C, a microstructural study of the second-phase precipitates

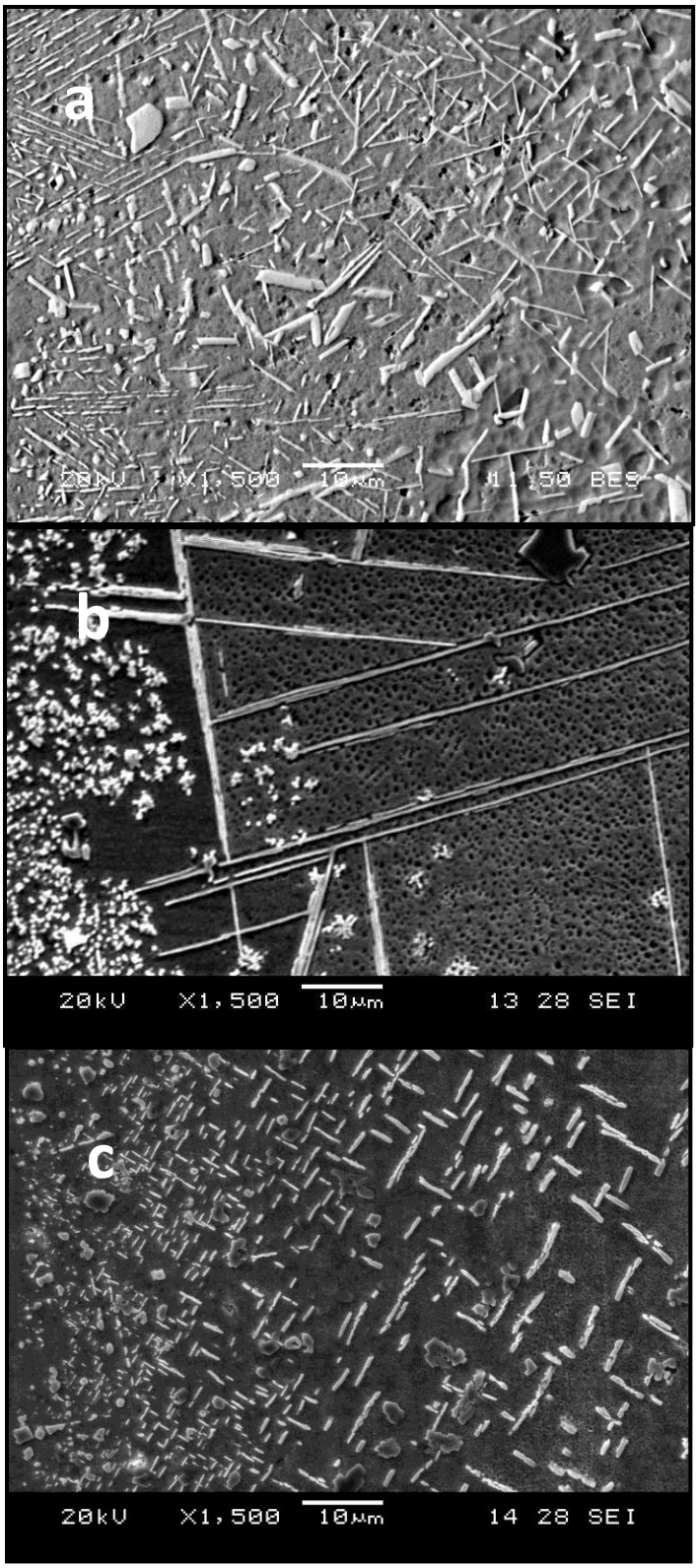

Figure 4.18: SEM micrograph of second phase precipitates in DAZ of (a) DS IC6. , (b) IN738, and (c) DS Rene80, bonded at 1150 °C for 12 hrs using NB150 filler alloy

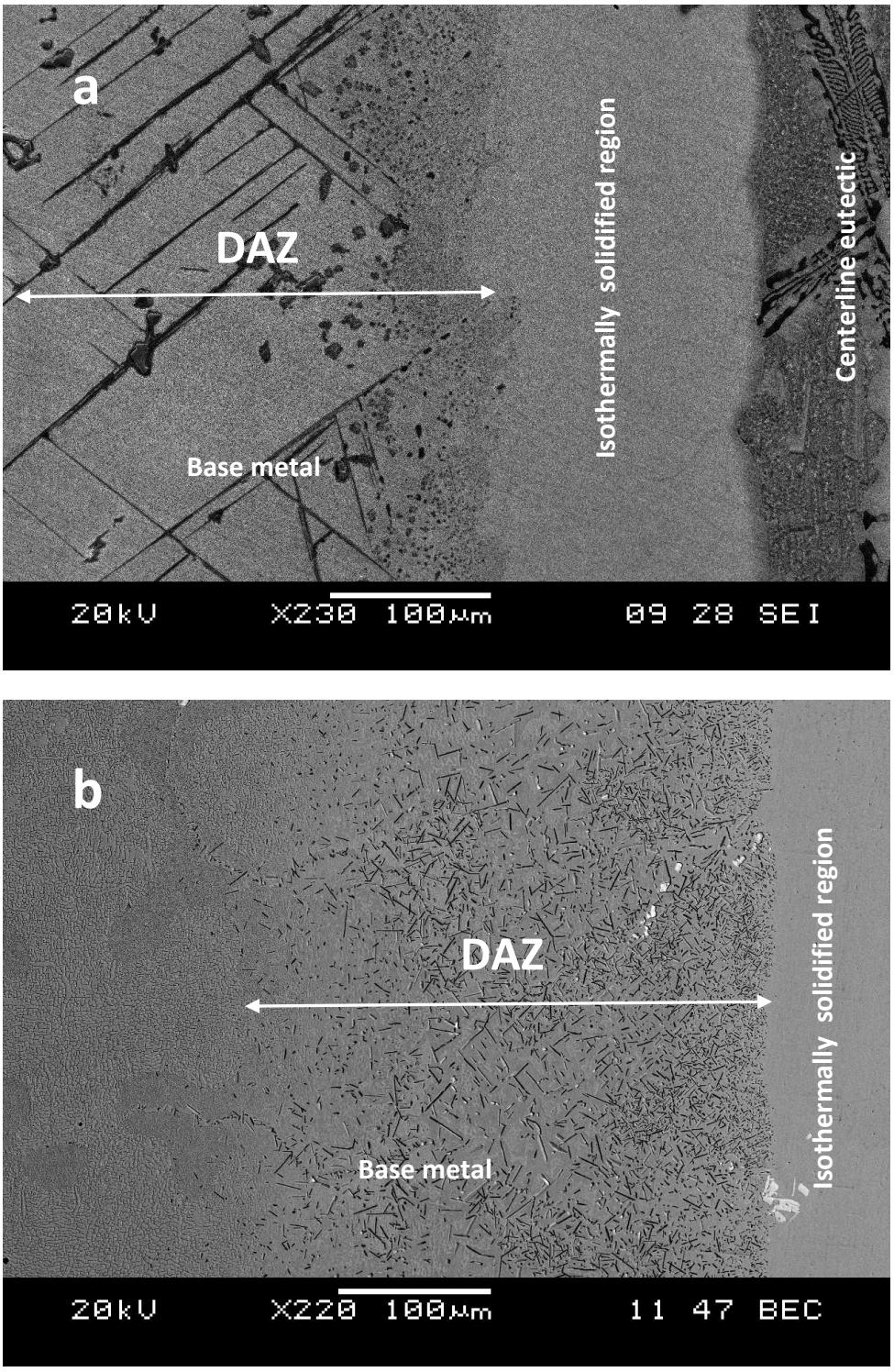

Figure 4.19: SEM micrograph of DAZ of (a) IN738 and (b) DS IC6, bonded at 1150 ^{o}C for 12 hrs using NB150 filler alloy

formed in the DAZ was carried out for samples bonded for 12 hrs. These second-phase precipitates, as suggested by the EDS X-ray mapping, were found to be rich Mo-B particles in alloy DS IC6 (Figure 4.20) and in alloy IN738, observed to be Cr-Mo-B rich particles (Figure 4.21). Mo is known to have a high affinity for B and several Mo-rich borides, such as M_3B_2 and M_5B_3 forms in Ni-base alloys [81, 82]. The EDS compositional analysis, coupled with the volume fraction of the second-phase precipitates formed in the DAZ of both alloys IN738 and DS IC6, would suggest that alloy DS IC6, which is richer in Mo, has a higher capability to accommodate diffusing B atoms from the liquated interlayer, through the formation of an extensive mesh of Mo-rich borides.

To further study the enhanced solute accommodation capability of alloy DS IC 6, a technique known as laser ablation-inductively coupled plasma-mass spectrometry (LAICP-MS), which is becoming popular for quantifying light trace elements like B, was used to determine the B concentration profile in the base-metal region adjacent to the joint (DAZ) in specimens bonded at 1150^{o}C, for both alloys IN738 and DS IC 6, where deviation from parabolic behaviour had occurred in alloy IN738. The technique involves the use of an ultraviolet laser to ablate material in air-tight cells and form a stream of fine particles from the specimen surface. The ablated material is subsequently carried in a helium aerosol carrier system into an inductively coupled plasma mass-spectrometer (ICP-MS) where ionisation occurs in argon-plasma at approximately 6000 K. Figures 4.22 and 4.23 show the laser ablation B concentration profile of the bonded materials as compared to that of the as-received material. In both alloys, the DAZ shows a high concentration of B compared to the rest of the matrix and the as received specimen. In

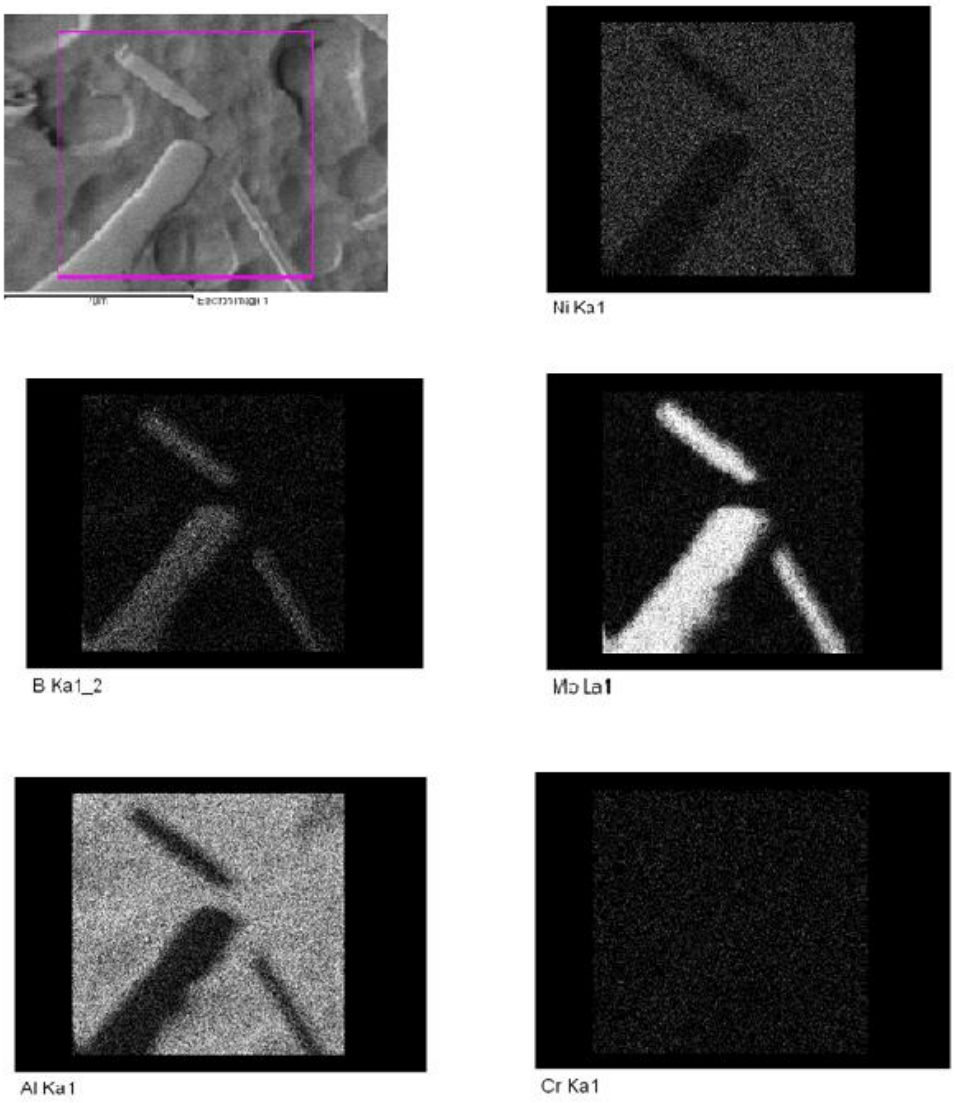

Figure 4.20: EDS X-ray maps analysis of second phase precipitates in DAZ of DS IC6 bonded at 1150 ^{o}C for 12 hrs using NB150 filler alloy

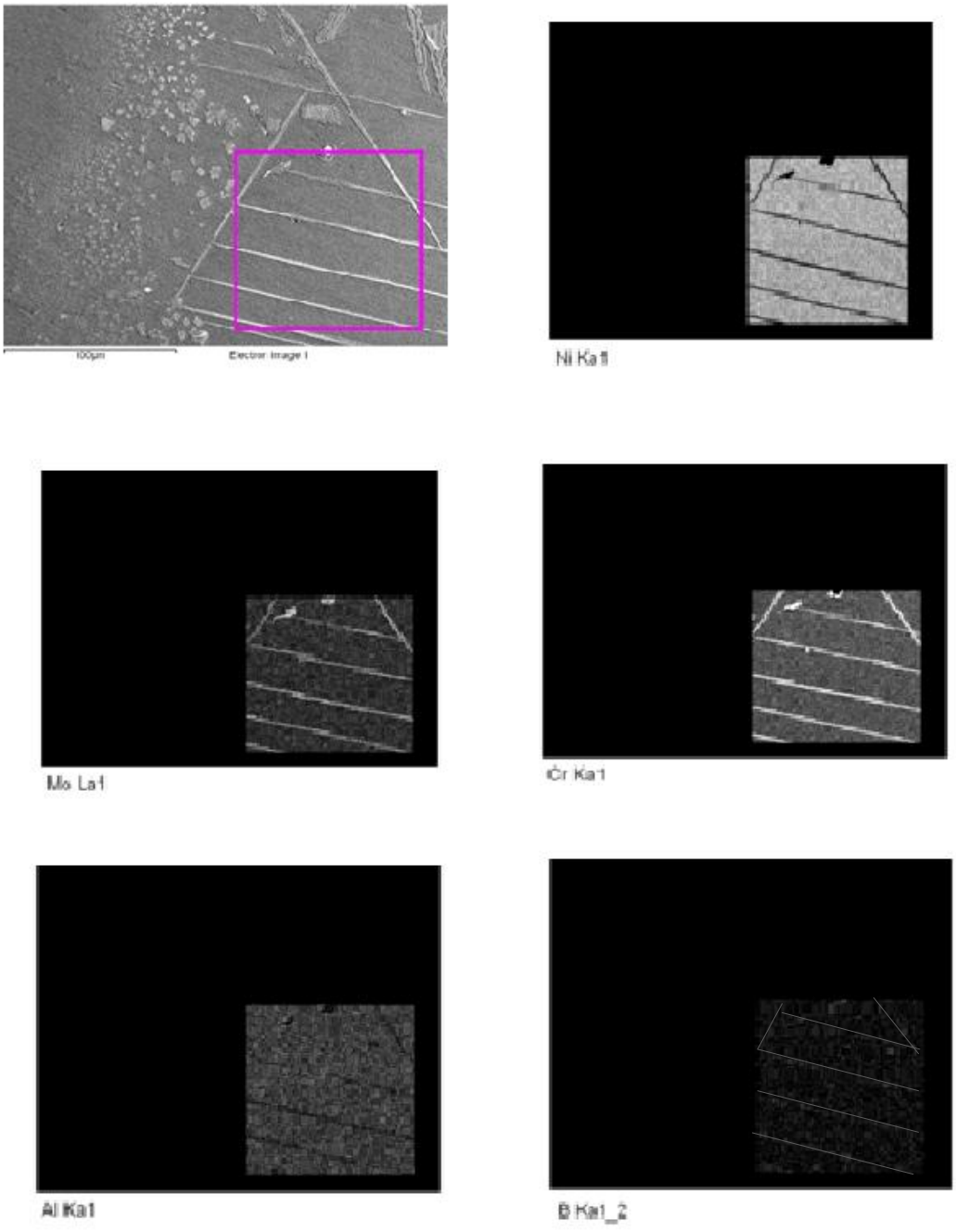

Figure 4.21: EDS X-ray maps analysis of second phase precipitates in DAZ of IN738 bonded at 1150 ^{o}C for 12 hrs using NB150 filler alloy

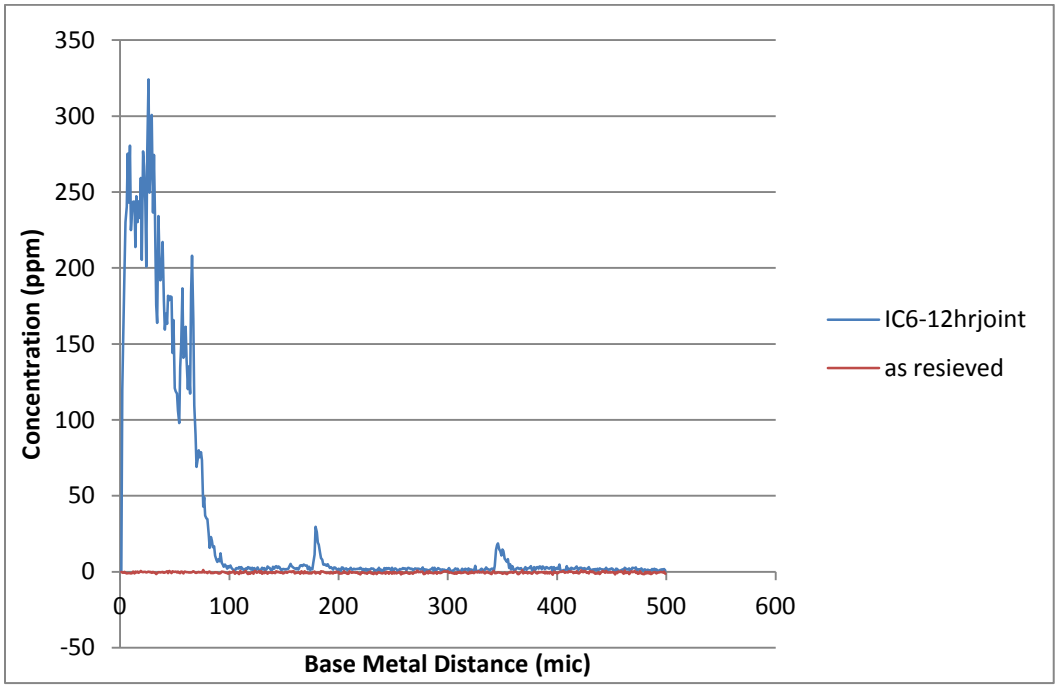

Figure 4.22: MPD solute (B) in TLP bonded and as received DS IC6 performed by laser ablation analysis

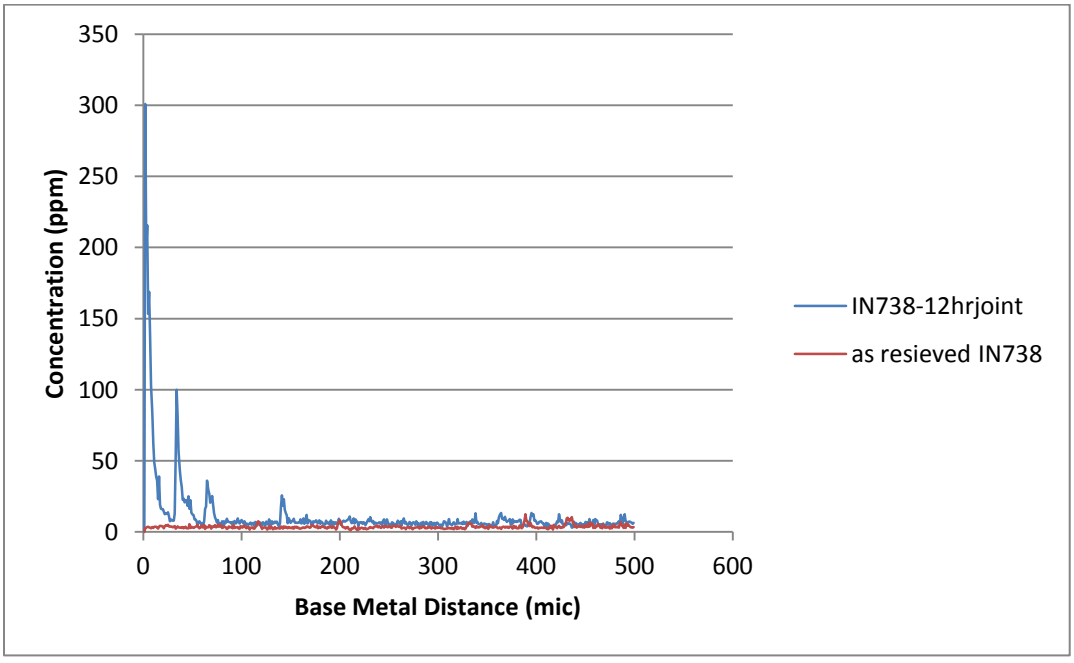

Figure 4.23: MPD solute (B) in TLP bonded and as received IN738 performed by laser ablation analysis

comparing the B concentration profile of the bonded materials to one another (Figure 4.24), a much higher concentration of B in the DAZ of DS IC 6 is evident as opposed to IN738. Interestingly, the concentration profile in the DAZ of alloy IN738 shows high peaks and depressions, thus indicating the detection of B rich particles and base-metal B concentration respectively. However, these depressions in the concentration profile are not observed for the DAZ of alloy DS IC 6. This observation, coupled with the fact that the concentration of B in the DAZ of DS IC 6 is higher than that of IN738, indicates the formation of a highly dense mesh of B rich particles, such that it is difficult to detect base-metal B concentration by using this particular mapping speed.

In view of the preceding discussion, it can be said that the timely finish of the isothermal solidification stage of alloy DS IC6 with increase in bonding temperature (compared to alloy IN738, which suffered a significant extension in t_f) cannot be attributable to higher MPD solute diffusivity in DS IC6 compared to IN738, especially as the t_f was comparable in both alloys at lower bonding temperatures. Additionally, the extension in the t_f experienced by IN738 with increase in temperature, as a result of the deviation from the parabolic rule, is independent of the solute diffusivity. As such, the enhanced capability of alloy DS IC6 to host diffusing B (by forming extensive boride particles), rather than higher diffusivity of B in DS IC6, is the responsible factor for the timely termination of the isothermal solidification stage which leads to a reasonable t_f.

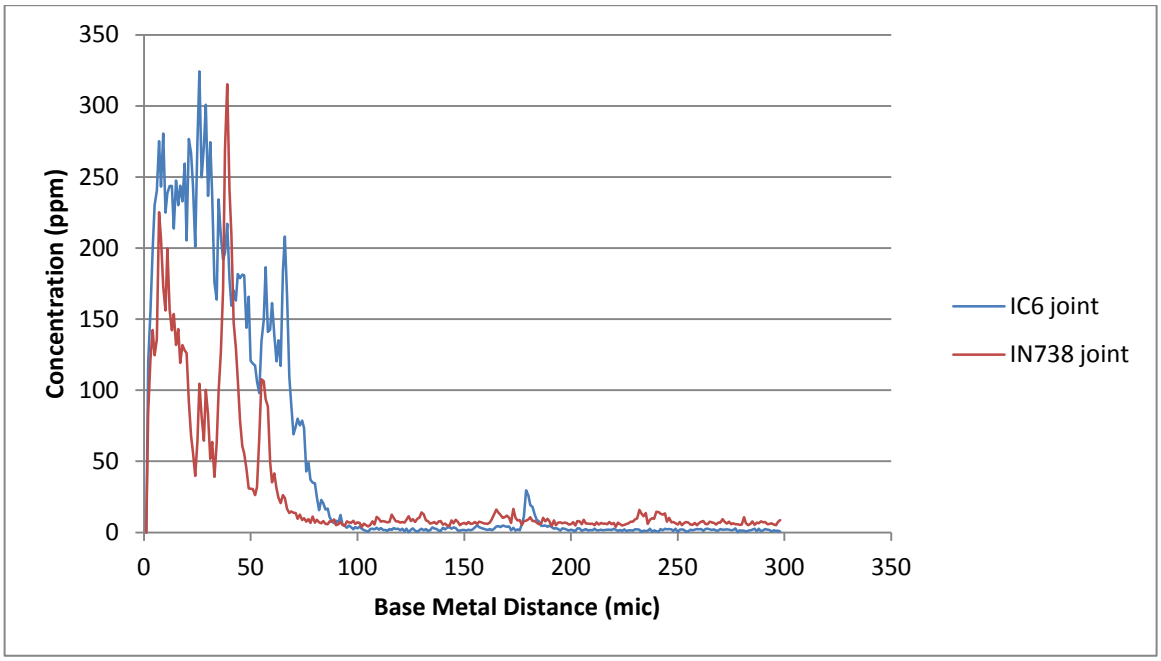

Figure 4.24: MPD solute (B) in TLP bonded DS IC6 and IN738 performed by laser ablation analysis

4.3 Reduction in t_f in materials that exhibit significant deviation from parabolic rule

As discussed in the previous section, the fundamental factor that causes an extension in the t_f upon increase in temperature during TLP bonding is the deviation of diffusion-controlled liquid-solid interface migration from its parabolic relationship with holding time [76]. Since the occurrence of deviation from parabolic behaviour is attributed to the reduction of $\partial C/\partial x$ below $(\partial C/\partial x)_c$ due to the continuous diffusion of the MPD solute into the base metal, it is therefore, theoretically speaking, possible to reduce the TLP processing time, t_f, by limiting the extent of reduction in the $\partial C/\partial x$ within the base metal. A reduction in the amount of MPD solute that must diffuse out of the joint into the base metal substrate to achieve complete isothermal solidification can be effective in limiting the reduction in the $\partial C/\partial x$. A reported practical way to achieve this [83] is by using a composite powder interlayer that consists of a mixture of a commercial filler alloy powder which contains an MPD solute and a base metal-like powder (called gap-filler) that is essentially free of MPD solute. This approach is typically used for wide-gap brazing of polycrystalline materials and reported to be beneficial in reducing liquid-phase erosion of substrate material, as well as enriching the joint with base material alloying elements [66, 67, 84].

In the current work, an experimental study is carried out to investigate the possibility of reducing the t_f by using the composite powder mixture method for alloys, such as IN738, where significant deviation from parabolic behaviour unavoidably occurs with increase in bonding temperature. To study this, 350 µm gap-sized butt-joint IN 738 samples were

TLP bonded in vacuum for various periods of times, which ranged from 1 to 36 hrs at a temperature of 1150^{o}C. For one set of samples, NB 150 filler alloy alone (conventional method) was used as the brazing alloy, while the other set of samples was joined by using a composite powder with a filler alloy (NB 150) to a gap filler (IN 738) powder ratio of 7:3 ($R_{7:3}$) by weight.

A plot of the average eutectic widths at the end of each holding time against the bonding time for both the conventional TLP bonding method (by using 100% NB 150 filler alloy) and the composite powder mixture method (by using a powder mixture with $R_{7:3}$) is presented in Figure 4.25. While both curves follow a similar trend, the composite powder method has the advantage of starting the isothermal solidification stage with less B to diffuse out of the joint, as indicated by the average eutectic width that represents the amount of liquid present at each time. A similar plot (Figure 4.26) was also constructed, by bonding sets of butt-joint samples joined at a temperature of 1180^{o}C by using filler alloy alone and composite powder mixtures of $R_{7:3}$ and $R_{1:1}$. While it is true that the onset of deviation from parabolic behaviour will take place in both cases at the same time, it must be noted that the rate of isothermal solidification continuously slows down with time within the deviation zone. As such, the use of a powder composite with less MPD solute as opposed to the filler alloy alone, would imply that complete isothermal solidification could be achieved at an earlier stage in the case of using a powder composite, whereas more MPD solute would have to diffuse out of the joint at an ever decreasing rate in the case where a filler alloy alone is used.

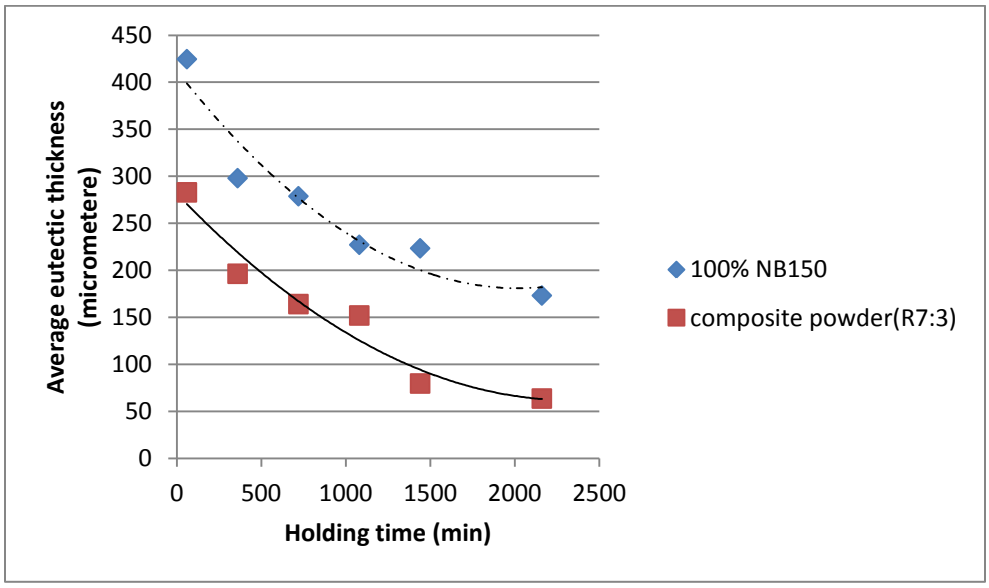

Figure 4.25: Plot of average eutectic width vs. holding time for alloy IN738 bonded at 1150 °C using 100% filler alloy and composite powder with $R_{7:3}$

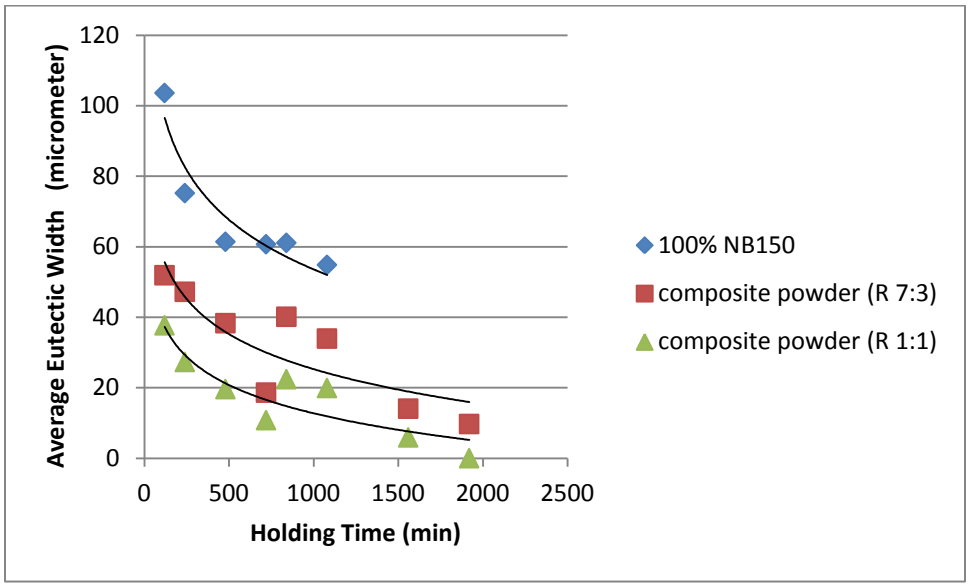

Figure 4.26: Plot of average eutectic width vs. holding time for alloy IN738 bonded at 1150 °C using 100% filler alloy and composite powders with $R_{7:3}$ and $R_{1:1}$

To clearly demonstrate the effectiveness of using the composite powder mixture method as a means of minimising t_f, an experiment was carried out at a temperature of 1150^{o}C by using a butt-joint IN738 sample with a gap size of 200 µm. It was found that the composite powder mixture with a mixing ratio of $R_{7:3}$ is able to achieve complete isothermal solidification within 26 hrs compared to the 52 hrs needed to produce a eutectic-free joint when using filler alloy alone. In addition to minimising t_f, the composite powder mixture method can aid in reducing liquid-phase erosion of the substrate, which is particularly important in thin sections to prevent compromising of the integrity of the joined or repaired component. This method can also be useful in favourably enriching the joint with base metal alloying elements provided by the gap filler present in the composite powder mixture.

4.4 Factors that affect dissolution of gap-filler powder particles

In the course of this investigation, it was observed (and contrary to what is normally reported in the literature for wide-gap TLP bonding) that for some bonding conditions, complete dissolution of the gap-filler within the powder composite occurred. Moreover, this complete melting of the gap-filler was found to be beneficial for the general quality (mainly presence of porosity) of the joint produced. Figure 4.27 is an example of two joints produced by using the powder composite method. It can be clearly seen that the joint that contains the powder composite with $R_{1:1}$ (in which the gap-filler particles are partially melted, see Figure 4.27a) suffers from severe void formation, while the joint

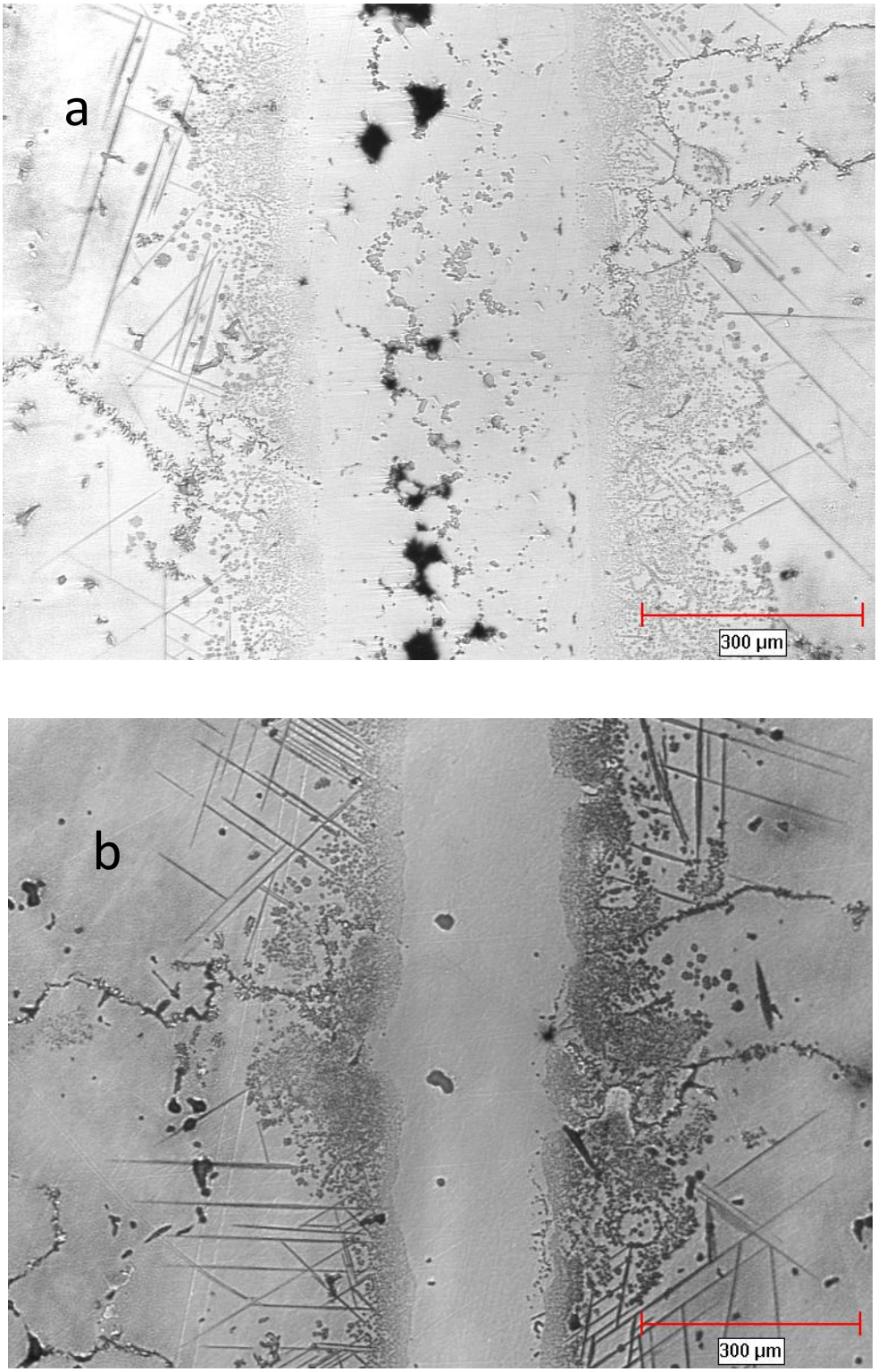

Figure 4.27: Optical micrograph showing a joint bonded at 1150 ^{o}C using a composite powder mixture with (a) $R_{1:1}$ and (b) $R_{7:3}$

that contains the powder composite with $R_{7:3}$ (where complete dissolution of the gap-filler has occurred, see Figure 4.27b) appears to be visually sound. In light of this important observation, an experimental study of some of the factors (material and process variables) that affect the extent of the gap-filler dissolution was carried out. The factors investigated in this work include: bonding temperature, mixing ratio of filler alloy to gap filler alloy ($R_{F:G}$), type of MPD solute, type of gap filler, and size of gap filler powder particles. Unless otherwise stated, it should be noted that the filler alloy referred to in the following discussion is NB150 powder and the gap-filler is IN738 powder and deposited onto an IN738 substrate.

Effect of bonding temperature

For a composite powder mixture that comprises a specific filler alloy and a gap-filler with a constant particle size, it was found that an increase in the bonding temperature of a mixture with a fixed $R_{F:G}$ aids to dissolve gap-filler particles, until a temperature is reached where complete dissolution of the gap-filler would occur. Figure 4.28 depicts a case where a composite powder with $R_{7:3}$ shows incomplete melting of the gap-fillerwhen held at 1100^{o}C (Figure 4.28a); however, when the temperature is increased to 1150^{o}C, the microstructure shows solidification dendrites, which is indicative of the complete melting of the gap-filler particles.

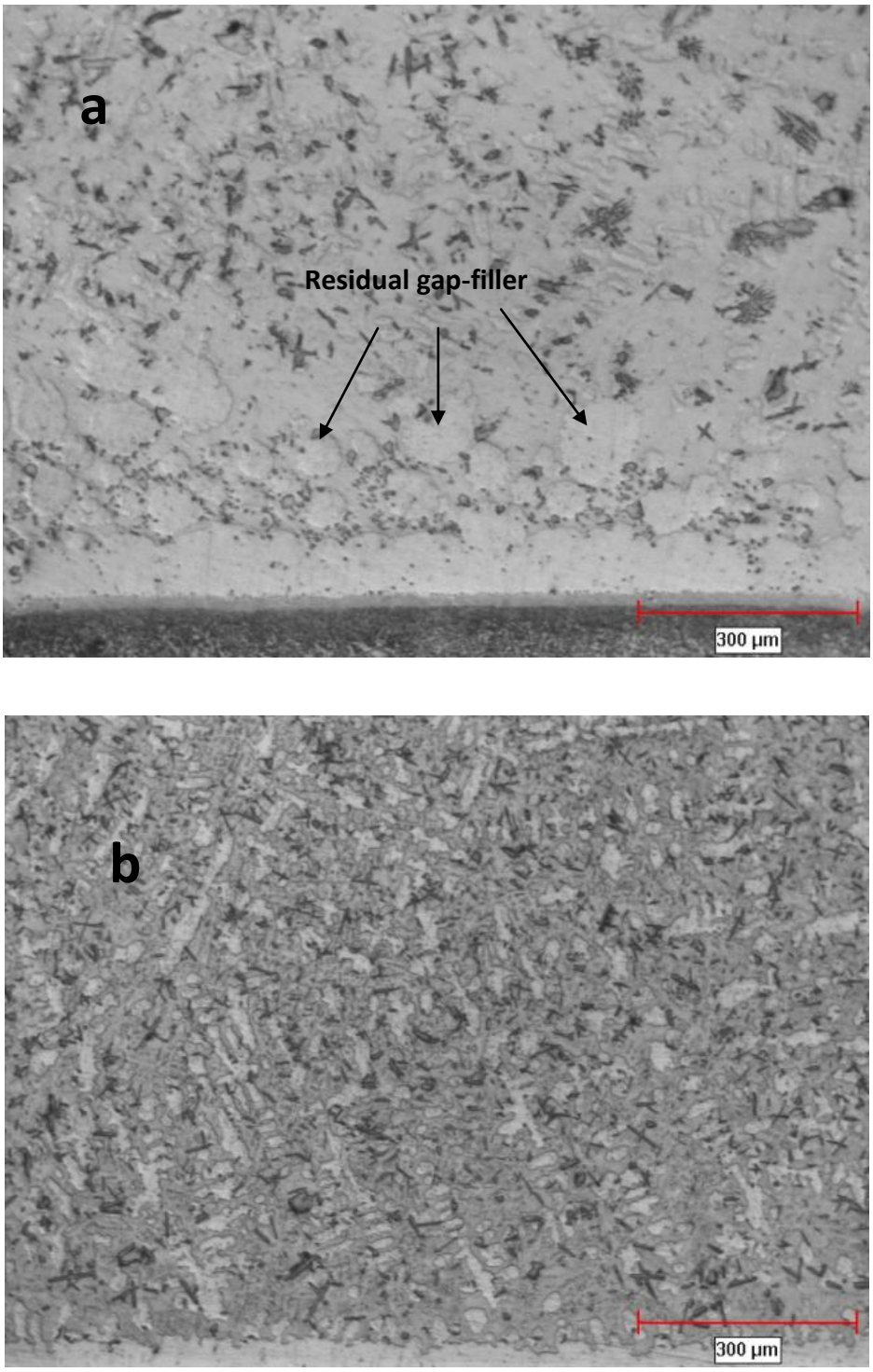

Figure 4.28: Optical micrograph showing a composite powder mixture with $R_{7:3}$ at (a) 1100 ^{o}C and (b) 1150 ^{o}C

Effect of mixing ratio $R_{F:G}$

If it is not possible to increase the bonding temperature above a certain value, for reasons such as compromising the properties of the base metal, complete dissolution of gap-filler particles that have not melted at the bonding temperature can be achieved by altering the $R_{F:G}$ of the composite powder mixture. Figure 4.29 shows how altering the mixing ratio from $R_{1:1}$ to $R_{7:3}$ can induce complete melting of the gap filler at 1150^{o}C.

Effect of gap-filler powder size

Another important variable that influences the extent of gap-filler melting is the size of the gap-filler powder particles. For two composite powder mixtures which have the same mixing ratio of $R_{1:1}$, with one that contains a fine gap-filler powder (Amdry7380) and the other a coarse gap-filler powder (Amdry7381), Figure 4.30 shows the resultant microstructure at 1180^{o}C. The mixture that contains the coarse gap-filler (Figure 4.30a) shows remnants of unmelted gap-filler particles. However, at the same temperature, the mixture that contains the fine gap-filler (Figure 4.30b) exhibits a solidification dendritic microstructure, thus indicating complete melting of the gap-filler particles.

Effect of type of gap-filler powder

To examine the effect of the type of gap-filler on the general melting behaviour, two different gap-fillers, namely Nicrogap 108 (15 Cr - 0.75 Si – 7 Fe - 0.2 B – bal. Ni) wt.% and HY282 (20 Cr – 10 Co – 8.5 Mo – 2.1 Ti – 1.5 Al – 1.5 Fe – 0.3 Mn – 0.15 Si – 0.06 C – 0.005 B – bal. Ni) wt.%, were used for comparison with the general melting trend exhibited by the IN738 gap-filler. Figure 4.31 shows the microstructure of composite

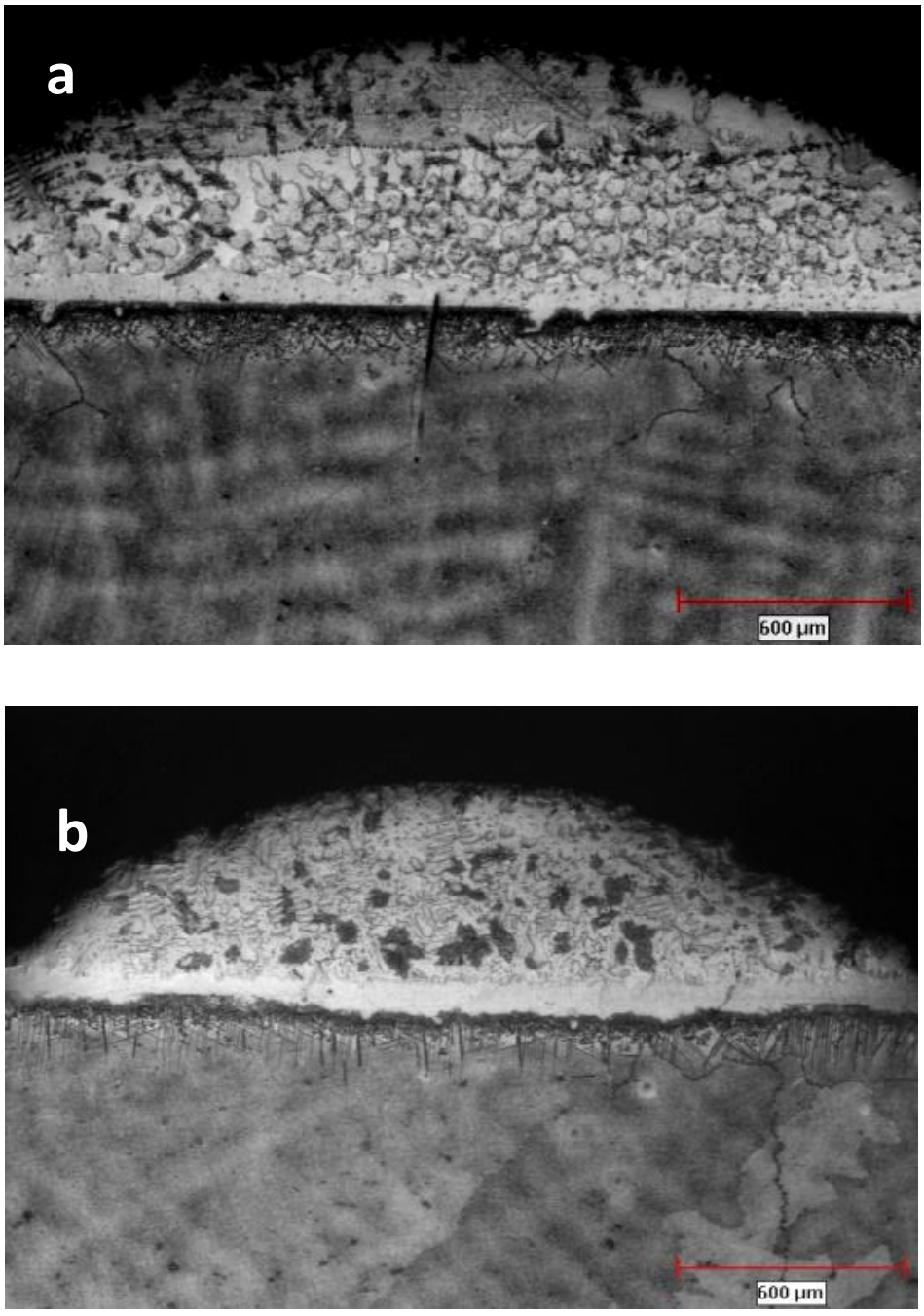

Figure 4.29: Optical micrograph showing a composite powder mixture at 1150 ^{o}C, with (a) $R_{1:1}$ and (b) $R_{7:3}$

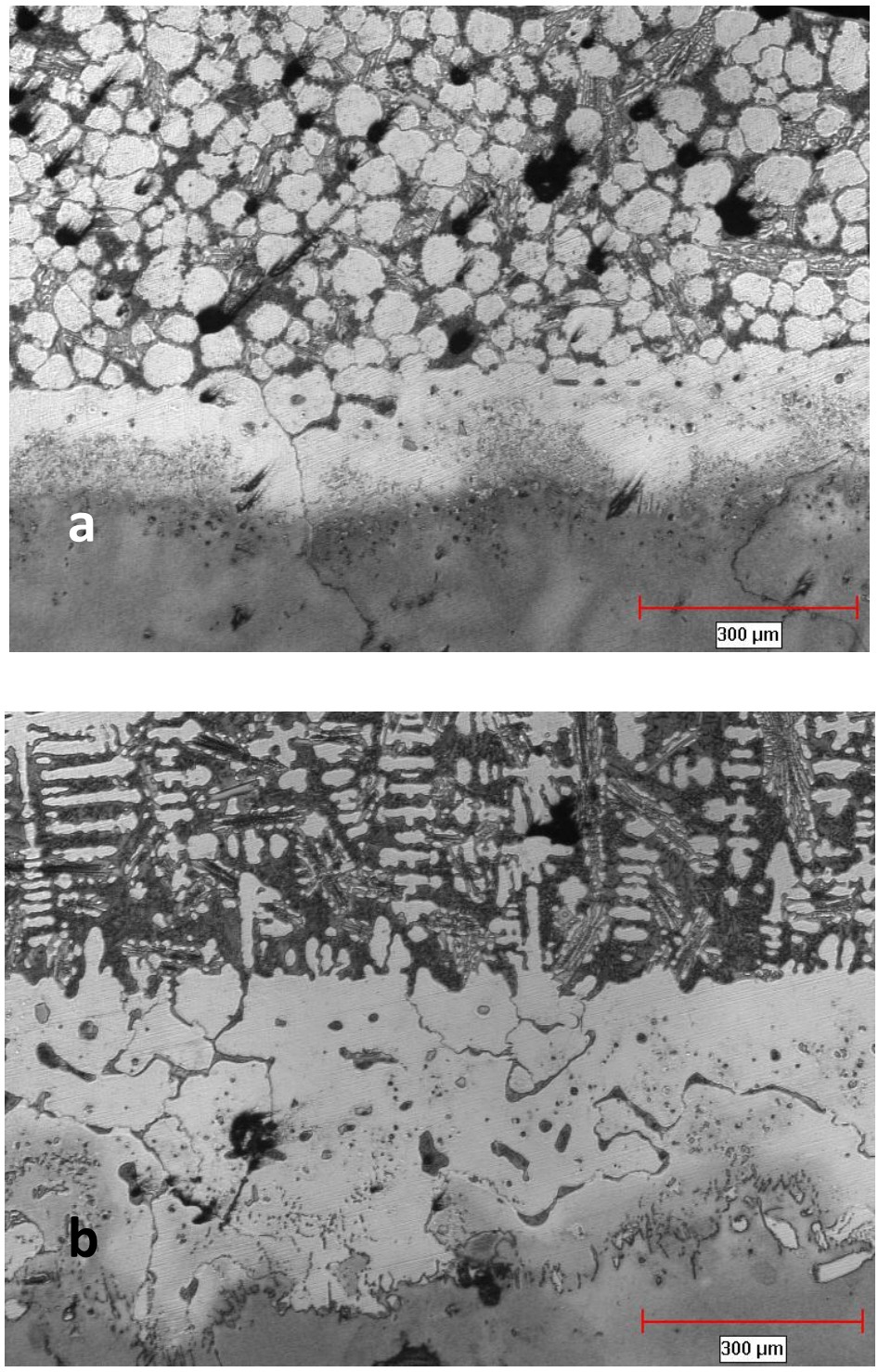

Figure 4.30: optical micrograph showing a composite powder mixture with $R_{1:1}$ at 1180 ^{o}C using (a) coarse and (b) fine gap-filler

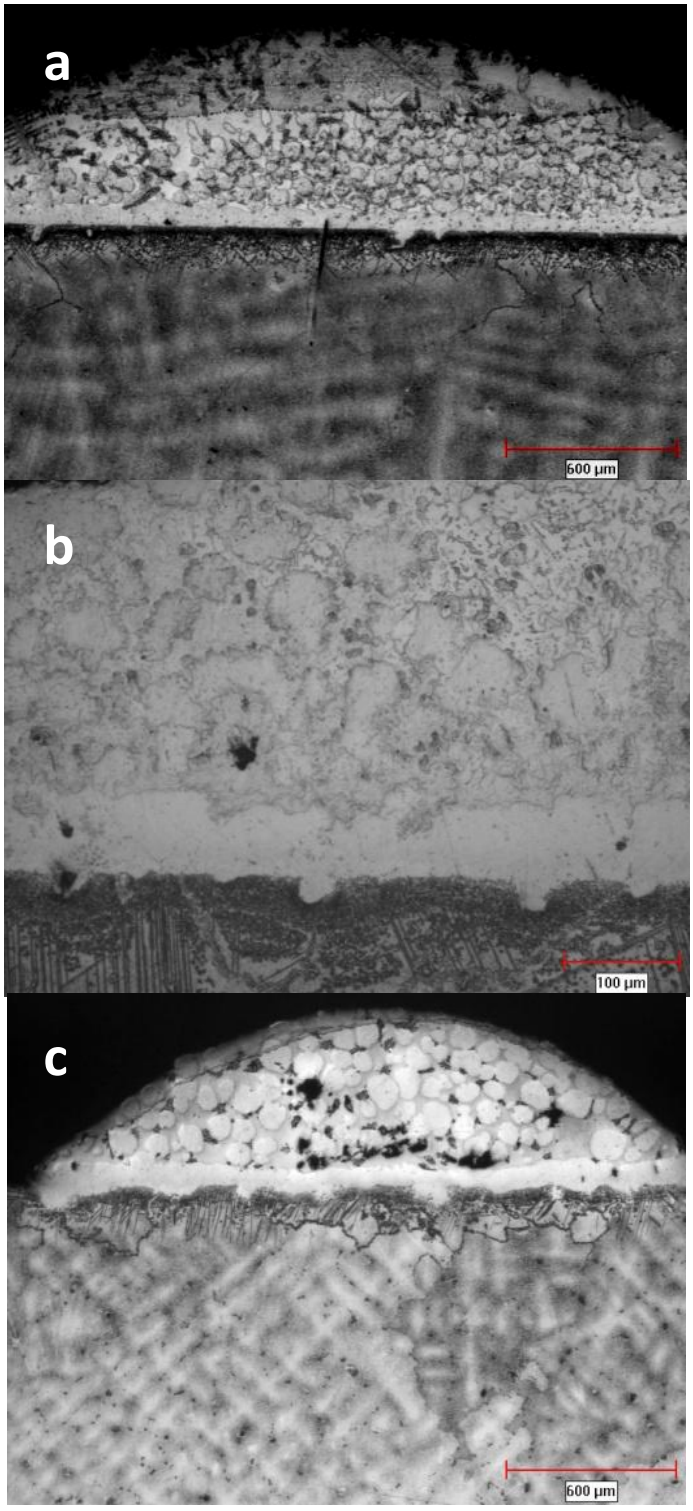

Figure 4.31: Optical micrograph showing a composite mixture containing (a) IN738, (b) HY282 and (c) Nicrogap108 gap-fillers at 1150 ^{o}C with $R_{1:1}$

powder mixtures with $R_{1:1}$ for gap-fillers IN 738, HY 282 and Nicrogap 108, at a temperature of 1150^{o}C. Like the mixture that contained gap-filler IN 738, the other two mixtures also show residual unmelted powder particles at this temperature. For the same temperature of 1150^{o}C, reduction in the amount of gap-filler in all mixtures, such that the mixing ratio is altered to $R_{7:3}$, means that complete dissolution of all gap-filler types would occur, as shown in Figure 4.32. Other experiments were also conducted, in which the temperature and/or mixing ratio were altered, and the melting behaviour of the three gap-fillers examined followed a similar pattern. This would imply that rather than gap-filler powder type, it is the proper combination of temperature and mixing ratio that is imperative to achieving complete dissolution of the composite powder. Thus, the choice of gap-filler would be based on the microstructural features desired within the joint.

Effect of type of MPD solute

Finally, the effect of the type of MPD solute on the dissolution behaviour of gap-filler powder particles was studied. Filler alloys that contained B as the MPD are usually preferred, owing to its high diffusivity in Ni based alloys, thus leading to shorter processing times. However, the use of B filler alloys is prohibited in the repair of nuclear power plant parts by TLP bonding. This is because of two reasons; one is that material that contain B have a large neutron absorption cross-section, thus resulting in reduced nuclear reactor performance, and second, when B is subjected to radiation, it transforms to helium, thus causing swelling of the structural material [85]. For this study, a filler alloy that bears Si as its MPD solute, namely, Amdry 100 with the

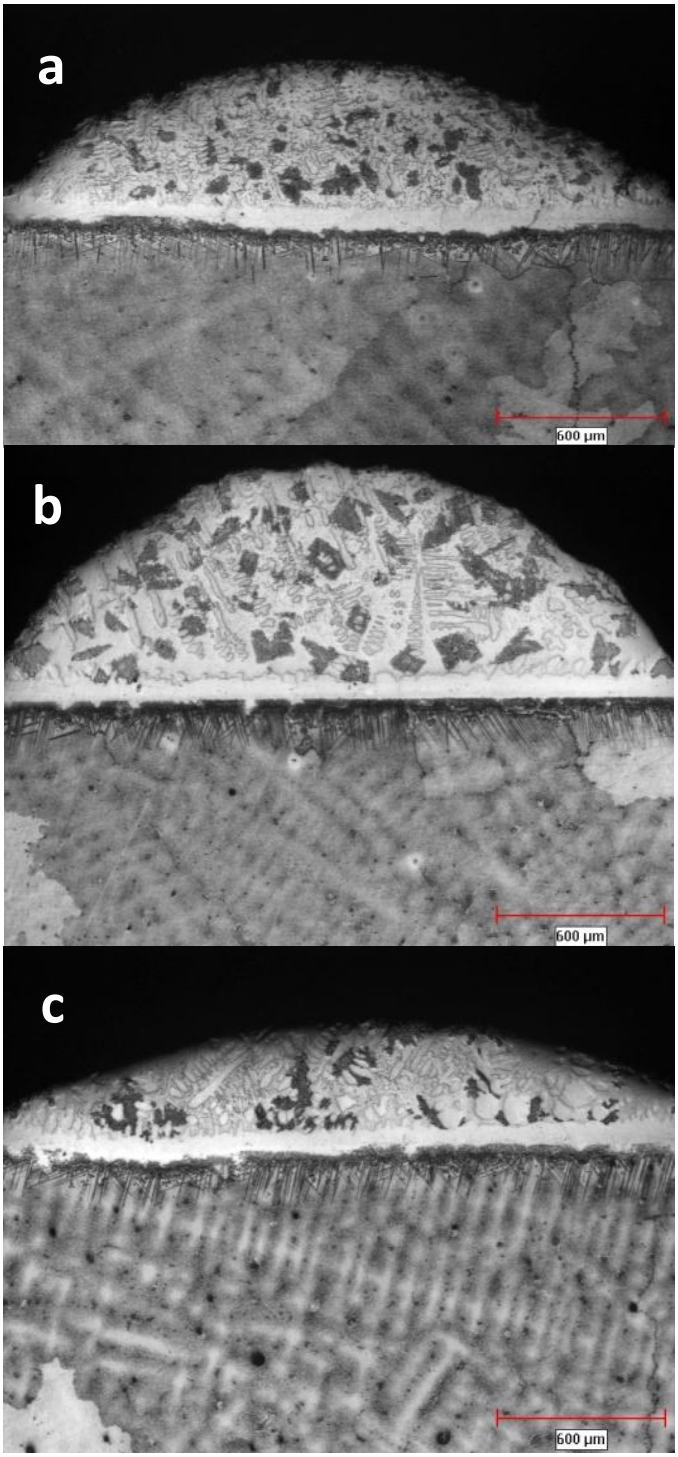

Figure 4.32: Optical micrograph showing a composite mixture containing (a) IN738, (b) HY282 and (c) Nicrogap108 gap-fillers at 1150 ^{o}C with $R_{7:3}$

composition (Ni –19 Cr– 10 Si) wt.%, was used for comparison with the NB150 filler alloy. Figure 4.33 shows a composite powder mixture ($R_{1:1}$) at 1150^{o}C, with Amdry 100 as the filler alloy and IN738 as the gap-filler. The gap-filler particles are largely unmelted at this temperature. When the amount of gap-filler is decreased, such that the mixing ratio becomes $R_{7:3}$, this is sufficient enough to induce complete melting in the mixture that contains NB 150 (Figure 4.29b); however, in the mixture that contained Amdry 100, with $R_{7:3}$, unmelted particles are evident (Figure 4.34). In an attempt to induce complete melting of the $R_{7:3}$ mixture, the temperature was increased to 1200^{o}C. This, however, did not produce complete melting of the gap-filler particles. To explain this, it should be recalled that from the mechanisms of the TLP bonding process, the melting of the gap-filler occurs in order to dilute the solute concentration in the liquated filler to the solidus and liquidus compositions, in order to achieve equilibrium at the bonding temperature. Looking at Figures 4.35 and 4.36 which show the Ni-B and Ni-Si phase diagrams respectively, it can be seen that for filler alloy NB 150 which melts at 1055^{o}C, large amounts of the solid particles (solid substrate) would have to be melted at a high temperature, such as 1150^{o}C, to achieve equilibrium solidus and liquidus compositions. In contrast, filler alloy Amdry100, which melts at 1140^{o}C, would only have to melt small amounts of the solid particles at a temperature such as 1150^{o}C, because its composition is already close to that of equilibrium. Therefore, if a Si-containing filler alloy must be used, and complete melting is desired, a very fine gap-filler powder would be favourable.

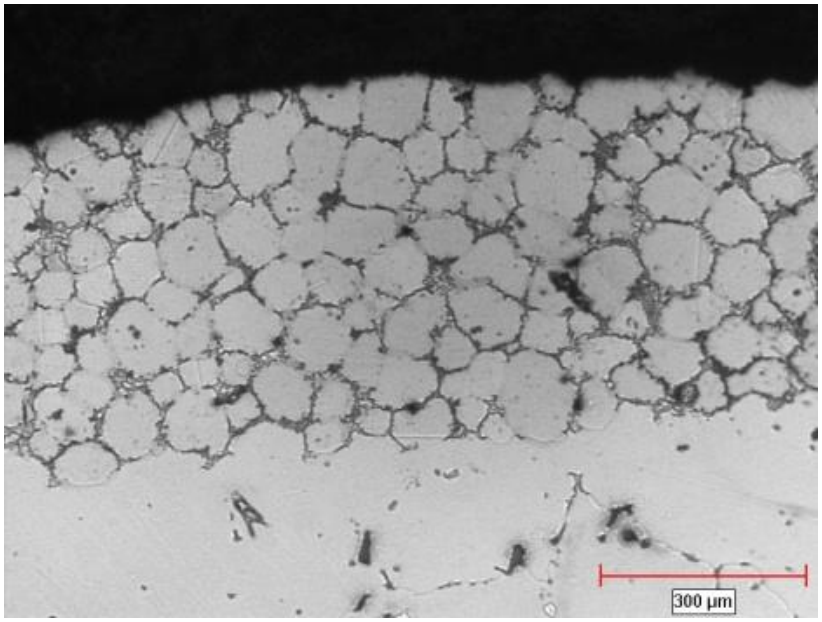

Figure 4.33: Optical micrograph showing a composite powder containing Amdry100 filler alloy at 1150 ^{o}C with $R_{1:1}$

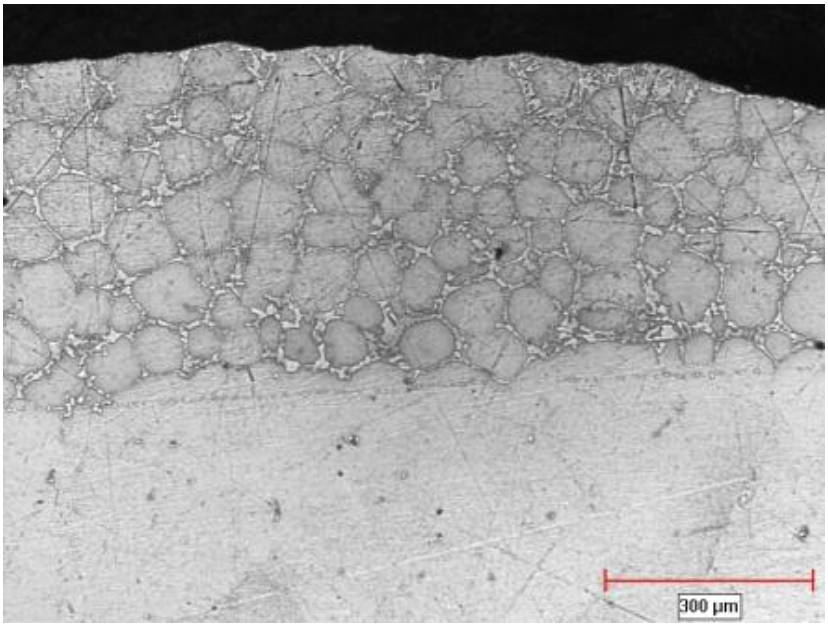

Figure 4.34: Optical micrograph showing a composite powder containing Amdry100 filler alloy at 1150 ^{o}C with $R_{7:3}$

4.35: The Nickel-Boron Phase Diagram [86]

4.36: The Nickel-Silicon phase diagram [86]

5 Summary and Conclusions

The influence of base alloy composition on the time required to achieve complete isothermal solidification (t_f) during the TLP bonding of three Ni-base superalloys was experimentally studied. The summary and main conclusions of the study are as follows:

1. The three alloys (IN738, DS Rene80 and DS IC 6) showed similar behaviour, with comparable t_f, when bonded at 1100 ^{o}C. The experimental data are concurrent with conventional TLP bonding analytical models, which assume a parabolic relationship between solid/liquid interface migration and holding time. This is an indication that the rate at which the MPD solute diffuses into the base alloy is comparable in all three alloys.
2. An incomparable behaviour is evident in these three alloys when bonded at 1150 ^{o}C. Alloy IN738 shows deviation from the expected parabolic behaviour, while alloy DS IC6 maintains a parabolic relationship to the end, and alloy DS Rene80 suffers a slight deviation towards the end of the isothermal solidification stage. This incomparable behaviour of the alloys at higher temperatures results in an excessively prolonged holding time in alloy IN738 (52 hrs), compared to DS IC6 (16 hrs) and DS Rene80 (26 hrs).
3. The fundamental factor that causes the prolonged t_f during TLP bonding is the deviation of diffusion-controlled liquid-solid interface migration from its parabolic relationship with holding time. This deviation from parabolic behaviour occurs due to diffusion-induced reduction of solute concentration gradient ($\partial C / \partial x$) in the base material below a critical value $(\partial C / \partial x)_C$.

4. This investigation shows that the ability of alloy DS IC6 to complete isothermal solidification within a reasonable time frame is attributable to its capability to accommodate the diffusing MPD solute, through the formation of a densely packed second-phase precipitates in diffusion affected zone.
5. A composite powder mixture (which comprises filler and base alloy powders) is used as an alternative to filler alloy alone to reduce the t_f in the alloy IN738, which shows deviation from parabolic behaviour. It is found that by using a composite powder with a 7:3 mixing ratio of NB150 filler alloy powder to IN738 base alloy powder, this can reduce the t_f by 50%, as compared to using NB150 filler alloy alone. The presence of base alloy powder within the joint reduces the amount of filler alloy used, thus reducing the amount of boron required to diffuse out of the joint to achieve complete isothermal solidification.
6. It is found that a composite powder mixture, in which the gap-filler particles remain unmelted at the bonding temperature, would produce a joint with large porosity. In contrast, complete melting of the gap-filler in the composite powder mixture would produce a joint free of porosity. Some of the factors that can affect the extent of dissolution of gap-filler powder particles include: bonding temperature, mixing ratio of filler alloy to gap-filler alloy ($R_{F:G}$), type of MPD solute, type of gap filler, and size of gap filler powder particles.
7. Normally, when joining or repairing components using TLP bonding, the main factor that is usually considered in order to achieve complete isothermal solidification of the joint within an economical time frame is selection of

appropriate filler alloy containing a fast diffusing MPD solute. However, this work shows that another very important factor, namely, base alloy composition, ought to be considered as it can in some cases effectively override the effect of high diffusivity at high temperatures and lead to an undesirable extension of in processing time.

6 Suggestions for Future Work

The following are possible work suggestions for future study:

1. Design a post-bond heat treatment to homogenize bonded materials and remove boron-rich precipitates in the DAZ, which have been reported to degrade properties of bonded material.

2. Perform mechanical tests to evaluate properties of bonded and homogenized joined components.

3. Study other superalloy families such as Cobalt-based in order to assess the influence of base-alloy composition on processing time during TLP bonding.

7 Bibliography

[1] D. S. Duvall and W. A. Owczarski, "Further Heat-Affected-Zone studies in heat resistant nickel alloys," *Weld. J,* vol. 46, no. 9, pp. 423s-432s, 1967.

[2] D. S. Duvall, W. A. Owczarski and D. F. Paulonis, "TLP* Bonding: A New Method for Joining Heat Resistant Alloys," *Weld. J.,* vol. 53, no. 4, pp. 203-214, 1974.

[3] C. Sims, N. Stoloff and W. Hagel, Super Alloys II, new york: John Wiley & Sons, 1987, pp. 97-118.

[4] A. K. Jena and M. C. Chaturvedi, "The Role of Alooying Elements in the Design of Nickel-Base Superalloys," *J. Mat. Sci.,* vol. 19, pp. 3121-3139, 1984.

[5] M. Durand-Charre, The Microstructure of Superalloys, Amsterdam: Gordon and Breach Science Publishers, 1997.

[6] R. Reed, The Superalloys: Fundamentals and Applications, New York: Cambridge Press, 2006, pp. 33-103.

[7] W. C. Hagel and H. J. Beattie, "Iron and Steel Institute Special Report," London 64, 1959.

[8] H. E. Collins and R. J. Quigg, "Carbide and Intermetallic Instability in Advanced Nickel-Base Superalloys," *Trans. ASM,* vol. 61, no. 1, pp. 139-148, 1968.

[9] Q. Z. Chen and D. M. Knowles, "The microstructures of base/modified RR2072 SX superalloys and their effects on creep properties at elevated temperatures," *Acta. Mat.,* vol. 50, no. 5, pp. 1095-1112, 2002.

[10] O. E. Oshobe, *MSc Dessertation,* Winnipeg, Manitoba: University of Manitoba, 2012.

[11] M. J. Donachie and S. J. Donachie, Superalloys- A Technical Guide, 2nd Edition ed., Ohio, USA: ASM International, 2002.

[12] A. K. Sinha, "Topologically close-packed structures of transition metal alloys," *Progress in Materials Science,* vol. 15, pp. 79-185, 1972.

[13] S. Kou, Welding Metallurgy, second ed., Wiley & Sons Inc., 2003, pp. 3-32.

[14] H. G and D. M. Jacobson, principles of soldering and brazing, Ohio, USA: ASM International, 1996, pp. 128-129.

[15] M. H. Haafkens and G. H. Matthey, "A new approach to the weldability of nickel-base as-cast and powder metallurgy superalloys," *Weld. J,* vol. 61, no. 25, pp. 25-30, 1982.

[16] O. A. Ojo, N. L. Richards and M. C. Chaturvedi, "Contribution of constitutional liquation of gamma prime precipitate to weld HAZ cracking of cast inconel 738 superalloy," *Scripta Mater.,* vol. 50, pp. 642-646, 2004.

[17] N. F. Kazakof, Diffusion Bonding of Materials, New York: Pergamon Press, 1985.

[18] M. W. Mahoney and C. C. Bampton, "Fundamentals of Diffusion Bonding," *ASM Handbook,* vol. 6, pp. 156-159, 1993.

[19] M. Schwartz, Brazing, 2nd ed., Ohio, USA: ASM International, 2003, pp. 1-382.

[20] H. G. Jacobson D. M., Principles of Brazing, ASM International, 2005, pp. 3-45, 105-141.

[21] D. M. Jacobson and G. Humpston, Principles of Brazing, Ohio, USA: ASM International, 2005, pp. 3-45.

[22] J. C. Ambrose, M. G. Nicholas and A. M. Stoneham, "Kinetics of Braze Spreading," in *Proc. Conf. British Association for Brazing and Soldering*, Conventry, U.K., 1992.

[23] K. B. Gove, "Braze Repair of Aero-engine Components," 1989.

[24] D. Manente, "Brazing of Heat-Resistant Alloys, Low Alloy Steels, and Tool Steels," *ASM Handbook, Volume 6 (Welding, Brazing, and Soldering),* vol. 6, pp. 925-930, 1993.

[25] W. F. Gale and D. A. Butts, "Overview: Transient liquid phase bonding," *Sci. and Tech. of Weld. and Joining,* vol. 9, no. 4, pp. 283-300, 2004.

[26] W. D. MacDonald and T. W. Eagar, "TRANSIENT LIQUID PHASE BONDING," *Annu.Rev.Mater.Sci.,* vol. 22, pp. 23-46, 1992.

[27] I. Tuah-Poku, M. Dollar and T. B. Massalski, "A Study of the Transient Liquid Phase Bonding Process applied to a Ag/Cu/Ag Sandwich Joint," *Metall. Tras. A,* vol. 19A, pp. 675-686, 1988.

[28] E. R. Maddrell and E. R. Wallach, "In Proc. Conf. Recent Trends in Welding Science and Technology," in *Materials Park*, Ohio, 1990.

[29] R. Thamburaj, W. Wallace and J. A. Goldak, "Post-weld heat-treatment cracking in superalloys," *Int. Mater. Rev,* vol. 28, no. 1, pp. 1-22, 1983.

[30] K. Nishimoto, K. Saida, D. Kim and Y. Nakao, "Transient liquid phase bonding of Ni-base

single crystal superalloy, CMSX-2," *ISIJ Int.,* vol. 35, no. 10, pp. 1298-1306, 1995.

[31] J. T. Niemann and R. A. Garret, "Eutectic bonding of boron-aluminum structural components," *Weld. J.,* vol. 52, pp. 175-184, 1974.

[32] H. Nakagawa, C. H. Lee and T. H. North, "Modeling of base metal dissolution behaviour during transient liquid phase brazing," *Metall. Trans. A,* vol. 22A, no. 2, pp. 543-555, 1991.

[33] W. F. Gale, "Applying TLP Bonding to the Joining of Structural Intermetallic Compounds," *JOM,* pp. 49-52, 1999.

[34] Y. Zhou and T. H. North, "Kinetic Modeling of Diffusion-Controlled, Two-Phase Moving Interface Problems," *Modeling and Simulation in Mater. Sci. Eng.,* vol. 1, no. 4, pp. 505-516, 2003.

[35] Y. Zhou, W. F. Gale and T. H. North, "Modeling of Transient Liquid Phase Bonding," *International Materials Reviews,* vol. 40, no. 5, pp. 181-196, 1995.

[36] Y. Zhou, Uneversity of Toronto, 1994.

[37] Y. Zhou, "Analytical Modeling of Isothermal Solidification during Transient Liquid Phase (TLP) bonding," *J. of Mat. Sci. Letters,* vol. 20, pp. 841-844, 2001.

[38] T. Onzawa, A. Suzamura and J. H. Kim, *J. Jpn. Weld.,* vol. 8, no. 4, p. 74, 1990.

[39] H. Ikawa, Y. Nakao and T. Isai, "Theoritical Considerations on Metallurgical Processes in TLP Bonding of Nickel-Based Superalloys," *Trans. Jpn. Weld. Soc.,* vol. 10, no. 1, pp. 24-29, 1979.

[40] Y. Nakao, K. Nishimoto, K. Shinozaki and C. Y. Kang, "Theoritical research on transient liquid insert metal diffusion bunding of nickel base alloys," *Trans. Jpn. Weld. Soc.,* vol. 20, no. 1, pp. 60-65, 1989.

[41] G. Lesoult, "Center for Joining of Materials Report," Carnegie Mellon University, Pittsurgh, PA, Sept.1976.

[42] A. Sakamoto, C. Fujiwara, T. Hattori and S. Sakai, "Optimizing processing variables in high-temperature brazing with Nickel-based filler metals," *Weld. J,* vol. 68, no. 3, pp. 63-71, 1989.

[43] J. E. Ramirez and S. Liu, "Diffusion Brazing in the Nickel-Boron System," *Weld. J.,* vol. 71, pp. 365s-375s, 1992.

[44] W. F. Gale and E. R. Wallach, "Microstructural Development in Transient Liquid Phase

Bonding," *Metall. Trans. A.,* vol. 22A, no. 10, pp. 2451-2457, 1991.

[45] W. F. Gale and E. R. Wallach, "Influence of Isothermal Solidification on Microstructural Developement in Ni-Si-B Filler Metals," *Mat. Sci. Tech.,* vol. 7, no. 12, pp. 1143-1148, 1991.

[46] C. H. Lee and T. H. North, *71st American Welding Society Convention, Anaheim, CA, April 1990, Preprint, AWS, Miami, FL.,* pp. 273-276, 1990.

[47] O. A. Ojo, *MSc Dessertation,* Winnipeg, Manitoba: University of Manitoba, 2002.

[48] T. C. Illingworth, I. O. Golosnoy, V. Gergely and T. W. Clyne, "Numerical modelling of transient liquid phase bonding and other diffusion controlled phase changes," *J. Mat. Sci.,* vol. 40, no. 9-10, pp. 2505-2511, 2005.

[49] J. F. Lynch, L. Feinstein and R. A. Huggins, "Brazing by the Diffusion Controlled Formation of a Liquid Intermediate Phase," *Welding Journal,* vol. 38, no. 2, pp. 85s-89s, 1959.

[50] W. A. Owczarski, *Welding Journal,* vol. 42, no. 2, pp. 78s-83s, 1962.

[51] L. Bernstein and H. Bartholomew, "Applications of Solid-Liquid Interdiffusion (SLID) Bonding in Integrated-circuit Fabrication," *Trans. Metall. Soc. AIME,* vol. 236, pp. 405-412, 1966.

[52] L. Bernstein, "Semiconductor joining by the solid-liquid-interdiffusion process," *Journal of the Electrochemical Soc.,* vol. 113, no. 12, pp. 1282-1288, 1966.

[53] G. S. Hoppin and T. F. Berry, "Activated Diffusion Bonding," *Welding Journal,* vol. 49, no. 11, pp. 505s-509s, 1970.

[54] W. A. Owczarski, W. H. King and D. F. Paulonis.United States Patent 3,530,568, 1970.

[55] D. S. Duvall, W. A. Owczarski, D. F. Paulonis and W. H. King, "Methods for Diffusion Welding the Superalloy Udimet 700," *Welding Journal,* vol. 51, no. 2, pp. 41s-49s, 1972.

[56] B. K. Lee, W. Y. Song, D. U. Kim, I. S. Woo and C. Y. Kang, "Effect of Bonding Temperatures on the Transient Liquid Phase Bonding of a Directionally Solidified Ni-based Superalloy, GTD-111," *Met. Mat. Int.,* vol. 13, no. 1, pp. 59-65, 2007.

[57] K. Nishimoto, K. Saida and Y. Shinohara, "Computer aided alloy design of insert metal for transient liquid phase bonding of γ/γ'/β type high aluminium nickel base superalloy," *Sci. and Tech. of Weld. and Joining,* vol. 8, no. 1, pp. 29-38, 2003.

[58] O. A. Ojo, N. L. Richards and M. C. Chaturvedi, "Isothermal solidification during transient liquid phase bonding of Inconel 738 superalloy," *Sci. and Tech. of Weld. and Joining,* vol. 9,

no. 6, pp. 532-540, 2004.

[59] A. Schnell, A. Stankowski and E. deMarcos, "ASME Turbo Expo 2006: power for land, sea, air," in *proceedings of GT2006*, Barcelona, 2006.

[60] X. Wu, R. S. Chandel and H. Li, "Evaluation of transient liquid phase bonding between nickel-based superalloys," *Journal of Mat. Sci.,* vol. 36, no. 6, pp. 1539-1546, 2001.

[61] O. A. Idowu, N. L. Richards and M. C. Chaturvedi, "Effect of bonding temperature on isothermal solidification rate during transient liquid phase bonding of Inconel 738LC superalloy," *Mat. Sci. Eng. A,* vol. A397, no. 1-2, pp. 98-112, 2005.

[62] B. Norris, "Designing with Titanium," in *Proceedings of the Institute of Metals Conference*, Bristol, 1986.

[63] Y. Nakao, K. Nishimoto, K. Shinozaki and C. Kang, in *Superalloys 1988*, Warrendale PA, 1989.

[64] Y. Nakao, K. Nishimoto, K. Shinozaki and C. Kang, *Trans. Japan Welding Soc.,* vol. 20, no. 1, pp. 60-65, 1989.

[65] Y. Nakao, K. Nishimoto, K. Shinozaki and C. Kang, "The 5th International Symposium of the Japan Welding Soc.," pp. 139-144, 1990.

[66] W. D. Zhuang and T. W. Eagar, "Transient Liquid-Phase Bonding Using Coated Metal Powders," *Weld. Journal,* vol. 76, no. 4, pp. 157s-162s, 1997.

[67] Y. S. Kwon, J. S. Kim, J. S. Moon and M. J. Suk, "Transient liquid phase bonding process using liquid phase sintered alloy as an interlayer material," *Journal of Mat. Sci.,* vol. 35, no. 8, pp. 1917-1924, 2000.

[68] A. A. Shirzadi and E. R. Wallach, "Temperature gradient transient liquid phase diffusion bonding: a new method for joining advanced materials," *Sci. and Tech. of Weld. and Joining ,* vol. 2, no. 3, pp. 89-94, 1997.

[69] A. A. Shirzadi, "Development and modelling of temperature gradient TLP bonding: a new method for joining advanced materials," *Welding in the World,* vol. 41, no. 5, pp. 435-442, 1998.

[70] A. Thakur, *MSc Dessertation,* Winnipeg, Manitoba: University of Manitoba, 1997.

[71] K. Ohsasa, T. Shinmura and T. Narita, "Numerical Modeling of Transient Liquid Phase Bonding Process of Ni using Ni-B-Cr Ternary filler metal," *J. of Phase Equlib.,* vol. 20, no. 3, pp. 199-206, 1999.

[72] Y. Nakao, K. Nishimoto, K. Shinozaki and C. Kang, Internationa Institute for Welding, UK, 1986.

[73] C. W. Sinclair, G. R. Prudy and J. E. Morell, "Transient Liquid-Phase bonding in Two-phase ternary systems," *Metall. and Mat. Trans.,* vol. 31, no. 4, pp. 1187-1192, 2000.

[74] W. D. MacDonald and T. W. Eager, "Isothermal solidification kinetics of diffusion brazing," *Metall. Mat. Trans. A,* vol. 29A, no. 1, pp. 315-325, 1998.

[75] K. Tokoro, N. P. Wikstrom, O. A. Ojo and M. C. Chaturvedi, "Variation in diffusion-induced solidification rate of liquated Ni–Cr–B insert during TLP bonding of Waspaloy superalloy," *Mat. Sci. Eng.A,* vol. 477, no. 1-2, pp. 311-318, 2008.

[76] M. M. Abdelfatah and O. A. Ojo, "On the Extension of Processing Time with Increase in Temperature during Transient-Liquid Phase Bonding," *Metall. Mat. Trans. A,* vol. 40, no. 2, pp. 377-385, 2009.

[77] M. Abdelfattah, *MSc Dissertation,* Winnipeg, Manitoba: University of Manitoba, 2008.

[78] A. Ghoneim and O. A. Ojo, "Asymmetric Diffusional Solidification during Transient Liquid Phase Bonding of Dissimilar Materials," *Metall. Mat. Trans. A,* vol. 43, no. 3, pp. 900-911, 2012.

[79] A. Ghoneim and O. A. Ojo, "Microstructure and mechanical response of transient liquid phase joint in Haynes 282 superalloy," *Mat. Charact.,* vol. 62, no. 1, pp. 1-7, 2011.

[80] A. Le Blanc and R. Mevrel, High Temperature Materials for Power Engineering, vol. II, Kluwer Academic, 1990, pp. 1451-1461.

[81] H. R. Zhang, A. Ghoneim and O. A. Ojo, "TEM Analysis of Diffusion Brazement Microstructure in a Ni3Al- based Intermetallic Alloy," *J. Mat. Sci.,* vol. 46, no. 2, pp. 429-437, 2011.

[82] S. M. Seo, I. S. Kim, J. H. Lee, C. Y. Jo, H. Miyahara and K. Ogi, "Eta Phase and Boride Formation in Directionally Solidified Ni-Base Superalloy IN792 + Hf," *Metall. Mat. Trans. A,* vol. 38A, no. 4, pp. 883-893, 2007.

[83] O. A. Ojo, "On an effective approach for reducing TLP bonding time in single crystal superalloys," *J. Maater. Sci.,* vol. 47, no. 3, pp. 1598-1602, 2012.

[84] W. F. Gale, D. A. Butts, M. Di Ruscio and T. Zhou, "Microstructure and mechanical properties of titanium aluminide wide-gap, transient liquid-phase bonds prepared using a slurry-deposited composite interlayer," *Metall. Mat. Trans. A,* vol. 33A, no. 10, pp. 3205-

3214, 2002.

[85] B. Zorc and L. Kosec, "Comparison of brazed joints made with BNi-1 and BNi-7 nickel-base brazing alloys," *Revista de Metalurgia Madrid,* vol. 36, no. 2, pp. 100-107, 2000.

[86] ASMHandbook, "Vol. 3 Alloy Phase Diagrams," Materials Park, Ohio, USA, ASM Internationa, 1992.